Fundamental and Applied Studies on Friction/Lubrication of Concentrated Polymer Brushes

Akihiro Nomura

2011

Contents

Chapter 1

General Introduction

1-1-1. Tribology and Lubrication

Tribology, which is defined as "*the science and technology of interacting surfaces in relative motion and of related subjects and practices*",[1] plays crucial roles on our lives. One of the most important contents in tribology is friction. When two solid surfaces in contact are sliding against each other, a friction force resisting the relative motion is produced (as shown in Figure 1-1). We live our lives by controlling the friction, which dominates almost all of our physical activities such as blinking, eating and moving his or her joints. Although the friction is very important for our lives, it is often cumbersome for machines or instruments we devised for our purposes. That is because the friction causes wear to shorten the machine life and to waste plenty of operational energy. Lubrication is the term of methodology for reducing such unfavorable friction between the relatively moving two surfaces.

Lubrication has been explored since the dawn of civilization. For example, ancient people around 5000 B.C. invented a wheel, which is a round-shaped machine component, to transport materials efficiently.[2] Ancient wall paintings tell us ancient people's efforts for lubrication. Egyptian around 1800 B.C. spread some kind of oil as lubricant between the ground and sledge carrying a stone statue. Mesopotamian around 700 B.C. used logs to move huge statues efficiently. In the course of development of our modern civilization, various kinds of lubrication techniques have been devised and improved.[3] Nevertheless, we can not still completely eliminate the friction, or at least, today's lubrication technology does not satisfy the demands for our modern high-performance machines progressing day by day, such as micro gadgets, space equipments, and medical instruments. Lubrication is one of the biggest issues of our modern science and technology.[4]

In spite of the importance of lubrication, our understanding of friction is still rudimentary. This

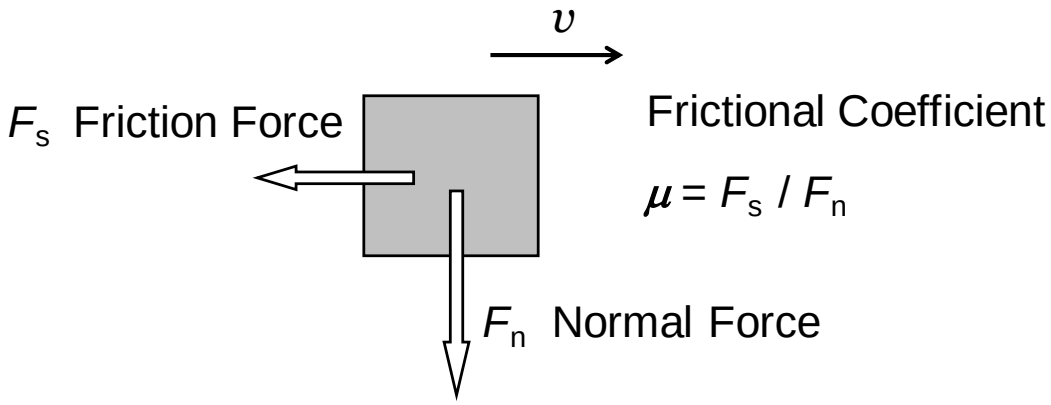

Figure 1-1. Force diagram of block material on ground surface. Normal force F_n is caused with a gravity proportional to the block mass. When the block moves on the ground surface with a velocity υ, friction force F_s is generated. Frictional coefficient μ is expressed by F_n and F_s as $\mu = F_s/F_n$.

results from the complexity of tribology; namely, a wide range of factors including not only the chemical and physical properties of contact surfaces, surface asperity (convexity and concavity), surface aging (wear), rheological character of lubricant are dynamically involved and mutually related. The experimental technique to directly observe the interface between two lubricating surfaces under the condition controlling such factors is now limited, which also hinders the development of tribology.[5]

1-1-2. Lubrication Mechanism

Recent development of new experimental technique, such as quartz crystal microbalance (QCM),[6] surface force apparatus (SFA)[7] and atomic force microscope (AFM),[8] has enabled us to study the friction at the molecular scale. Many of experimental results obtained through these new techniques, however, can not describe the equation of friction. We still have to rely on empirical knowledge and extensive experience for the prediction of friction.

Stribeck et al found out two distinctive friction regions from empirical study of friction with lubricant oil.[9] They had measured the frictional coefficient μ, the ratio of friction force to normal load (Figure 1-1), of rolling bearing with a wide range of controlled load, velocity and viscosity of lubricant. He compiled the data of frictional coefficient μ as a function of $\upsilon\eta/p$, where υ is the shear velocity, η the viscosity and p the pressure normal to the contacted interface. The parameter, $\upsilon\eta/p$ is

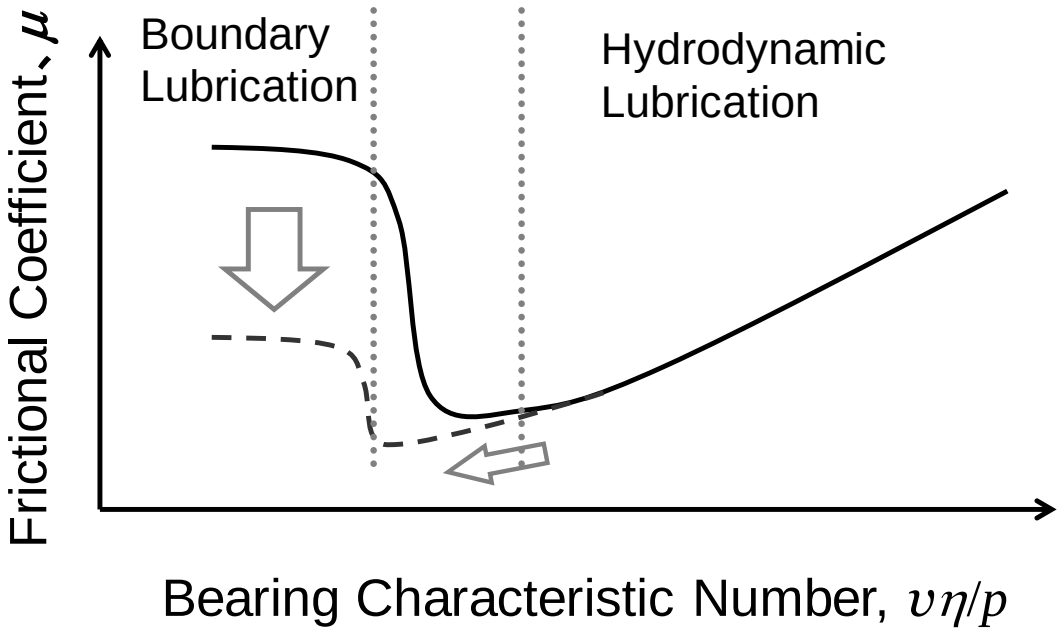

Figure 1-2. Stribeck diagram for lubricated friction surfaces. Frictional coefficient μ is depicted against $\upsilon\eta/p$. There are two distinct friction regimes; boundary lubrication with a relatively high frictional coefficient, and hydrodynamic lubrication with a low frictional coefficient with apparent dependence on bearing characteristic number. In the diagram, the strategy for better lubrication is indicated by a grey arrow; decreasing μ in boundary lubrication and expanding hydrodynamic lubrication region.

called the bearing characteristic number. This is shown in the so-called Stribeck diagram (Figure 1-2). According to the results, he divided the friction state into two distinctive regimes in a view of what determines the friction force. These regimes are called (I) Hydrodynamic lubrication and (II) Boundary lubrication, as will be summarized below.

(I) Hydrodynamic lubrication is the lubrication in which a fluid lubricant is filled between relatively moving two surfaces. The fluid lubricant hydrodynamically prevents direct contact of two surfaces, decreasing the friction (typically to be 0.001~0.01 in μ), minimizing the frictional wear, and then attaining an ideal frictional state. The friction force in hydrodynamic lubrication is determined by rheological character of the fluid lubricant. If the fluid lubricant is a Newtonian fluid, the friction force can be formulated from the equation of viscosity resistance as,

$$\mu = \upsilon\eta/dp \tag{1-1}$$

where d denotes the thickness of a fluid lubricant layer.

(II) The fluid lubricant is squeezed out between two lubricating surfaces with increasing normal load or decreasing velocity, and finally their direct contact occurs. This state is the boundary lubrication. Some overcoats of lubricating surfaces prevent adhesion of two solids, serving as a lubricant. Under ambient frictional condition, an oxide film or an adsorbed molecular layer (water or an organic molecule from air) can also be a lubricant.[10] Such overcoats are effective as lubricants even if they are monomolecular layer.[11]

It is considered that van der Waals force is the origin of friction under boundary lubrication. When the surfaces are in contact, molecules constructing two surfaces attractively interact each other with van der Waals force when the surfaces are in contact, producing adhesion force and hence friction force to break free from the adhesion. The Amontons-Coulomb law, an empirical rule about dry friction between solid materials, applicable to boundary lubrication, suggests that (i) the friction force is proportional to the applied load, (ii) the friction force is independent of the sliding velocity, and (iii) the friction force is independent of the apparent area of contact.[12] The frictional coefficient is difficult to be formulated due to the complexity in this friction state, but it is empirically known that the coefficient is typically 100 times higher than that under hydrodynamic lubrication.

Except for these lubrication mechanisms, there are several kinds of lubrication states such as elastohydrodynamic lubrication and mixed lubrication, which are now basically understood with combination of those two lubrication mechanisms.

1-1-3. Lubrication Technique

We can set guidance for lubrication techniques from the lubrication mechanisms as mentioned above. Briefly speaking, the key for lubrication is how we can afford or keep a hydrodynamic lubrication state by effectively holding a lubricant fluid between surfaces. At the same time, the

friction in boundary lubrication state should be also suppressed.

To reduce the friction in boundary lubrication, adhesion between the relatively moving two surfaces should be alleviated. While the molecule inside materials in a bulk state is stabilized by adjacent molecules with van der Waals force or covalent bonding, the molecule at the outermost surface is usually unstable, in other words, chemically activated because of the incomplete surrounding by neighbor molecules. The outermost-surface molecule more or less tries to seize other molecules out of the materials, leading to strong adhesion.[10] Effective lubrication can not be desired in this state. The surfaces should be covered with a chemically stable layer to prevent such adhesion.

In ambient friction of common solid substances, an oxide film or a molecule-absorbed layer functions as a protection layer against adhesion, giving μ of 0.4 - 1.0 on general metals as shown in Table 1-1. Polytetrafluoroethylene (PTFE, known as Teflon, a trade name of PTFE) is used as a material with high performance in lubrication. PTFE is much chemically stable and hardly react with anything. This feature of PTFE leads to less adhesive each other, which eventually develops a low μ value. Actually, PTFE shows particularly less μ (0.05 - 0.1) than that of other solid material, and is used as a self-lubricant material.[13] Molybdenum disulfide and graphite are also used as lubricants in particulate dispersion state in grease.[14] It is known that their molecular structures have lamellar morphology with very weak interaction between adjacent layers and that their layers are easy to be delaminated, which affords a low μ value.[15]

On the other hand, lubricant fluid should also be hold on for hydrodynamic lubrication. Viscous oil has been used for traditional lubricant fluid. Higher viscosity is required to maintain a fluid film between lubricating two surfaces but raises the μ as described in Equation (1-1). A precisely patterned and indented surface enables lubricant fluid to be kept, easily affording hydrodynamic lubrication at lower velocity, as is adopted as micro-groove bearing.[16] Gel is one of the most interesting materials as lubricant since it can contain much solvent in its polymer-network structure. Various kinds of hydro-gels are in our bodies, enabling us to blink, eat something, and move our joints very smoothly. Osada et al revealed that the friction of hydro-gels is dominated by adhesive or

Table 1-1. Examples of Frictional Coefficient μ

Materials		Frictional Coefficient, μ
General Metal		0.4 - 1.0
Polymer	PS	0.4 - 0.5
	PMMA	0.4 - 0.5
	PTFE	0.05-0.1
Hydro Gel	Adhesive	0.01-10
	Repulsive	10^{-3} ~
Polymer Brush	Semi-dilute	0.01-0.1
	Concentrated	10^{-4} ~

*Achievable minimum values are indicated.

repulsive interaction of network polymer chain.[17] They achieved a μ value as low as 10^{-4} order or less by introducing repulsive interaction between the surfaces of hydrogels (Table 1-1), e. g., electrostatic repulsion, which forms a water layer acting as a fluid lubricant and affords hydrodynamic lubrication effectively.

1-1-4. Model Surfaces for Tribology

As noted by the author, the key to improving the lubricating property is how the surface is precisely designed both in its chemical and physical structure. To conduct a fundamental study of tribology, we need model layers whose structures and configurations at the outermost surface are well controlled at a molecular level. Although there are several types of surfaces with molecularly controlled structure, such as a Langmuir-Blodgett (LB)[18] film and a self-assembled monolayer

(SAM),[19] an architecture consisting of polymer chains tethered to a solid surface at one end (polymer brush) has attracted increasing attention, because it plays an important role in many areas of science and technology, e.g., colloid stabilization, adhesion, rheology, and tribology.[20] Strategies have been developed to introduce polymer chains onto surfaces using chemical (through covalent bonding) and physical (by physisorption) methodologies.[21] Physisorption involves the absorption of a block copolymer with a segment which sticks to the substrate surface. Such polymer chains are not stably attached, particularly under conditions in which high shear forces are involved. In order to achieve stable interfacial compatibility, covalent bonding is preferred. Techniques for graft polymer chains can be categorized into two methods. The first method is called as the "grafting-to" method, which involves preformed polymers with reactive sites.[22] The second method is called as "grafting-from" method which conducts the direct growth of polymer chains from the surface, the details of which will be described below.

1-1-5. Friction of Polymer Brush

The controlled fabrication of model surfaces as well as recent improvement in SFA and AFM as nano-tribometers have enabled us to study the origins of friction forces. Klein et al studied the friction of a solvent swollen polymer brushes prepared by the "grafting-to" method and found that the polymer brush considerably decreased the friction force in a wide range of normal loads and sliding velocities as compared to the case of the absence of polymer chains.[23] This decrease corresponded to a reduction in the frictional coefficient by two to three orders of magnitude. This study also revealed that the so-called stick-slip behavior characterizing the trace in the case without brushes was less marked and was seen to come into effect only at very high compressions on polymer-attached surfaces. The lubrication effect of the brush layer is attributed first to the adhesion of relatively moving surfaces being prevented via steric repulsion of the swollen brush layers. Klein et al. also presented a theoretical derivation on the friction of brushes and explained that the limited interpenetration of brush layers facilitated the effective lubrication.[24] Their theoretical expression predicts that the smaller the screening length is at the anchoring surface (i.e. the denser brush), the

greater the effective lubrication is. However, the graft densities of their brushes considered were limited to small values that corresponded to that of a dilute polymer solution, because the polymer-tethered surfaces were assumed to have been fabricated by the grafting-to method.

1-1-6. Surface-Initiated Polymerization

The grafting-from method, referred to as surface-initiated polymerization and first investigated by Prucker and Rühe,[25] makes it possible to achieve denser grafting of polymers than the "grafting-to" one. This method is divided into two processes. First, an initiator is introduced onto a solid surface using, e.g., a bifunctional compound that is capable of covalently bonding with a surface and initiating polymerization. Second, polymerization is carried out from initiating sites on the surface. In this technique, the addition of a monomer to the end of a growing chain is less hindered by chains that have been grafted. Therefore, the grafting-from method is more suitable than the grafting-to one to produce polymer-grafted surfaces with greater thicknesses and higher graft densities.

Surface-initiated polymerization has been carried out using a variety of polymerization techniques, including free radical,[25] ionic,[26] and ring-opening methathesis[27] polymerizations. In particular, the application of living polymerizations offers clear advantages in that it provides not only a fine control of chain length, its distribution, monomer sequence and topology of graft polymers (e.g., random/block/gradient copolymers, comb-like or branched polymers, and crosslinked polymers) but also a dramatic increase in graft density. The reason for this increase is that all the graft chains grow more or less simultaneously, with their active chain ends concentrated near the outermost surface of the graft layer. Among living polymerization techniques, living radical polymerization (LRP) is one of the most promising routes for densely grafting functional polymers owing to its tolerance to impurities and versatility in relation to various monomers. A variety of LRPs, including nitroxide-mediated polymerization (NMP),[28] atom transfer radical polymerization (ATRP),[29] and reversible addition-fragmentation chain transfer (RAFT)[30] polymerization, have already been applied to surface-initiated polymerization by immobilizing either a dormant species or

a conventional radical initiator on the surface. In the latter case, a capping agent is added in a solution phase (reverse LRP). Recently, organotellurium-mediated radical polymerization (TERP)[31] and reversible chain transfer catalyzed polymerization (RTCP)[32] have also been gaining attention as new classes of LRP with good controllability.

1-1-7. Concentrated Polymer Brushes

The conformation, in a solvent, of polymer chains end-tethered on a solid surface can be dramatically changed depending on the graft density.[33] At low graft densities, the polymer chains will assume a "mushroom" conformation with a coil dimension similar to that of free (ungrafted) polymer chains (Figure 1-3a). With increasing graft density, graft chains are obliged to stretch away from the surface, forming the so-called "polymer brush". Polymer brushes may be categorized into two types according to their graft density. One is the "semi-dilute polymer brush" (SDPB, Figure 1-3b), in which polymer chains overlap each other, but their volume fraction is still so low that the free energy of interaction can be approximated by a binary interaction, and the elastic free energy, by that of a Gaussian chain.[34] The second is the "concentrated polymer brush" (CPB, Figure 1-3c), for

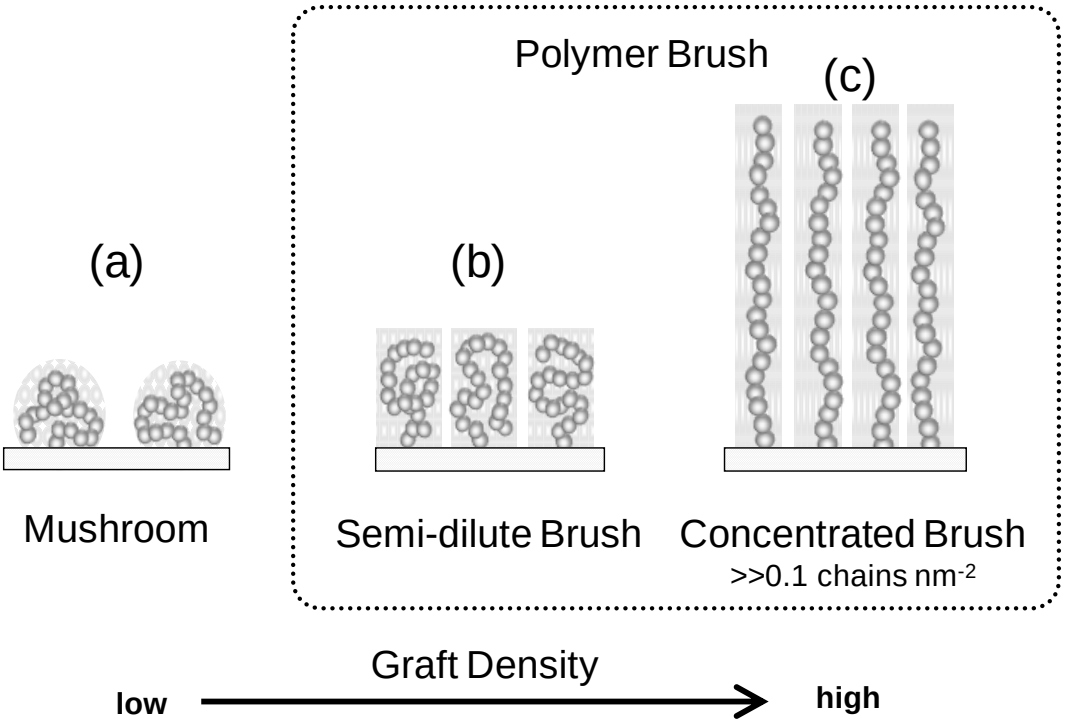

Figure 1-3. Schematic illustrations of tethered polymer chains.

which the above-mentioned approximations are no longer valid and higher-order interactions must be taken into account. Theoretical analyses taking these interactions into account have predicted that the repulsive force will increase much more steeply with increasing graft density.[35]

Fukuda et al. firstly conducted systematic studies on CPBs using samples of low-polydispersity poly (methyl methacrylate) (PMMA) that was densely grafted onto a surface by surface-initiated ATRP. Recent studies have revealed that the CPBs indeed have both the structure and properties significantly different from those of SDPBs. In particular, the CPB of PMMA formed on a silicon wafer is highly swollen in a good solvent, such that it gives an equilibrium swollen thickness as large as 80 - 90% of the full contour length of the graft chains, suggesting that these chains are extended to an exceptionally high degree.[36] Microtribological studies have revealed that the frictional coefficient between the swollen CPBs is extremely small (μ~10^{-4}) even at high compression (Figure 1-4).[37] The features specific to the CPB, including such super lubrication, were reasonably interpreted by the entropic interaction related to extremely high osmotic pressure and highly stretched chain

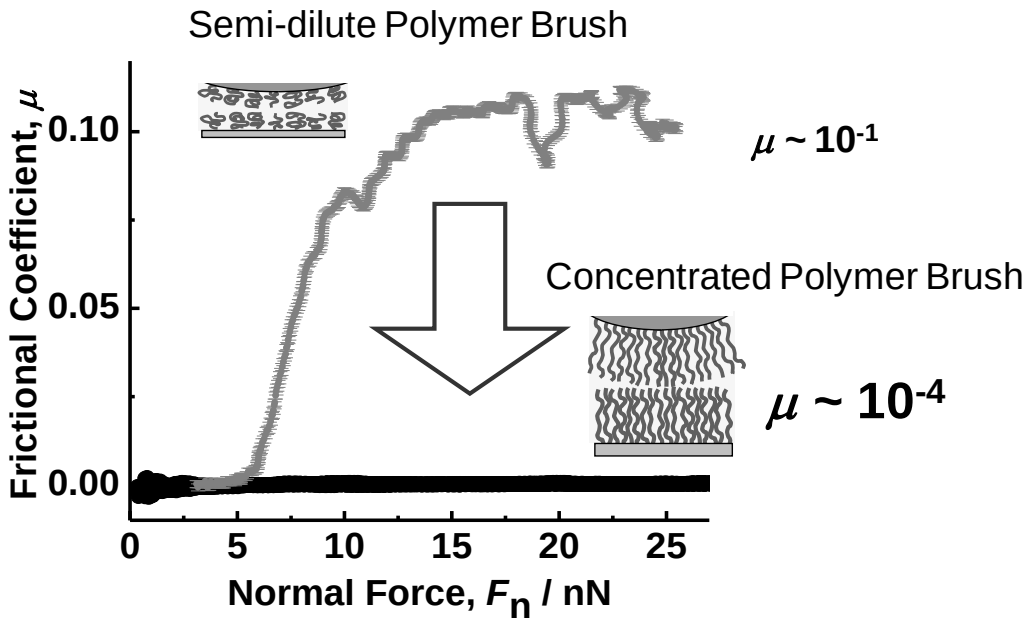

Figure 1-4. Normal force dependence on the frictional coefficients of semi-dilute and concentrated PMMA brushes. The data was reprocessed from reference 36.

conformation and termed as the “concentrated-brush effect”.

1-2. Background and Purpose of This Thesis

Although the CPB is already known to afford an extremely small frictional coefficient, a number of problems remain unsolved in order to put this excellent function into a practical lubrication system. One of these problems stems from our lack of a detailed understanding of the lubrication mechanism of the CPB. Fundamental and mechanistic study of the subject has hardly been carried out because of the difficulty not only in preparing such well-defined brush samples but also in precisely measuring their frictional property as a function of the viscosity and quality of solvent as well as the brush-structure characteristics such as chain length, brush thickness, and degree of swelling. Another challenge is the precise design of the CPBs for practical use, which requires, among other factors, better control of the tribology (stimuli responsibility) and tolerance to wearing and in some cases those as an aqueous system.

In light of the present situation, the author determined that the first objective of this thesis would be to verify the lubrication mechanism of the CPB with precise control of the brush structure. The ultra-low frictional property of the CPB is discussed in terms of whether or not the confronted graft chains interpenetrate each other. Such interpenetration occurs at a certain level of compression between SDPBs, affording a frictional transition from low to high frictional stages (μ ~ 0.01 - 0.1), but it is dramatically suppressed between the CPBs because of entropic origins. According to the lubrication mechanisms discussed in Section 1-1-2, the above-mentioned frictional state is categorized as boundary lubrication, since the outermost-surface property determines the friction. On the contrary, the regime of hydrodynamic lubrication for a solvent-swollen CPB remains little understood. The author achieves his first objective by analyzing the friction/lubrication data as a function of normal force, shear velocity, solvent quality (hence, degree of swelling), and solvent viscosity. The frictional property between immiscible CPBs is also evaluated in order to confirm the hydrodynamic and boundary lubrication proposed for the CPB.

The achievement of the first objective enables us to then develop new designs for lubricating materials equipped with the concentrated-brush effect. Such an ultra-low frictional property has previously been demonstrated only for nonpolar polymer brushes of limited thicknesses owing to the easy preparation of such brush samples. Thus, the author set up a second objective, which was to establish newly designed CPBs of functional polymers for practical use. Water-swellable and thermo-responsible CPBs are synthesized and investigated in terms of their frictional property in water media, with the aim of eventual applications in biomedical materials. Another application of this design is a polymer gel of bottle-brush type, in which the network structure of the polymer chains can contain much solvent inside and the precise structural control of the bottle-brush polymer, i.e., the control of the side-chain length and graft density, can be expected to introduce the concentrated-brush effect. The author uses the most appropriate LRP technique as a versatile and robust tool for the preparation of well-defined polymer-brush samples. In addition to this, a methodology to precisely measure the surface interaction and swelling and friction/lubrication properties is newly devised, particularly using a colloidal-probe technique on AFM. Such newly designed materials may concurrently give rise to other factors, that were not previously taken into account. The author also discusses such factors in regard to the frictional property of the CPB.

1-3. Outline of This Thesis

The purpose of this thesis is to clarify the correlation between the structure and the surface property of a CPB and to thereby provide new guideline for the novel design of tribomaterials.

In **Chapter 2**, the author measures the friction force and hence the frictional coefficient μ between CPBs of polystyrene (PS) in solvents as a function of shear velocity and degree of swelling (Figure 1-5). The degree of swelling of a polymer-brush layer is successfully controlled by the solvent composition of a mixture containing toluene (a good solvent for PS) and 2-propanol (non-solvent for PS). The author analyzes the friction data collected under a wide range of conditions, ranging from a highly stretched brush to almost shrunken states, and discusses these

mechanisms in terms of boundary lubrication and hydrodynamic lubrication.

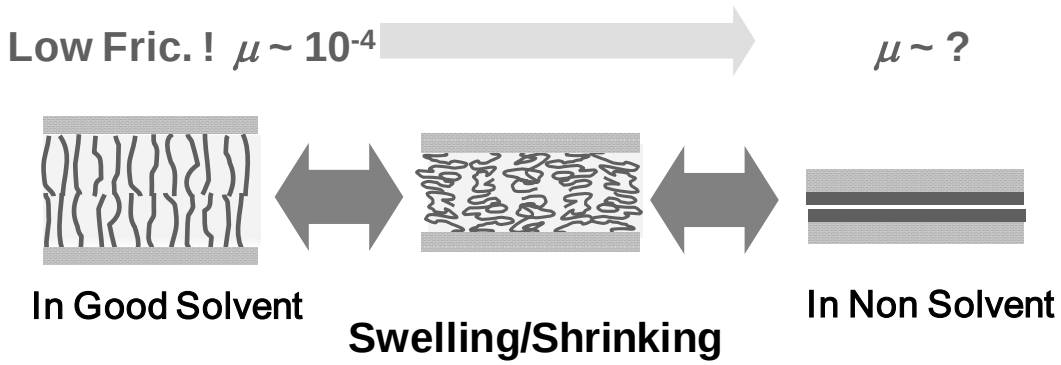

Figure 1-5. Schematic representation of the frictional property of swelling degree controlled CPBs of PS.

In **Chapter 3**, the frictional property between CPBs of PMMA immersed in highly viscous ionic liquids (ILs) is measured in order to demonstrate the effects of solvent viscosity (Figure 1-6). As ILs which can swell PMMA brushes, DEME-TFSI and EMI-TFSI are used. The results obtained clearly reveal the hydrodynamic-lubrication regime. The author discusses the effects of solvent viscosity in terms of the local viscosity at or inside the brush in order to quantitatively clarify the

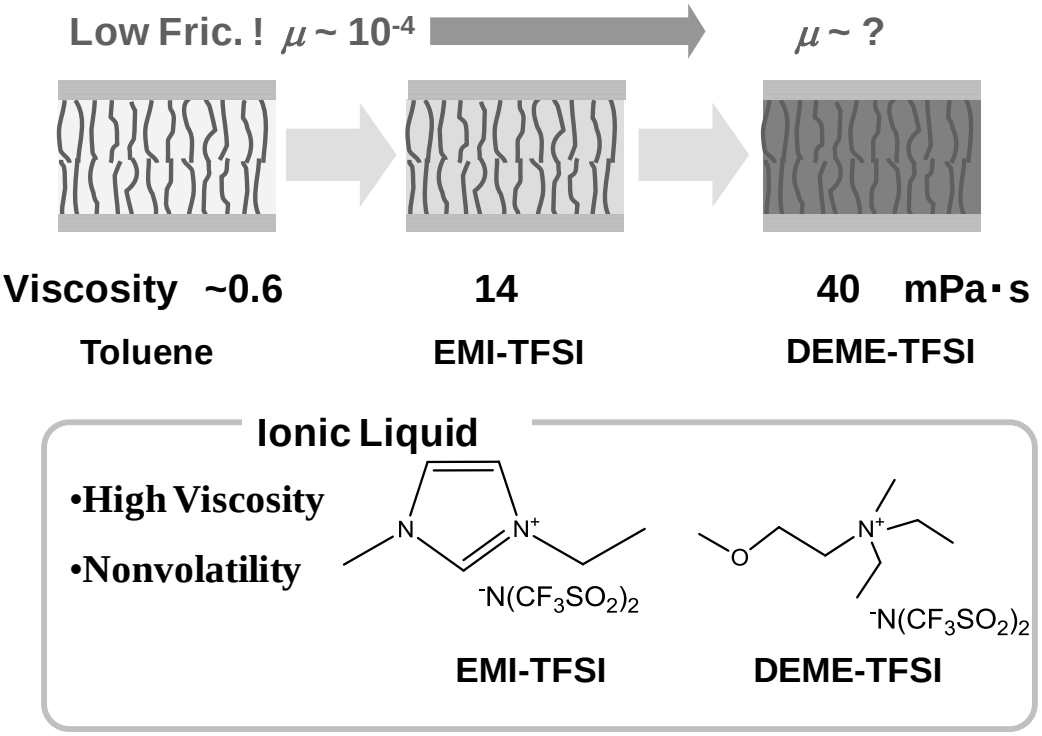

Figure 1-6. Schematic representation of the frictional property of CPBs of PMMA in ionic liquids.

hydrodynamic lubrication of the CPB.

In **Chapter 4**, the frictional property between CPBs of immiscible polymers (PMMA and PS) is compared with that between the identical ones in order to reveal the nature of the boundary lubrication of the CPB. The most important issue in this regard is the degree of interpenetration (Figure 1-7) between confronted graft chains, which should dominate the boundary lubrication.

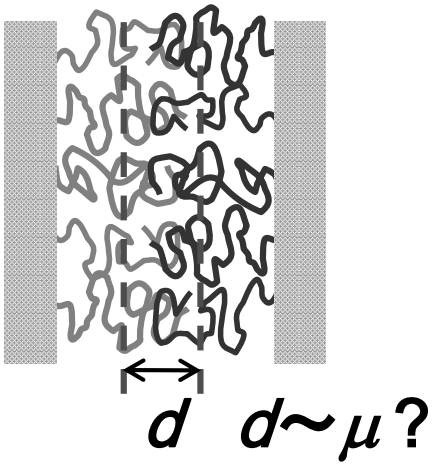

Figure 1-7. Schematic representations of the graft chains interpenetration.

In **Chapter 5**, the CPBs of hydrophilic polymers, poly (2-hydroxyethyl acrylate) (PHEA) and poly (poly(oxyethyleneglycol)methylether acrylate) (PPEGA), are newly synthesized with surface-initiated TERP (Figure 1-8). The frictional property of these polymer brushes in water media is evaluated. The results are then discussed in terms of the hydrodynamic and boundary lubrications described in the previous chapters.

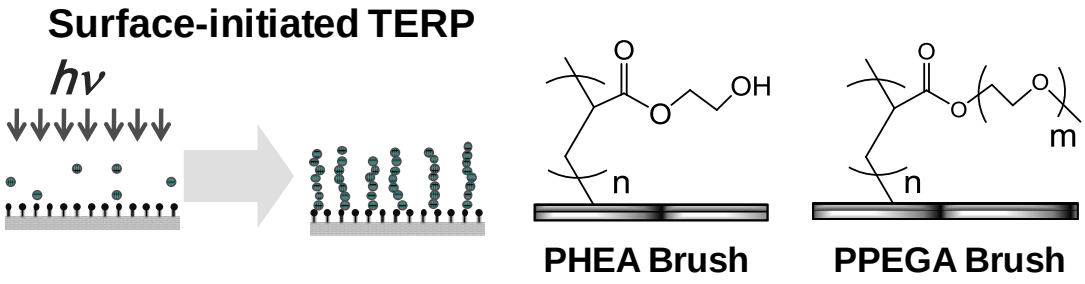

Figure 1-8. Schematic representation of the synthesis of CPBs of PHEA and PPEGA.

In **Chapter 6**, the CPB of a thermo-responsible polymer, poly (*N*-isopropyl acrylamide) (PNIPAM), is newly synthesized via the surface-initiated ATRP in order to fabricate a lubricating surface with stimuli responsibility. The degree of swelling and frictional property is minutely evaluated as a function of temperature (Figure 1-9).

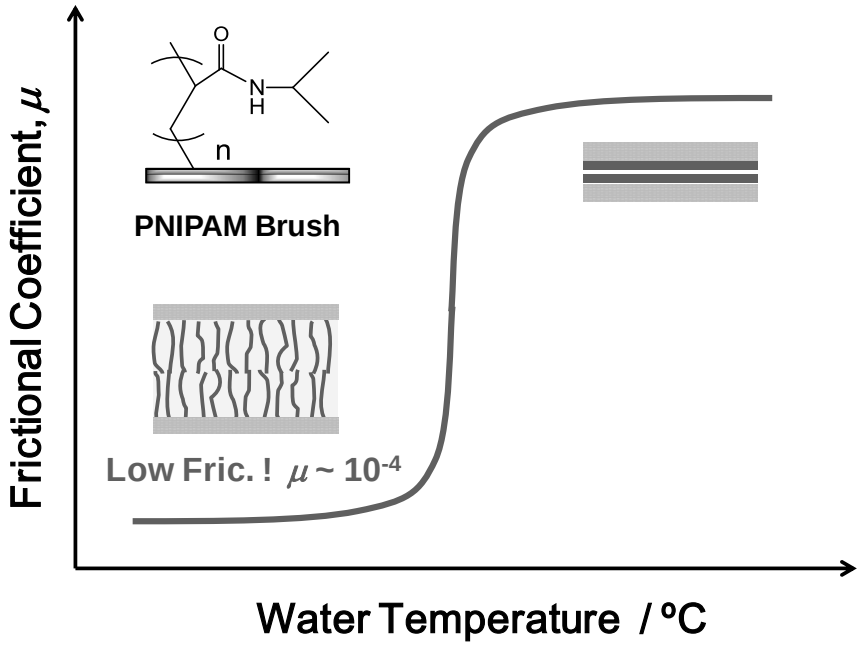

Figure 1-9. Schematic representation of the frictional property of CPBs of PNIPAM.

In **Chapter 7**, bottle-brush polymers that potentially possess an ultra-low frictional property comparable to that of a CPB are fabricated via the ATRP from a multi-initiator polymer (Figure 1-10). The bottle-brush polymer is processed into a thin gel film via newly established radical coupling that employs an amine catalyst, and its frictional property is evaluated. The results are discussed in terms of the side-chain length and the effective graft density.

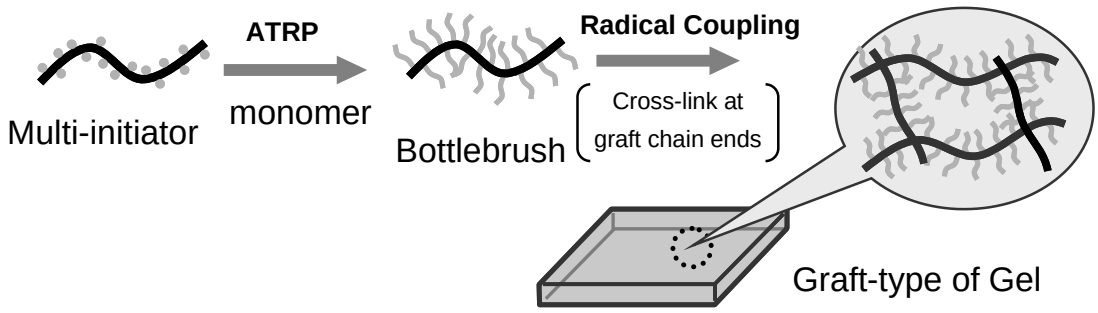

Figure 1-10. Schematic representation of the synthesis of bottle brush polymer gel.

References

(1) The term “tribology” is derived from the ancient Greek word “tribein” (meaning rubbing) and was first used in 1966 in a publication titled, *The Jost Report: Lubrication Education and Research*, published by Her Majesty’s Stationary Office (HMSO) in the United Kingdom.

(2) The earliest image of what may be a wheeled vehicle is depicted in the *Bronocise pot* dated to around 3500 BC, discovered in 1976 at south of Poland.

(3) Dowson, D. *History of Tribology, Second Edition*; Professional Engineering Publishing: London, 1999.

(4) (a) Jost, H. P. *Wear* **1990**, *136*, 1-17. (b) D. Tabor. *Tribol. Int.* **1995**, *28*, 7-10.

(5) (a) Butt, H. J.; M. Kappl. *Surface and Interfacial Forces*; Whiley-VCH: Weinheim, 2010. (b) Ludema, K. C. *Friction, Wear, Lubrication: A Textbook in Tribology*; CRC Press: Boca Raton, 1996. (c) Bhushan, B. *Introduction to Tribology*; John Wiley & Sons Inc: New York, 2002 (d) Persson, B. N. J. *Sliding Friction: Physical Principles and Applications, Second Edition*; Springer: Berlin, 1998 (e) Krim, J. *Surf. Sci.* **2002**, *500*, 741-758. (f) Krim, J. *Am. J. Phys.* **2002**, *70*, 890-897.

(6) (a) Krim, J.; Widom, A. *Phys. Rev. B* **1988**, *38*, 12184-12189. (b) Krim, J.; Solina, D. H.; Chiarello, R. *Phys. Rev. Lett.* **1991**, *66*, 181-184. (c) Cieplak, M.; Smith, E. D.; Robbins, M. O. *Science* **1994**, *265*, 1209-1212. (d) Daly, C.; Krim, J. *Phys. Rev. Lett.* **1996**, *76*, 803-806. (e) Mak, C.; Krim, J. *Phys. Rev. B* **1998**, *58*, 5157-5159. (f) Dayo, A.; Alnasrallah, W.; Krim, J. *Phys. Rev. Lett.* **1998**, *80*, 1690-1693. (g) Dultsev, F. N.; Ostanin, V. P.; Klenerman, D. *Langmuir* **2000**, *16*, 5036-5040. (f) Mason, B. L.; Winder, S. M.; Krim, J. *Tribol. Lett.* **2001**, *10*, 59-65. (g) Bruschi, L.; Mistura, G. *Phys. Rev. B* **2001**, *63*, no. 235411.

(7) (a) Thompson, P. A.; Grest, G. S.; Robbins, M. O. *Phys. Rev. Lett.* **1992**, *68*, 3448-3451. (b) Yoshizawa, H.; Chen, Y. -L.; Israelachvili. J. *J. Phys. Chem.* **1993**, *97*, 4128-4140. (c) Idziak, S. H. J.; Safinya, C. R.; Hill, R. S.; Kraiser, K. E.; Ruths, M.; Warriner, H. E.; Steinberg, S.; Linang, K. S.; Israelachvili, J. N. *Science* **1994**, *264*, 1915-1918. (d) Demirel, A. L.; Granick, S.

Phys. Rev. Lett. **1996**, *77*, 4330-4333. (e) Campbell, S. E.; Luengo, G.; Srdanov, V. I.; Wudi, F.; Israelachvili, J. N. *Nature* **1996**, *382*, 520-522. (f) Golan, Y.; Martin-Herranz, Y. A.; Li, Y.; Safinya, C. R.; Israelachvili, J. *Phys. Rev. Lett.* **2001**, *86*, 1263-1266. (g) Raviv, U.; Giasson, S.; Kampf, N.; Gohy, J. F.; Jerome, R.; Klein, J. *Nature* **2003**, *425*, 163-165. (h) Yamada, S. *J. Chem. Phys.* **2009**, *131*, 184708.

(8) (a) Mate, C. M.; Mcclelland, G. M.; Erlandsson, R.; Chang, S. *Phys. Rev. Lett.* **1987**, *59*, 1942-1945. (b) Mayer, E.; Overney, R. M.; Howald, L.; Luthi, R.; Frommer, J.; Gunngherodt, J. *Phys. Rev. Lett.* **1992**, *69*, 1777-1780. (c) Germann, G. J.; Cohen, S. R.; Neubauer, G.; Mcclelland, G. M.; Seki, H.; Coulman, D. *J. Appl. Phys.* **1993**, *73*, 163-167. (d) Binggeli, M.; Mate, C. M. *Appl. Phys. Lett.* **1994**, *65*, 415-417. (e) Xiao, X.; Hu, J.; Charych, D. H.; Salmeron, M. *Langmuir* **1996**, *12*, 235-237. (f) Hirano, M.; Shinjo, K.; Kanko, R.; Murata, Y. *Phys. Rev. Lett.* **1997**, *78*, 1448-1451. (g) Enachescu, M.; Van den Oetelaar, R. J. A.; Carpick, R. W. *Tribol. Lett.* **1999**, *7*, 73-78. (h) Tutein, A. B.; Stuart, S. J; Harrison, J. A. *Langmuir* **2000**, *113*, 8249-8252. (i) Jung, Y. C.; Bhushan, B. *Nanotechnology* **2006**, *17*, 4970-4980. (j) Szlufarska, I.; Chandross, M.; Carpick, R. W. *J. Phys. D* **2008**, *41*, 123001.

(9) (a) Stribeck, R. *Zeitschrift des Vereines deutscher Ingenieure* **1901**, *45*, 73-79 (Part I). & **1901**, *45*, 118-125 (Part II). (b) Stribeck, R. *Zeitschrift des Vereines deutscher Ingenieure*. **1902**, *46*, 1341-1348 (Part I). & **1902**, *46*, 1432-1438 (Part II). & **1902**, *46*, 1463-1470 (Part III). (d) for recent comment, see, Jacobson, B. *Tribol. Int.* **2003**, *36*, 781-789.

(10) (a) Buckley, D. H. *Surface effects in Adhesion, Friction, Wear, and Lubrication*; Elsevier: Amsterdam, 1981. (b) Feng, Z.; Tzeng, Y.; Field, J. E. *J. Phys.* **1992**, *25*, 1418-1424.

(11) Bhushan, B.; Israelachvili, J. N.; Landman, U. *Nature* **1995**, *374*, 607-616.

(12) Amonton, G. *Mem. del'Academie Royale A* **1699**, 275-282.

(13) (a) Fusaro, R. L. *Tribol. Int.* **1990**, *23*, 105-122. (b) Lu, Z. P.; Friedrich, K. *Wear* **1995**, *181*, 624-631. (c) Yamada, S.; Israelachvili. J. *J. Phys. Chem. B* **1998**, *102*, 234-244. (d) Theiler, G.; Hubner, W.; Gradt, T.; Klein, P.; Friedrich, K. *Tribol. Int.* **2002**, *35*, 449-458.

(14) (a) Kustas, F. M.; Misra, M. S.; Shepard, D. F.; Froechtenigt, J. F. *Surf. Coat. Tech.* **1991**, *48*, 113-119. (b) How, K. P.; Kalousek, J.; Magel, E. *Wear* **1997**, *211*, 134-140. (c) Chhowalla, M.; Amaratunga, G. A. J. *Nature* **2000**, *407*, 164-167. (d) Zhang, X. -T.; Liao, G. -X.; Jin, Q. -F.; Feng, X. -B.; Jian, X. -G. *Tribol. Int.* **2008**, *41*, 195-201.

(15) Bowden, F. P.; Tabor, D. *The Friction and Lubrication of Solid*; Oxford University Press: New York, 1986.

(16) (a) Etsion, I.; Burstein, L. *Tribol. Trans.* **1996**, *39*, 677-683. (b) Wang, X.; Kato, K.; Adachi, K.; Aizawa, K. *Tribol. Int.* **2003**, *36*, 189-197. (c) Wakuda, M.; Yamauchi, Y.; Kanzaki, S.; Yasuda, Y. *Wear* **2003**, *254*, 356-363. (d) Costa, H. L.; Hutchings, I. M. *Tribol. Int.* **2007**, *40*, 1227-1238.

(17) (a) Gong, J.; Higa, M.; Iwasaki, Y.; Katsuyama, Y.; Osada, Y. *J. Phys. Chem. B* **1997**, *28*, 5487-5489. (b) Gong, J.; Osada, Y. *J. Chem. Phys.* **1998**, *109*, 8062-8068. (c) Gong, J.; Kagata, G.; Osada, Y. *J. Phys. Chem. B* **1999**, *103*, 6007-6014. (d) Gong, J.; Kurokawa, T.; Narita, T.; Kagata, G.; Osada, Y.; Nishimura, G.; Kinjo, M. *J. Am. Chem. Soc.* **2001**, *123*, 5582-5583.

(18) Zasadzinski, J. A.; Viswanathan, R.; Madsen, L.; Garnaes, J.; Schwarts, D. K. *Science* **1994**, *263*, 1726-1733.

(19) Schreiber, F. *Prog. Surf. Sci.* **2000**, *65*, 151-256.

(20) (a) Napper, D. H., Eds.; *Polymeric Stabilization of Colloidal Dispersions*; Academic Press: London, 1983. (b) Raphael, E.; de Gennes, P. G. *J. Phys. Chem.* **1992**, *96*, 4002-4007. (c) Klein, J. *Annu. Rev. Mater. Sci.* **1996**, *26*, 581-612. (d) Klein, J.; Kumacheva, E. *Science* **1995** *269*, 816-819. (e) Parnas, R. S.; Cohen, Y. *Rheol. Acta* **1994**, *33*, 485-505.

(21) Advincula, R. C.; Britain, W. J.; Caster, K. C.; Rühe, J., Eds.; *Polymer Brushes*; Whiley-VCH: Weinheim, 2004.

(22) (a)Tsubokawa, N.; Hosoya, M.; Yanadori, K.; Sone, Y. *J. Macromol. Sci. - Chem.* **1990**, *A27*, 445-457. (b) Bridger, K.; Vincent, B. *Eur. Polym. J.* **1980**, *16*, 1017-1021. (c) Kishida, M.; Mishima, K.; Corretge, E.; Konishi, H.; Ikeda, Y. *Biomaterials* **1992**, *13*, 113-118. (d) Tezuka,

Y.; Nobe, S.; Shiomi, T. *Macromolecules* **1995**, *28*, 8251-8258. (e) Pitsikaris, M.; Woodward, J.; Mays, J. W.; Hadjichristidis, N. *Macromolecules* **1997**, *30*, 5384-5389. (f) Mousanda, B. *Polymer* **1997**, *38*, 5301-5306.

(23) (a) Klein, J.; Kumacheva, E.; Mahalu, D.; Pherahia, D. *Macromol. Symp.* **1995**, *98*, 1149-1158. (b) Klein, J.; Kumacheva, E.; Mahalu, D.; Perahia, D.; Fetters, L. J. *Nature* **1994**, *370*, 634-636. (c) Klein, J.; Kumacheva, E.; Perahia, D.; Mahalu, D.; Warburg, S. *Faraday Disc*. **1994**, *98*, 173-188. (d) Luckham, P. F.; Manimaaran, S. *Adv. Colloid Interface Sci*. **1997**, *73*, 1-46.

(24) Klein, J. *Ann. Rev. Mat. Sci.* **1996**, *26*, 581-612.

(25) (a) Prucker, O.; Rühe, J. *Macromolecules* **1998**, *31*, 592-601. (b) Prucker, O.; Rühe, J. *Macromolecules* **1998**, *31*, 602-613.

(26) (a) Zhao, B.; Brittain, W. J. *Macromolecules* **1998**, *31*, 592-601. (b) Jordan, R.; Ulman, A.; Rafailovick, M. H.; Sokolov, J. *J. Am. Chem. Soc.* **1999**, *121*, 1016-1022. (c) Advincula, R.; Zhou, Q. G.; Park, M.; Wang, S. G.; Mays, J.; Sakellariou, G.; Pispas, S.; Hadjichristidis, N. *Langmuir* **2002**, *18*, 8672-8684

(27) (a) Kim, N. Y.; Jeon, N. L.; Choi, I. S.; Takami, S.; Harada, Y.; Finnie, K. R.; Girolami, G. S; Nuzzo, R. G.; Whitesides, G. M.; Laibinis, P. E. *Macromolecules* **2000**, *33*, 2793-2795. (b) Juang, A.; Scherman, O. A.; Grubbs, R. H.; Lewis, N. S. *Langmuir* **2001**, *17*, 1321-1323. (c) Moon, J. H.; Swager, T. M. *Macromolecules* **2002**, *35*, 6086-6089.

(28) (a) Husseman, M.; Malmström, E. E.; McNamara, M.; Mate, M.; Mecerreyes, D.; Benoit, D. G.; Hedrick, J. L.; Mansky, P.; Huang, E.; Russel, T. P.; Hawker, C. J. *Macromolecules* **1999**, *32*, 1424-1431. (b) Shah, R. R.; Mecerreyes, D.; Husseman, M.; Rees, I.; Abbott, N. L.; Hawker, C. J.; Hedrick, J. L. *Macromolecules*. **2000** *33*, 597-605. (c) Devaux, C.; Chapel, J. P.; Beyou, E.; Chaumont, P. *Eur. Phys. J. E* **2002**, *7*, 345-352.

(29) (a) Ejaz, M.; Yamamoto, S.; Ohno, K.; Tsujii, Y.; Fukuda, T. *Macromolecules* **1998**, *31*, 5934-5936. (b) Huang, W. X.; Wirth, M. J. *Macromolecules* **1999**, *32*, 1694-1696. (c) Matyjaszewski, K.; Miller, P. J.; Shukla, N.; Immaraporn, B.; Gelman, A.; Luokala, B.B.;

Siclovan, T. M.; Kickelbick, G.; Vallant, T.; Hoffmann, H.; Pakula, T. *Macromolecules* **1999**, *32*, 8716-8724. (d) Xiao, D. Q.; Wirth, M. J. *Macromolecules* **2002**, *35*, 2919-2925. (f) Jeyaprakash, J. D.; Samuel, S.; Dhamodharan, R.; Rühe, J. *Macromol. Rap. Comm.* **2002**, *23*, 612-616. (g) Ramakrishnan, A.; Dhamodharan, R.; Rühe, J. *Macromol. Rap. Comm.* **2002**, *23*, 612-616. (h) Parvole, J.; Laruelle, G.; Guimon, C.; Francois, J.; Billon, L. *Macromol. Rap. Comm.* **2003**, *107*, 10198-10205. (i) Yu, W. H.; Kang, E. T.; Neoh, K. G.; Zhu, S. P. *J. Phys. Chem. B* **2003**, *107*, 10198-10205. (j) Kim, J. -B.; Bruening, M. L.; Baker, G. L. *J. Am. Chem. Soc.* **2000**, *122*, 7616-7617. (k) Kim, J. -B.; Huang, W. X.; Miller, M. D.; Baker, G. L.; Bruening, M. L. *J. Polym. Sci. Part A: Polym. Chem.* **2003**, *41*, 386-394. (l) Huang, W.; Kim, J. -B.; Bruening, M. L.; Baker, G. L. *Macromolecules* **2002**, *35*, 1175-1179. (m) Jones, D. M.; Brown, A. A.; Huck, W. T. S. *Langmuir* **2002**, *18*, 1265-1269. (n) Desai, S. M.; Solanky, S. S.; Mandale, A. B.; Rathore, K.; Singh, R. P. *Polymer* **2003**, *44*, 7645-7649.

(30) (a) Baum, M.; Brittain, W. J. *Macromolecules* **2002**, *35*, 610-615. (b) Zhai, G.; Yu, W. H.; Kang, E. T.; Neoh, K. G.; Huang, C. C.; Liaw, D. J. *Indust. Eng. Chem. Res.* **2004**, *43*, 1673-1680. (c) Tsujii, Y.; Ejaz, M.; Sato, K.; Goto, A.; Fukuda, T. *Macromolecules* **2001**, *34*, 8872-8878.

(31) (a) Yamago, S.; Lida, K.; Yoshida, J. *J. Am. Chem. Soc.* **2002**, *124*, 13666-13667. (b) Yamago, S.; Iida, K.; Nakajima, M.; Yoshida, J. *Macromolecules* **2003**, *36*, 3793-3796. (c) Yamago, S. *Chem. Rev.* **2009**, *109*, 5051-5068. (d) Yamago, S.; Ukai, Y.; Matsumoto, A.; Nakamura, Y. *J. Am. Chem. Soc.* **2009**, *131*, 2100-2101.

(32) (a) Goto, A.; Zushi, H.; Hirai, N.; Wakada, T.; Tsujii, Y.; Fukuda, T. *J. Am. Chem. Soc.* **2007**, *129*, 13347-13354. (b) Goto, A.; Tsujii, Y.; Fukuda, T. *Polymer* **2008**, 49, 5177-5185. (c) Goto, A.; Wakada, T.; Fukuda, T.; Tsujii, Y. *Macromol. Chem. Phys.* **2010**, *211*, 594-600. (d) Goto, A.; Hirai, N.; Nagasawa, K.; Tsujii, Y.; Fukuda, T.; Kaji, H. *Macromolecules* **2010**, *43*, 7971-7978.

(33) (a) Israelachvili, J. N. *Intermolecular and Surface Forces, Second Edition.*; Academic Press: London, 1992. (b) Halperin, A.; Tirrell, M.; Lodge, T. P. *Adv. Polym. Sci.* **1992**, *100*, 31-71. (c) Kawaguchi, M.; Takahashi, A. *Adv. Colloid. Interface Sci.* **1992**, *37*, 219-317.

(34) (a) Taunton, H. J.; Toprakcioglu, C.; Fetters, L. J.; Klein, J. *Macromolecules* **1990**, *23*, 571-580. (b) Courvoisier, A.; Isel, R.; Francois, J.; Maaloum, M. *Langmuir* **1998**, *14*, 3727-3729. (c) Satija, S. K.; Majkrzak, C. F.; Russell, T. P.; Sinha, S. K.; Sirota, E. B.; Hughes, G. J. *Macromolecules* **1990**, *23*, 3860-3864. (d) Levicky, R.; Koneripalli, N.; Tirrell, M.; Satija, G. J. *Macromolecules* **1998**, *31*, 3731-3734. (e) Cosgrove, T.; Heath, T. G.; Phipps, J. S.; Richardson, R. M. *Macromolecules* **1991**, *24*, 94-98. (f) Field, J. B.; Toprakcioglu, C.; Ball, R. C.; Stanley, H. B.; Dai, L.; Barford, W.; Penfold, J.; Smith, G.; Hamilton, W. *Macromolecules* **1992**, *25*, 434-439. (g) Anastassopoulos, D. L.; Vradis, A. A.; Toprakcioglu, C.; Smith, G. S.; Dai, L. *Macromolecules* **1998**, *31*, 9369-9371.

(35) (a) Shim, D. F. K.; Cates, M. E. *J. Phys. (France)* **1989**, *50*, 3535-3551. (b) Lai, P. Y.; Halperin, A. *Macromolecules* **1991**, *24*, 4981-4982.

(36) (a) Yamamoto, S.; Ejaz, M.; Tsujii, Y.; Matsumoto, M.; Fukuda, T. *Macromolecules* **2000**, *33*, 5602-5607. (b) Yamamoto, S.; Ejaz, M.; Tsujii, Y.; Fukuda, T. *Macromolecules* **2000**, *33*, 5608-5612.

(37) (a) Tsujii, Y.; Okayasu, K.; Ohno, K.; Fukuda, T. *Polym. Prep. (Am. Chem. Soc., DiV. Polym. Chem.)* **2005**, *46* (2), 85-86. (b) Tsujii, Y.; Nomura, A.; Okayasu, K.; Gao, W.; Fukuda, T. *J. Phys.: Conference Series* **2009**, *184*, 012031.

Chapter 2

Lubrication Mechanism of Concentrated Polymer Brushes in Solvents: Effect of Solvent Quality and Thereby Swelling State

2-1. Introduction

The friction/lubrication property of polymer-coated surfaces is an important characteristic in many areas of science and technology.[1] Polymer brushes, in particular, have been extensively studied because of their efficiency at modifying the equilibria and dynamic properties of surfaces.[2] In solvents, they have been shown to be efficient lubricants by forming layers at moderate shear velocities and loads.[2f-h] Previously, well-defined polymer brushes were prepared using end-functionalized polymers or block copolymers with the terminal group or one of the blocks selectively adsorbed onto a surface. These systems possess rather low graft densities of typically 0.001 - 0.05 chains/nm^2, corresponding to the regime of "semi-dilute polymer brush (SDPB)", which limits their practical application requiring a brush layer thick enough to hold a wide range of pressure and shear velocity.

Densely grafting well-defined polymers on various kinds of materials including inorganic substrates was achieved using the living radical polymerization technique.[3] The graft density of thus obtained polymer brushes was about an order of magnitude higher than those of typical SDPBs, penetrating deep into the regime of "concentrated polymer brush (CPB)", which had been little explored systematically because of the unavailability of such brush samples. Recent studies revealed that these CPBs have structures and properties quite different and even unpredictable from those of SDPBs: most strikingly, the CPBs of poly (methyl methacrylate) (PMMA) swollen in a good solvent (toluene) exhibit equilibrium film thicknesses as large as 80% - 90% of the full (contour) length of the graft chains.[4] More interestingly, the microtribological analysis using an atomic force microscope

(AFM) revealed that in a good solvent, the CPBs of PMMA exhibit super lubrication with an extremely low frictional coefficient ($\mu \sim 10^{-4}$) for any applied load.[5] Other examples of polymer brushes with excellent lubrication properties have been reported for the SDPBs of polyelectrolyte and for a polyzwitterionic brush (whose graft density was not reported).[2f] The excellent water-lubrication characteristics were ascribed to the osmotic pressure of counter ion and the strong hydration of charged groups. By contrast, the super lubrication observed for the swollen CPBs of PMMA was previously attributed to the strong resistance of CPBs against mixing with each other: that is, confronted CPBs (of the same kind) do not mix with each other at high compression. This new mechanism was expected to be common to CPB/good solvent systems.

Parallel to the friction studies of CPBs, Kobayashi et al. studied the tribological properties of densely grafted polymer brushes of various polymers using a tribometer with a probe ball 5 mm in diameter.[6] They revealed lower frictional forces and improved wear resistance as compared with the corresponding spin-cast polymer film. The frictional coefficient μ for these systems was not of the same value reported above; the discrepancy may be attributed to the different experimental conditions employed. Microtribological measurements are suitable for revealing the intrinsic friction/lubrication properties of solvent-swollen polymer brushes with, for example, sub-micron thickness.

As mentioned above, CPB successfully achieved super lubrication. The solvent-swollen polymer brush can be regarded as a thin lubricating layer. Concerning the fluid character of the brush layers, the thickness and viscosity of the lubricating layer and the shear velocity should affect the frictional/lubrication property.[7] However, these effects warrant further investigation. In this work, AFM-microtribological studies were carried out on well-defined CPBs of polystyrene (PS) under varying degrees of swelling, which was precisely controlled by changing the composition of good/non-solvent mixtures. The lubrication mechanism of CPBs is discussed in detail in terms of

hydrodynamic and boundary lubrications.

2-2. Experimental Section

2-2-1. Materials

Styrene (99%, Nacalai Tesque, Inc., Japan) was passed through a column of basic alumina to remove inhibitors. Cu(I)Br (99.9%, Wako Pure Chemical Ind., Ltd., Japan), ethyl 2-bromoisobutylate (EBIB, 99%, Wako), and 4,4'-dinonyl-2,2'-bipyridine (dNbipy, 97%, Aldrich) were used as received. (2-bromo-2-methyl) propionyloxyhexyltriethoxysilane (BHE, a fixable initiator for ATRP) was prepared as previously reported.[8] All other reagents were obtained from commercial source and used as received.

A silicon wafer (Ferrotec Corp., Japan, one side chemicaly/mechanicaly polished, 525 μm thickness) was cleaned by ultrasonication in $CHCl_3$ for 15 min and ultraviolet (UV) / ozone treatment for 10 min before fixation of BHE. A silica particle (SiP, HIPRESICA SP, radius R of 5 μm) used as a probe for the AFM measurement was obtained from Ube Nitto Kasei Co., Ltd., Japan.

2-2-2. Synthesis of Concentrated PS Brushes via Surface-Initiated ATRP

Well-defined CPBs of PS were prepared by surface-initiated ATRP. To immobilize the surface initiator, BHE, a silicon wafer was immersed in an ethanol solution containing BHE (1 wt%) and 28%-aqueous ammonium (5 wt%) for 12 h at room temperature, copiously rinsed with ethanol, and then dried. The BHE-immobilized silicon wafer was subjected to graft polymerization at 110^{o}C for 2 h in a styrene solution containing Cu(I)Br (87 mM), dNbipy (170 mM), and EBIB (8.7 mM) under argon atmosphere. EBIB was added as a free initiator not only to control the polymerization by the so-called persistent radical effect but also to yield free polymers, which are useful as a measure of the molecular weight M_n and molecular weight distribution M_w/M_n of the graft chains.[3] Good agreement in M_n and M_w/M_n between the graft and free polymers has been reported by several research groups.[9] After polymerization, the substrate was rinsed in a Soxhlet extractor with toluene

Table 2-1. Characteristics of PS-Brush Samples

Sample	M_n	M_w/M_n	L_d /nm	σ /chains nm^{-2}	σ*
1	34,000	1.29	25	0.46	0.30
2	38,000	1.19	26	0.44	0.29
3	37,000	1.27	29	0.49	0.32
probe	33,000	1.17	-	-	-

for 8 h to remove physisorbed polymers and impurities. The thickness L_d of the polymer layer in a dry state was determined by ellipsometry (M-2000U, J.A. Woolam, Lincoln, NE, USA). The characteristics of the PS brushes are summarized in Table 2-1. The M_n and the M_w/M_n values are those of the free polymer analyzed by gel permeation chromatography (GPC). The graft density σ was calculated from the determined values of M_n and L_d by the following equation $\sigma = \rho L_d N_A/M_n$, where ρ is the bulk density of a PS film (= 1.05 g/cm^3)[10] and N_A is Avogadro constant. As a good measure of graft density for various kinds of polymer brushes, the surface occupancy, σ*, was defined as $\sigma^* = s_c \sigma$, where s_c is the cross-sectional area per monomer unit given by $s_c = v_0/l_0$ with v_0 being the molecular volume per monomer unit (estimated from bulk density of monomer in this case) and l_0 being the chain length per monomer unit (l_0 = 0.25 nm for vinyl polymers).

The PS brush was also fabricated on the SiP as described above. The SiP was dispersed by 0.5 wt% in the BHE solution, magnetically stirred for 12 h at room temperature, and then solvent-exchanged to styrene, to afford a 0.5 wt%-SiP dispersion that was then subjected to ATRP of styrene. Finally, the PS-grafted SiP was copiously washed with chloroform.

2-2-3. AFM Measurements

The degree of swelling of a polymer brush in a solvent was estimated by force measurements and scratched groom imaging on an AFM (Seiko Instruments Inc., Japan, SPI3800 controller with SPA400 unit). This procedure has been described in detail elsewhere.[4] A V-shaped cantilever

OMCL-TR800 (Olympus Corp., Japan, normal spring constant k_n = 0.15 N/m) was used with a bare (unmodified) SiP probe attached using a two-component epoxy-resin adhesive. The R of the probe particle was 5.0 μm, much larger than the size of graft layer so that the graft chains could be viewed as being compressed by a flat surface. A liquid cell was used for the measurement in mixtures of toluene and 2-propanol with different compositions (f_{TOL}, volume fraction of toluene). The mixed solvents were filtered through a cellulose porous membrane (Whatman, diameter 0.1 μm) before use. The normal displacement Δz of the cantilever was monitored as a function of separation in approaching/retracting modes; typically, an approaching/retracting speed of 80 nm/s, and at least 8 force curves were taken at different locations. The interaction force, i.e., the normal force, F_n, was estimated as follows,

$$F_n = k_n \cdot \Delta z = k_n \cdot (DIF \cdot S_{DIF}) \quad (2\text{-}1)$$

where DIF (V) and S_{DIF} (m/V) are the signal intensity and sensitivity of the vertical deflection, respectively. The latter value was determined for each force curve in the so-called constant-compliance region where the cantilever deflection increased linearly with decreasing separations. The AFM raw data of cantilever deflection vs displacement were converted into F_n as a function of separation D' according to the principle of Ducker et al.[11] The separation D' is not the distance from the substrate but that from the constant-compliance region. In a system with a dense polymer layer, the distance between D' = 0 plane and the substrate surface, which is called as "offset distance D_0", can be very large. The offset distance D_0 was measured by AFM-imaging under a constant force mode by applying the force corresponding to the constant compliance region in the force measurements. The true distance D between the surfaces of the substrate and the probe sphere was defined as $D = D' + D_0$. The determination of D_0 and hence D in each solvent condition gives the equilibrium thickness L_e of the brushes in solvent, where L_e is the critical true distance at a repulsive force onset (0.05 nN was employed as onset value of F_n).

The frictional measurement was performed by the so-called force-curve method. The same procedures outlined above were employed unless otherwise stated. The PS-brush-grafted SiP was mounted on a rectangular-shaped cantilever OMCL-RC800 (Olympus, k_n = 0.1 N/m) for the friction measurement. The lateral displacement Δx as well as Δz of the cantilever were simultaneously monitored in approaching/retracting modes, while the substrate was slid back and forth in the horizontal plane normal to the cantilever by applying a triangular-wave oscillation on a piezo actuator via a function generator (Wave Factory 1945, NF Corp, Japan). The normal and frictional forces (F_n and F_s) were evaluated according to Equations (2-1) and (2-2), respectively.

$$F_s = k_s \Delta x = k_s \cdot (\mathrm{FFM} \cdot S_{\mathrm{FFM}}) \quad (2\text{-}2)$$

where k_s, FFM (V) and S_{FFM} (m/V) are the torsional spring constant of the cantilever, the signal intensity and sensitivity of the torsional deflection, respectively. The torsional-deflection sensitivity was estimated from S_{DIF} by correcting the difference in geometry of the reflected-light path (L/2R) and amplification factor of the detectors, where L is the cantilever length.[12] The k_s was calculated to be 23 N/m using the following equation,[13]

$$k_s = GWT^3/3L \quad (2\text{-}3)$$

where G, W, T are the shear modulus, width, and thickness of the cantilever, respectively. For some selected levers, the commercially reported k_n and above calculated k_s values were experimentally found to have an error of 10% and 20%, respectively, by the resonant technique.[14] The observed signal proportional to Δx was modulated by the reciprocal motion. Thus, the signal was processed through a high-pass filter (Multi-function filter 3611, NF Corp., Japan) to remove a lower-frequency component, which is mainly caused by vertical deflection of the cantilever, and finally converted to the FFM data as the root-mean-square value with AC-volt meter (M2170, NF Corp, Japan). Typically, the approaching/retracting speed and the distance of shearing was set to be 27 nm/s and 1 μm, respectively, and 4 force curves were recorded and averaged at different locations for each

measurement. The shear velocity v (4 ~ 1000 μm/s) was changed by adjusting the oscillating frequency (2 ~ 500 Hz). The distance of shearing was calibrated by AFM-observations of the scratched trace on a bare silicon wafer with a harder cantilever OMCL-AC160TS (Olympus, k_n = 42 N/m).

The F_s was also measured by the so-called "frictional-loop" method, in which the torsion of the cantilever was monitored during repeated reciprocal/lateral movement of the piezo with a constant F_n. The distance of shearing was 5 μm, and the shear velocity (4 ~ 1000 μm/s) was changed by adjusting the shearing frequency (0.4 ~ 100 Hz).

The frictional coefficient was defined as $\mu = F_s/F_n$.

2-3. Results and Discussion

2-3-1. Swelling in Mixed Solvents

Scaling theoretical analysis predicted that the L_e of polymer brushes in good solvent varies with $L_e \propto L_c \sigma^{*\alpha'}$, where L_c is the contour length of the graft chain and the α' value is 1/3 [15] and 1/2 [16] for SDPB and CPB, respectively. The L_e as a function of graft density for the brushes of PMMA in good solvent was measured using, e. g., a combinatorial method and the crossover density between SDPB and CPB was determined to be around 0.1 for σ*. Figure 2-1 shows the plot of $L_e / L_{c,w}$ vs σ* in logarithmic scale, where $L_{c,w}$ is the contour length of the graft chain calculated from the M_w value. In this figure, the data for various kinds of polymer brushes including the CPB of PMMA previously studied in toluene were also plotted. The present samples had a σ* value sufficiently higher than the above-mentioned criterion, and the graft chains were highly stretched, similarly to the previous results of CPB of PMMA in a good solvent. Thus the prepared samples can be justifiably categorized as belonging to the CPB regime.

Figure 2-2 shows the force curves of the CPB of PS against the bare SiP probe in solvents with

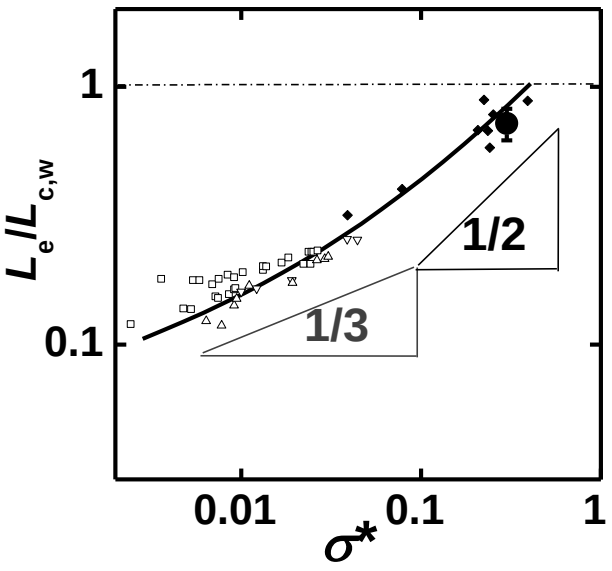

Figure 2-1. Plot of degree of stretching $L_e/L_{c,w}$ vs dimensionless graft density σ* of the PS brush (Sample 1) in toluene (●). Other symbols reprocessed from the reference 4(b) show the data for some other polymer brushes in good solvents including the CPB of PMMA in toluene (small closed symbols).

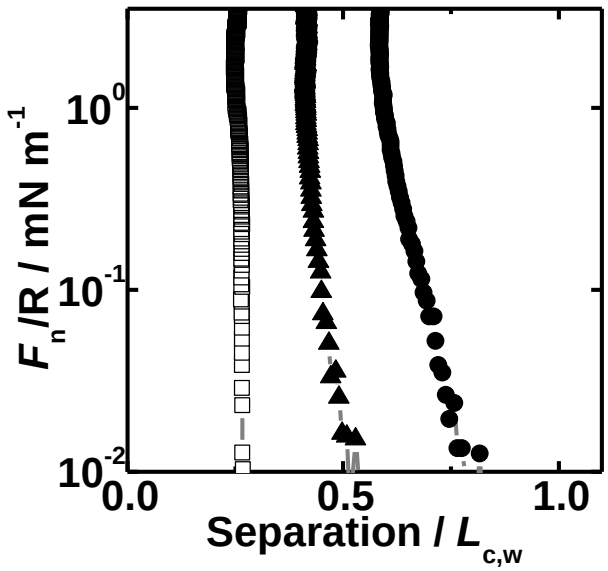

Figure 2-2. Force curves of the PS brush (Sample 1) measured in toluene/2-propanol-mixed solvents with different compositions; f_{TOL}=0.0 (□), 0.5 (▲) 1.0 (●). The bare SiP (R = 5 μm) mounted on triangular-shaped cantilever was used as a probe.

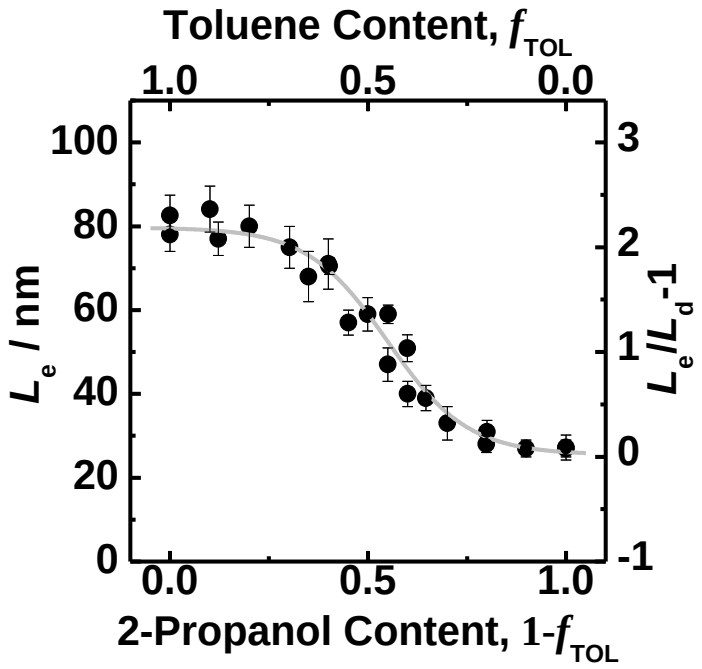

Figure 2-3. Plots of equilibrium thickness L_e and swelling ratio L_e/L_d -1 of the PS brush (Sample 1) in toluene/2-propanol-mixed solvents. The gray curve is the result fitted with sigmoid function.

f_{TOL} = 1 (pure toluene), 0.5, and 0 (pure 2-propanol). It should be noted that the horizontal axis in this figure was corrected to the true distance D between the surfaces of the base substrate and the probe sphere, thus corresponding to the thickness of the PS-brush layer if F_n is detected. In toluene (at f_{TOL} = 1.0), the equilibrium thickness L_e, defined as the maximum distance with F_n detectable, reached 80% of the $L_{c,w}$. This force curve indicates not only high stretching of chains but also strong resistance against compression as F_n steeply increases. This is one of the most important properties of CPB in good solvents. Figure 2-2 suggests that with decreasing f_{TOL} and hence decreasing the solvent quality, the PS brush increasingly shrank. Details are shown in Figure 2-3 as plots of L_e and L_e/L_d - 1 as a function of f_{TOL}, where the value of L_e/L_d - 1 gives the volume fraction of solvent absorbed in the polymer-brush layer. When f_{TOL} > 0.8, the solvent quality was sufficiently good to promote high extension of the chains of the polymer brushes. When f_{TOL} < 0.2, the PS brush swelled very little. In between these two limits, the degree of swelling gradually decreased with decreasing f_{TOL}. This dependency can be rationalized by taking account of mixing and conformational

entropies; the former causes brush swelling by osmotic pressure and the latter is responsible for the elastic stress. These two forces are balanced in equilibrium of swelling. The saturated degree of swelling can presumably be attributed to an rapid increase in conformational entropy (and hence extension stress) when the graft chain extends to almost full length.

2-3-2. Frictional Property and Mechanism in Mixed Solvents

Figures 2-4a and 2-4b show the F_s and μ values of the CPBs of PS against F_n at υ = 10 μm/s in solvents with f_{TOL} = 1.0 and 0.4, respectively. At f_{TOL} = 1.0 (Figure 2-4a), F_s is almost proportional to F_n, giving an almost constant value of $\mu = 2\times10^{-4}$, close to the value previously reported for the CPBs of PMMA.[5] At f_{TOL} = 0.4 (Figure 2-4b), the F_s linearly but not proportionally increased and hence the μ value gradually decreased with increasing F_n. As previously indicated,[17] one of reasons for this is an adhesion force acting as an additional normal force; friction is caused by this adhesion force even when the applied normal force is zero. As plotted by open symbols in Figure 2-4b, an almost constant μ value was obtained in this friction study when the sum of the applied force and the adhesion force was used as F_n to calculate the μ value. In the following section, the author will

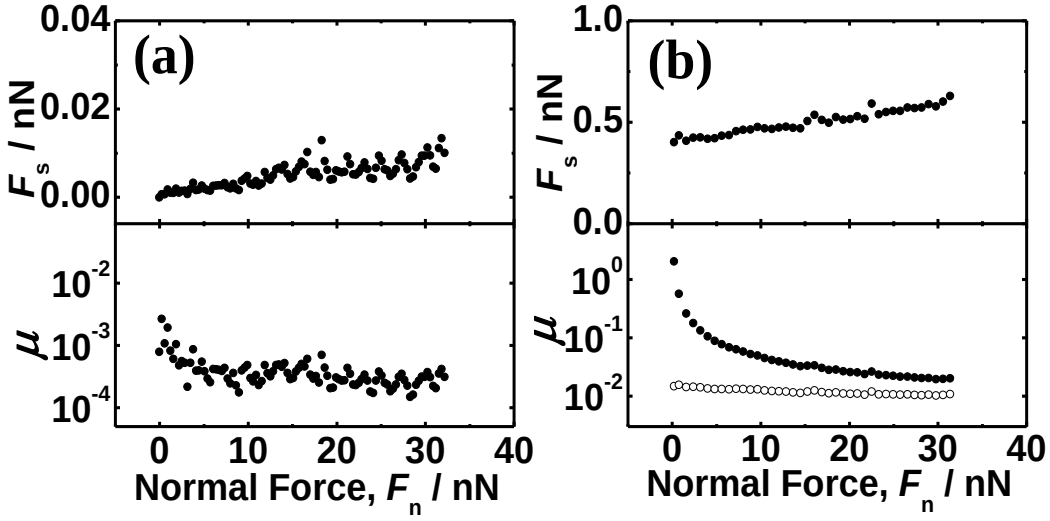

Figure 2-4. Plots of frictional force F_s and frictional coefficient μ (= F_s/F_n) vs normal force F_n measured at a shear velocity υ of 7 μm/s between the PS brushes (samples 2 and 3 against PS-brush modified particle) in solvents with (a) f_{TOL} = 1.0 and (b) f_{TOL} = 0.4. In Figure 2-4 (b), the frictional coefficient corrected with adhesion force as $\mu = F_s/(F_n$ +adhesion force in Figure 2-6) is also plotted (○). The friction force curve method (see experimental section) with PS-grafted SiP mounted on a rectangular-shaped cantilever was used to measure F_s.

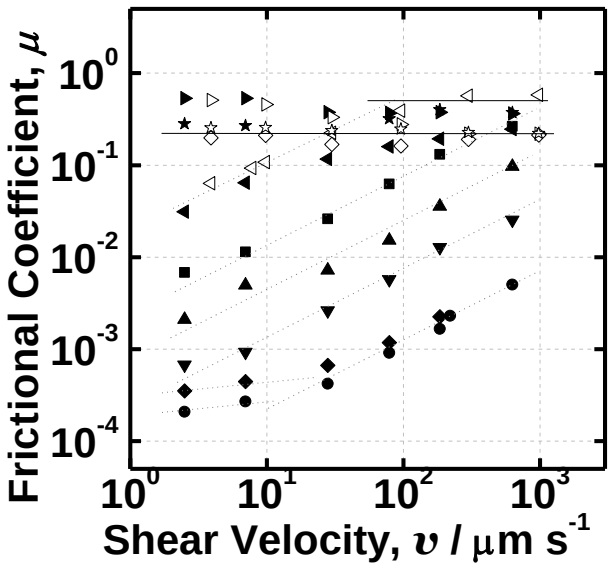

Figure 2-5. Plot of frictional coefficient μ vs shear velocity υ between the PS brushes (sample 2 and 3 against PS-brush modified particle) measured in toluene/2-propanol-mixed solvents at F_n = 20 nN; f_{TOL} = 1.0 (●), 0.7 (◆), 0.6 (▼), 0.5 (▲), 0.4 (■), 0.3 (◀), 0.2 (▶), 0.0 (★) for the force curve method, and 0.3 (◁), 0.2 (▷), 0.1 (◇), 0.0 (☆) for the frictional-loop method (see experimental section). The PS-grafted SiP mounted on a rectangular-shaped cantilever was used as a probe.

estimate the μ value by correcting the adhesion force.

Figure 2-5 shows the plot of μ vs υ in solvents with different values of f_{TOL}. Under good-solvent conditions, i.e., at f_{TOL} = 1.0 and 0.7, μ increased with increasing υ at high regions of υ, seemingly giving a constant slope in the logarithmic plot. In lower regions of υ, the slope decreased with decreasing υ. It is quite interesting that the observed μ value and its corresponding υ are very similar to the results obtained previously for the CPB of PMMA with similar σ* and M_n. Excellent lubrication common to the CPB (regardless of the kind of polymer chain) under good-solvent conditions is well understood by non-interpenetrating interactions as detailed in previous publication.[5] With decreasing f_{TOL} and hence decreasing the solvent quality, μ increased in almost all the υ regions. It is known that the force-curve method might not be able to adequately measure the friction force because the strong adhesion force may cause the probe sticking to a friction surface to prevent shear, especially under poor solvent conditions. Therefore, the author also measured the friction force by the friction-loop method with longer shear length (5 μm). Comparing μ data in

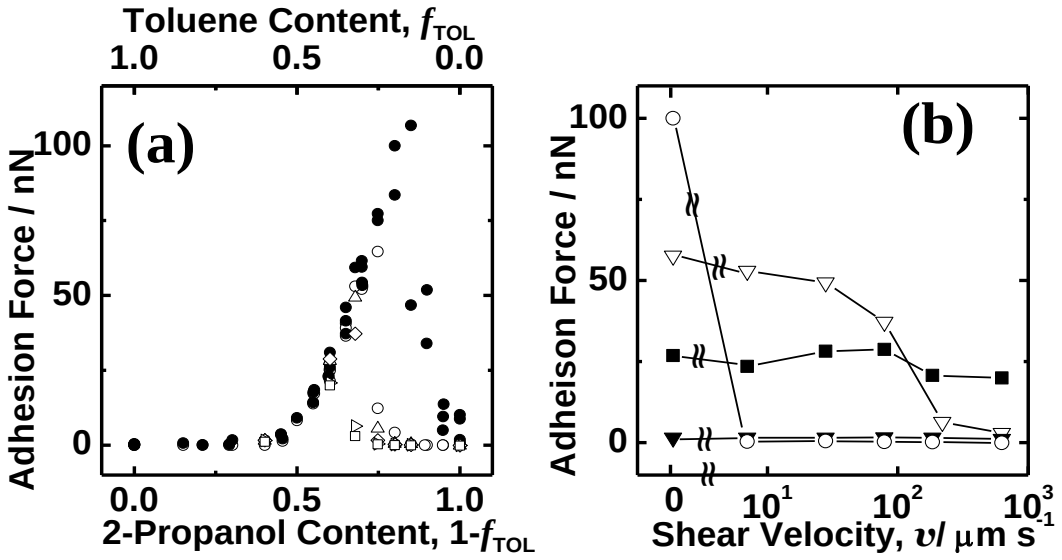

Figure 2-6. Plots of adhesion force between the PS brushes (samples 2 and 3 against PS-brush modified particle) as a function of (a) solvent composition f_{TOL} and (b) shear velocity v in toluene/2-propanol-mixed solvents; (a) v = 1000 (□), 320 (▷), 100 (◇), 32 (△), 10 (○) 0 (●) μm/s, and (b) f_{TOL}=0.6(▼), 0.4(■), 0.3(▽), 0.2(○). The PS-grafted SiP mounted on a rectangular-shaped cantilever was used as a probe.

Figure 2-5, both of these two methods work well to evaluate the friction force correctly with little differences in results. Interestingly, the data can be categorized into two regimes as a function of f_{TOL} and v. One is the v-dependent regime with almost the same slope, and the other has less dependence. The lubrication mechanism for these two regimes can be discussed in terms of the boundary and hydrodynamic lubrications, which were previously proposed for the CPB of PMMA in a good solvent. For the detailed discussion, the author measured the adhesion force as a function of f_{TOL} and v to take account of attractive interaction between the polymer brushes (see Figure 2-6).

2-3-2-1. Boundary Lubrication

Here, the author describe the boundary lubrication regime, in which the load is carried by the physical or chemical properties of confronted surfaces including asperities or adhesiveness rather than those of the lubricant.[18] The previous study on the PMMA brushes in toluene revealed that the degree of interpenetration between graft polymer chains impacts upon the friction;[5] the CPB was demonstrated to have an extremely low value of μ for any applied loads at a low v because the interpenetration was drastically suppressed due to the entropic effect of highly extended polymer

chains. The weak v-dependency was previously reported for a system in which the polymer brushes interpenetrate at a faster rate than the applied shear velocity.[19] In this study, a regime with μ on the order of 10^{-4} and a weak v-dependency was also observed at a low v regions between the CPBs of PS under good-solvent conditions, i.e., at f_{TOL} = 1.0 and 0.7, where the brush had a highly stretched conformation ~80% of the $L_{c,w}$ (as mentioned above) and little adhesion force (see the data plotted by closed symbols in Figure 2-6a).

In addition to these cases, a weak v-dependency was also observed in solvents with f_{TOL} lower than 0.2 (Figure 2-5). The PS-brush layer is in a glassy state and can no longer function as an effective lubricant layer. The small v-dependency of μ may be understood by considering Amonton's law, in which the kinetic frictional force between solid surfaces bears no relation to the shear velocity.[20] Figure 2-3 suggests that under these conditions, the PS brush is less swollen, giving a value of L_e/L_d - 1 (the solvent fraction in the brush) less than 0.1 at f_{TOL} = 0.2 and almost zero at f_{TOL} = 0 (pure 2-propanol, non-solvent). The presence of solvent somehow decreases the glass transition temperature T_g of the polymer due to the reduced barriers for the rotational and transitional motions of chain segments as the described by the following equation,

$$1/T_g = W_1/T_{g1} + W_2/T_{g2} \qquad (2\text{-}4)$$

where W is the weight fraction and the subscripts 1 and 2 refer to the polymer and the diluent, respectively.[21] Using the T_g data of PS (T_{g1}) as 100 ºC [10] and 2-propanol (T_{g2}) as -152 ºC,[22] the T_g of the swollen PS brush layer for W_1 = 0.9 and hence W_2 = 0.1 (at f_{TOL} = 0.2) was estimated to be about 30 ºC, which is approximately the room temperature at which the friction measurements were conducted. This glassy-state brush layer under poor solvent conditions with f_{TOL} lower than 0.2 should result in a loss in lubricant efficiency.

Figure 2-6a suggests that the adhesion force remained at ~0 nN for f_{TOL} > 0.7 and then increased with decreasing f_{TOL}, reaching a maximum and suddenly decreasing at a critical value

$f_{TOL,c}$. The sudden decrease in adhesion force can be attributed to asperities, i.e., decreasing area of contact due to the glass transition of the polymer-brush layer. Interestingly, the adhesion force followed the same f_{TOL} dependency up to its maximum at $f_{TOL,c}$ independent of v (with and without shearing), while the $f_{TOL,c}$ decreased with increasing v. Of course, the glass transition should be time-dependent. This is consistent from the data obtained at f_{TOL} = 0.3 as shown in Figure 2-6b; the adhesion force drastically falls at v = 200 μm/s. This is reflected in the data at f_{TOL} = 0.3 in Figure 2-5, where the μ value increased with increasing v, approaching an almost constant value beyond v = 100 μm/s.

2-3-2-2. Hydrodynamic Lubrication

The author now discusses hydrodynamic lubrication, in which the friction force is determined by the viscosity of solvent rather than the interactions between surfaces. From the viscosity law, the frictional force in hydrodynamic lubrication can be formulated as follows.[23]

$$\mu = \beta \cdot v^{\alpha} \quad (2\text{-}5)$$

where α is the parameter representing the shear-flow distribution in a lubricating layer and β is a function of viscosity and the effective thickness of the lubricating layer. This lubrication mechanism is expected to come into play when the shear velocity exceeds a certain value and the friction caused by boundary lubrication is relatively small. The α parameter is unity for Newtonian fluids but usually much smaller for polymer solutions behaving as non-Newtonian fluids,[23] in which the entanglement of polymer chains hinders uniform shear-flow distribution of solvent molecules. The data in Figure 2-5 except for those in the above-mentioned regime of boundary lubrication behaved in accordance with Equation (2-5). It is notable that the data at different f_{TOL} values ranging from 1.0 to 0.3 can be well fitted by a line with almost the same slope in the double logarithmic plot. An almost constant α value of ca. 0.7 is obtained, even though the degree of swelling changes significantly as shown in Figure 2-3. Another interesting point is that in those cases, the adhesion

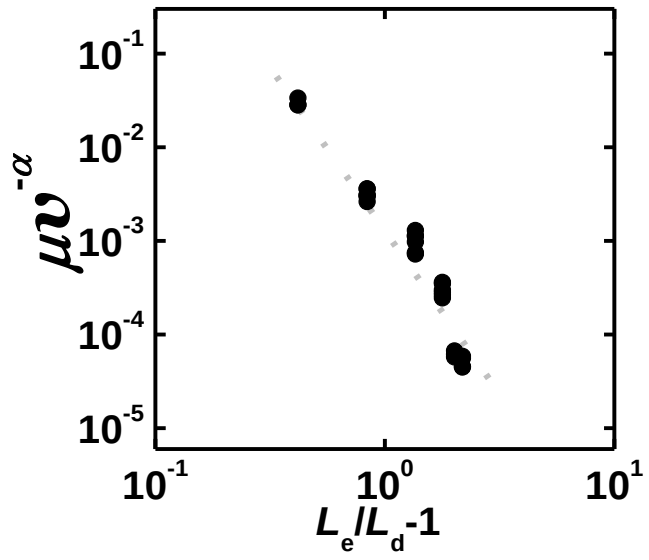

Figure 2-7. Plot of frictional coefficient μ reduced by shear velocity v with parameter α as a function of degree of swelling L_e/L_d-1 for the data in the regime corresponding to hydrodynamic lubrication.

force was detected as shown in Figure 2-6, indicating that the friction caused by this adhesive interaction should be low enough to achieve hydrodynamic lubrication.

The β parameter, corresponding to intercept of the graph in Figure 2-5, increased with decreasing f_{TOL}, as the above-mentioned fitted line shifted to higher values. This can be explained by decreasing degree of swelling. In Figure 2-7, the μ values scaled by $v^{-\alpha}$ (α = 0.7) were replotted in the double logarithmic scale against L_e/L_d-1 as a measure of the degree of swelling. This showed a good linearity, indicating that the β (= $\mu \cdot v^{-\alpha}$) parameter was scaled by the degree of swelling, which should result in increasing viscosity in the brush and its thickness. Further investigations are underway to fully characterize this relationship.

Three types of lubricating layers can be proposed for hydrodynamic lubrication; (a) a pure-solvent layer usually assumed for a system between solid surfaces under high shear conditions, (b) the swollen brush or its outermost part with a certain depth from the surface, and (c) their mixing. As shown in Figure 2-6b, a certain amount of adhesion force was observed between the PS-brush surfaces under reciprocal motion. One may suppose that the interaction around the turning points of

the reciprocating motion is the origin of this adhesion. However, this possibility was ruled out by the measurement of frictional loop, which detailed no enhanced interaction around these points. Thus, the confronted polymer-brush layers interacted with each other even in the regime of hydrodynamic lubrication. In addition to this consideration, the α value was close to unity when compared with the systems containing polymer solutions. This indicates that the hydrodynamically lubricating layer composed by the CPB caused less hindrance to the shear flow of solvent infiltrating into the brush layer. This might be the characteristic features of the lubrication mechanism of the CPB in addition to the ultra-low frictional property. These considerations suggest another method of possible lubrication whereby a pure-solvent layer might be produced between two brush surfaces at much higher shear velocity.

2-4. Conclusions

The friction/lubrication properties of the CPBs of PS in toluene/2-propanol-mixed solvents have been studied using an AFM-colloidal-probe technique. The PS brushes prepared in this study via surface-initiated ATRP were reasonably categorized in the CPB regime, on the basis that the graft density was sufficiently higher than the critical value for the CPB and that the graft chains were highly stretched to almost 80% of the contour length in a good solvent (pure toluene). The degree of swelling of the brush was successfully controlled by varying the solvent composition of toluene/2-propanol mixture.

The μ data as a function of shear velocity and solvent composition (and hence degree of swelling) was divided into two regimes corresponding to different lubrication mechanisms. One is boundary lubrication, in which the chemical or physical property of the outermost surface determines the frictional force. At low shear velocity in toluene-rich solvents, the boundary lubrication mechanism afforded μ values that are less dependent on shear velocity and are

exceptionally small (on the order of 10^{-4}), similar to the previous studies of the CPB of PMMA in toluene. This had been ascribed to effective suppression of interpenetration between polymer brushes. Boundary lubrication was also observed in 2-propanol-rich solvents, where the PS-brush layer was in a glassy state with μ on the order of 0.1 independent of shear velocity.

The second mechanism is hydrodynamic lubrication, in which the viscosity resistance owing to the solvent-swollen polymer brush dominates the friction. This was observed in a wide range of solvent compositions except for those in the glassy state. The data in this regime can be described by the relationship $\mu = \beta \cdot v^{\alpha}$. An almost constant value of $\alpha = 0.7$ was obtained and β depended on the solvent composition and was scaled by the degree of swelling. The measurement of the adhesion force revealed that the confronted polymer brushes interacted with each other in this regime, which is different from the usual hydrodynamic lubrication forming a pure-solvent layer. The CPB in solvents would be an efficient lubricating layer presumably because of its high osmotic pressure. This work allows for the design of friction/lubrication-controlled materials by taking advantage of novel properties of the CPBs.

References

(1) (a) Zhang, S. L.; Tsou, A. H.; Li, J. C. M. *J. Polym. Sci., Part B: Polym. Phys*. **2002**, *40*, 1530-1537. (b) Zappone, B.; Rosenberg, K. J.; Israelachvili. J. *Tribol. Lett.* **2007**, *26*, 191-201. (c) Hutchings, L. R.; Narrianen, A. P.; Thompson, R. L.; Clarke, N.; Ansari, L. *Polym. Int.* **2008**, *57*, 163-170.

(2) (a) Joanny, J. F. *Langmuir* **1992**, *8*, 989-995. (b) Klein, J.; Kumacheva, E.; Perahia, D.; Mahalu, D.; Warburg, S. *Faraday Discuss.* **1994**, *98*, 173-188. (c) Grest, G. S. *Curr. Opin. Coll. Interface Sci*. **1997**, *2*, 271-277. (d) Ndoni, S.; Jannasch, P.; Larsen, N. B.; Almdal, K. *Langmuir* **1999**, *15*, 3895-3865. (e) Klein, J.; Kumacheva, E.; Mahalu, D.; Perahia, D.; Fetters, L. J. *Nature* **1994**, *370*, 634-636. (f) Raviv, U.; Giasson, S.; Kampf, N.; Gohy, J. F.; Jerome, R.; Klein, J. *Nature* **2003**, *425*, 163-165. (g) Muller, M.; Lee, S.; Spikes, H. A.; Spencer, N. D. *Tribol. Lett.* **2003**, *15*, 395-405. (h) Yan, X. P.; Perry, S. S.; Spencer, N. D.; Pasche, S.; De Paul, S. M.; Textor. M.; Lim, M. S. *Langmuir* **2004**, *20*, 423-428.

(3) (a) Edmondson, S.; Osborne, V. L.; Huck, W. T. S. *Chem. Soc. Rev.* **2004**, *33*, 14-22. (b) Tsujii, Y.; Ohno, K.; Yamamoto, S.; Goto, A.; Fukuda, T. *Adv. Polym. Sci.* **2006**, *197*, 1-45. (c) Barbey, R.; Lavanant, L.; Paripovic, D.; Schuwer, N.; Sugnaux, C.; Tugulu, S.; Klok, H. A. *Chem. Rev.* **2009**, *109*, 5437-5527.

(4) (a) Yamamoto, S.; Ejaz, M.; Tsujii, Y.; Matsumoto, M.; Fukuda, T. *Macromolecules* **2000**, *33*, 5602-5607. (b) Yamamoto, S.; Ejaz, M.; Tsujii, Y.; Fukuda, T. *Macromolecules* **2000**, *33*, 5608-5612.

(5) Tsujii, Y.; Okayasu, K.; Nomura, A.; Ohno, K.; Fukuda, T. *submitted*.

(6) (a) Sakata, H.; Kobayashi, M.; Otsuka, H.; Takahara, A. *Polym. J.* **2005**, *37*, 767-775. (b) Kobayashi, M.; Terayama, Y.; Hosaka, N.; Kaido, M.; Suzuki, A.; Yamada, N.; Torikai, N.; Ishihara, K.; Takahara, A. *Soft Matter* **2007**, *3*, 740-746. (c) Kobayashi, M.; Takahara, A. *Chem.*

Rec. **2010**, *10*, 208-216. (d) Ishikawa, T.; Kobayashi, M.; Takahara, A. *ACS Appl. Mater. Interfaces* **2010**, *2*, 1120-1128.

(7) Bhushan, B. *Introduction to Tribology*; John Wiley & Sons Inc: New York, 2002.

(8) Ohno, K.; Morinaga, T.; Koh, K.; Tsujii, Y.; Fukuda, T. *Macromolecules* **2005**, *38*, 2137-2142.

(9) (a) Husseman, M.; Malmstrom, E. E.; McNamara, M.; Mate, M.; Mecerreyes, D.; Benoit, D. G.; Hedrick, J. L.; Mansky, P.; Huang, E.; Russell, T. P.; Hawker, C. J. *Macromolecules* **1999**, *32*, 1424-1431. (b) Von Werne, T.; Patten, T. E. *J. Am. Chem. Soc*. **1999**, *121*, 7409-7410. (c) Pyun, J.; Jia, S.; Kowalewski, T.; Patterson, G. D.; Matyjaszewski, K. *Macromolecules* **2003**, *36*, 5094-5104. (d) Blomberg, S.; Ostberg, S.; Harth, E.; Bosman, A. W.; Van Hor, B.; Hawker, C. J. *J. Polym. Sci., Part A: Polym. Sci.* **2002**, *40*, 1309-1320. (e) Tsujii, Y.; Ejaz, M.; Sato, K.; Goto, A.; Fukuda, T. *Macromolecules* **2001**, *34*, 8872-8878. (f) Morinaga, T.; Ohkura, M.; Ohno, K.; Tsujii, Y.; Fukuda, T. *Macromolecules* **2007**, *40*, 1159-1164.

(10) Brandrup, J.; Immergut, E. H.; Grulke, E. A., Eds.; *Polymer Handbook*; John Wiley & Sons Inc: New York, 1999.

(11) Ducker, W. A.; Senden, T. J.; Pashley, R. M. *Langmuir* **1992**, *8*, 1831-1836.

(12) Ogletree, D. F.; Carpick, R. W.; Salmeron, M. *Rev. Sci. Intrum*. **1996**, *67*, 3298-3306.

(13) Meyer, G.; Amer, N. M. *Appl. Phys. Lett.* **1990**, *57*, 2089-2091.

(14) Green, C. P.; Lioe, H.; Cleveland, J. P.; Proksch R.; Mulvaney, P.; Sader, J. E. *Rev. Sci. Inst.* **2004**, *75*, 1988-1966.

(15) (a) Taunton, H. J.; Toprakcioglu, C.; Fetters, L. J.; Klein, J. *Macromolecules* **1990**, *23*, 571-580. (b) Courvoisier, A.; Isel, F.; Francois, J.; Maaloum, M. *Langmuir* **1998**, *14*, 3727-3729.

(16) (a) Oshea, S. J.; Welland. M. E.; Rayment, T. *Langmuir* **1993**, *9*, 1826-1835. (b) Shim, D. F. K.; Cates, M. E. *J. Phys. (Paris)* **1989**, *50*, 3535-3551.

(17) Butt, H. J.; Kappl, M. *Surface and Interfacial Forces*; Wiley-VCH: Weinheim, 2006.

(18) (a) Kaneko, D.; Oshikawa, M.; Yamaguchi, T.; Gong, J. P.; Doi, M. *J. Phys. Soc. Jpn.* **2007**, *76*, 043601. (b) Wang, W. Z.; Hu, Y. Z.; Liu, Y. C.; Wang, H. *Tribol. Int.* **2007**, *40*, 687-693.

(19) Tadmor, R.; Janik, J.; Klein, J.; Fetters, L. J. *Phys. Rev. Lett.* **2003**, *91*, 115503.

(20) Amonton, G. *Mem. del'Academie Royale A* **1699**, 275-282.

(21) (a) Fox, T. G. *Bull. Am. Phys. Soc.* **1956**, *1*, 123. (b) Nielson, L. E. *Mechanical Properties of Polymers*; Reinhold: New York, 1962. (c) Sung, Y. K.; Gregonis, D. E.; Russell, G. A.; Andrade, J. D. *Polymer* **1978**, *19*, 1362-1363.

(22) Faucher, J. A.; Koleske, J. V. *Phys. Chem. Glasses* **1966**, *7*, 202.

(23) Barnes, H. A.; Hutton, J. F.; Walters, K. *An Introduction to Rheology*; Elsevier: Amsterdam, 1989.

Chapter 3

Lubrication Mechanism of Concentrated Polymer Brushes in Solvents: Effect of Solvent Viscosity

3-1. Introduction

The suppression of interpenetration and hence the decrease of friction in the boundary lubrication regime manifested the other mechanism of lubrication even at high loads, that is hydrodynamic lubrication. In this regime, the viscosity resistance between and/or in the solvent-swollen polymer brushes dominates the friction, giving v-dependency on μ. In Chapter 2, the author studied the CPB of PS in a mixture of good/non solvents in which the solvent quality was controlled. It was demonstrated that under the hydrodynamic lubrication regime, the confronted polymer brushes still had some interaction and that the frictional property could be scaled by the degree of swelling. This is a new mechanism characteristic to the CPB, in contrast to the usual hydrodynamic lubrication forming a pure-solvent layer. It may be expected that the hydrodynamic lubrication will be affected by viscosity and brush height concurrently. In order to test this assumption and also to clarify the mechanism of hydrodynamic lubrication for the CPB, the author will investigate the frictional property of the CPB of PMMA in ionic liquids (ILs) which have higher viscosities than typical organic solvents such as toluene.

Recently, ILs have attracted much attention as green solvents because of their characteristic properties such as nonvolatility, noncombustibility, wide solvent-temperature ranges, and electrochemical stability.[1] ILs can dissolve various kinds of chemical additives, including some polymers, by suitably designing the molecular structure of anionic and cationic species.[2] ILs usually have higher viscosities than general organic solvents of equivalent molecular weight because of

enhanced intermolecular interaction.[3] It has been reported that some organic solvents affect the clustering of IL molecules, so much so that a dramatic decreasing in the viscosity can be observed by the addition of a small amount of the solvent.[4] In recent years, efforts have been made to employ ILs as lubricants especially at a high temperatures and/or under vacuum.[5] Under these conditions, the evaporation of organic solvents is problematic.

Figure 3-1 shows the chemical structures of the ILs studied, *N*,*N*-diethyl-*N*-methyl-*N*-(2-methoxyethyl)ammonium bis(trifluoromethanesulfonyl)imide (DEME-TFSI) and 1-ethyl-3-methylimidazolium bis(trifluoromethanesulfonyl)imide (EMI-TFSI). The author discusses their ability to solubilize the CPB of PMMA and also investigates the relationship between solvent viscosity and frictional data in hydrodynamic lubrication.

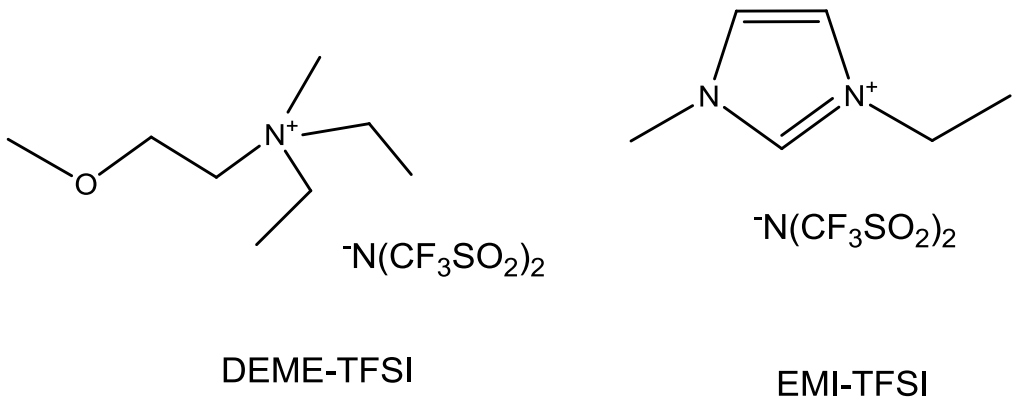

Figure 3-1. Chemical structures of DEME-TFSI and EMI-TFSI.

3-2. Experimental Section

3-2-1. Materials

Methyl methacrylate (MMA, 99% , Nacalai Tesque, Japan) was passed through a column of basic alumina to remove inhibitors. Cu(I)Cl (99.9%, Wako Pure Chemical, Japan), ethyl 2-bromoisobutylate (EBIB, 99%, Wako), 4,4’-dinonyl-2,2’-bipyridine (dNbipy, 97%, Sigma-Aldrich Co., USA), and hexamethyldisilazane (HMDS, Tokyo Chemical Industry Co., Ltd., Japan) were used

as received. (2-Bromo-2-methyl) propionyloxyhexyltriethoxysilane (BHE) was prepared as previously reported.[6] All other reagents were used as received from commercial sources.

A silicon wafer (Ferrotec Corp., Japan, one side chemical/mechanical polished, a thickness of 525 μm) was cleaned by ultrasonication in $CHCl_3$ for 15 min and ultraviolet (UV) / ozone treatment for 10 min before fixation of BHE. A silica particle (SiP, HIPRESICA SP, diameter 10 μm,) was obtained from Ube Nitto Kasei Co., Ltd., and was used as a probe for the AFM measurement.

3-2-2. Synthesis of Concentrated PMMA Brushes via Surface-Initiated ATRP

Well-defined CPBs of PMMA were prepared by surface-initiated atom transfer radical polymerization (SI-ATRP), as previously reported. Briefly, a silicon wafer was immersed in an ethanol solution of BHE (1 wt%) and 28%-aqueous NH_3 (5 wt%) for 12 h at room temperature and washed with ethanol. Thus obtained, BHE-immobilized silicon wafer was immersed in a degassed MMA (in bulk) containing EBIB (3 mM), Cu(I)Cl (16 mM), and dNbipy (37 mM), sealed under an argon atmosphere in a Schlenk flask, and heated at 70ºC for 2 h. EBIB was added as a free initiator not only to control the polymerization but also to yield free polymers which is a good measure of the molecular weights of graft polymers (see section 2-2-2). After polymerization, the solution was subjected to gel permeation chromatographic (GPC) measurements to determine the molecular weights of free polymer and monomer conversions. The PMMA grafted silicon wafer was copiously rinsed and then washed by ultrasonication in $CHCl_3$ to remove physisorbed free polymers and impurities. The thickness of PMMA-brush layer was determined using a spectroscopic ellipsometer

Table 3-1. Molecular Characteristics of PMMA-Brush Samples

Substrate	M_n	M_w/M_n	L_d /nm	σ /chains nm^{-2}
Wafer	57,000	1.24	41	0.52
Probe	49,000	1.21	-	-

(M-2000U, J. A. Woolam, Lincoln, NE). For the synthesis of the CPB of PMMA on a SiP, the same procedure followed except that the SiP concentration maintained at ~0.5 wt% for all steps. Table 3-1 lists the characteristics of the CPBs of PMMA studied in this paper. The number-average molecular weight, M_n, and the polydispersity index, M_w/M_n, are those of the free polymer analyzed by GPC calibrated with PMMA standards. The graft density σ was calculated from M_n, L_d, the bulk density of a PMMA film ρ (= 1.19 g/cm^3),[7] and Avogadro constant N_A, using $\sigma = \rho L_d N_A / M_n$.

3-2-3. Hydrophobic Treatment of Silicon Wafer and SiP

Hydrophobic treatment of a silicon wafer was performed according to the method of Chen et al.[8] a silicon wafer was immersed in a mixture of HMDS (10 wt%) and toluene (90 wt%), heated at 110ºC for 5 h, and then rinsed with chloroform. The same treatment was applied to a SiP with a concentration as low as ~0.3 wt%. After the treatment, the modified SiP was repeatedly washed with chloroform and stored in it prior to use.

3-2-4.AFM Force Measurements

Normal and frictional forces were measured by an atomic force microscope (AFM) (JPK Instruments Inc., Germany, NanoWizard) equipped with a rectangular-shaped cantilever (Olympus Optical Co., Ltd., Japan, OMCL-RC800, vertical spring constant, k_n = 0.1 N/m). A brush-modified or hydrophobized SiP was attached on the cantilever with a two-component epoxy resin adhesive. The detailed procedures are given in section 2-2-3.

3-2-5. Viscosities of ILs

The viscosities of DEME-TFSI and EMI-TFSI (Table 3-2) were determined with a rheometer (Malvern Instruments., UK, CVOR 150) equipped with a temperature control unit (Malvern Instruments, Melts Oven) and a cone/plate geometry with a diameter of 25 mm.

Table 3-2. Viscosities of DEME-TFSI, EMI-TFSI and Toluene

Solvent	Viscosity at 30 ºC / mPa·s	Viscosity at 58 ºC / mPa·s
DEME-TFSI	40	20
EMI-TFSI	14	9
Toluene	0.6 (room temperature) [(a)]	-

(a) The data was reprocessed from reference 12.

3-3. Results and discussion

The AFM measurement of the equilibrium thicknesses L_e revealed that ILs could swell the CPB of PMMA to similar levels as when toluene is employed. The $L_e/L_{c,w}$ value reached about 60% ± 10% in all cases, where $L_{c,w}$ is the contour chain length calculated from the M_w value. This value is slightly lower than a previously reported value (ca. 80%); the reason for this discrepancy is unclear. However, the value obtained was considered to be high enough to conclude that the studied ILs are solvents of similar quality to toluene from the viewpoint of the similarity in their values for all the systems. Sufficiently good solvent-quality was also confirmed by Figure 3-2, which shows the

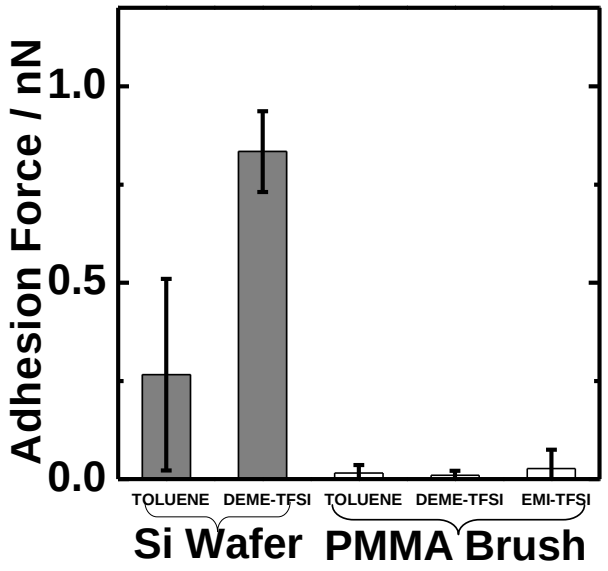

Figure 3-2. Adhesion forces observed by AFM in the retracting mode between hydrophobized silica surfaces and between PMMA-brush surfaces in ILs and toluene.

adhesion forces between the studied lubricating surfaces estimated from the retracting force profile in the AFM measurement. The CPB-modified surface gave little adhesion in all the solvents. In contrast adhesion forces of 0.2 - 1.0 nN were detected between the hydrophobized silica surfaces (unmodified with the CPB) in DEME-TFSI and toluene. The very low adhesion indicates that these solvents including the ILs are good enough to suppress the attractive interaction between polymer segments and that the graft density is high enough to effectively reduce the interpenetration between brushes, as was previously observed for SDPBs. Any adhesive interaction will, of course, increase friction to destroy the hydrodynamic lubrication layer and enter the boundary lubrication regime.

Figures 3-3 and 3-4 illustrate the results of the properties of friction/lubrication in these three solvents. For the silica surfaces without brushes, μ increased with increasing F_n, approaching almost constant value of ca. 0.2 in ILs and in toluene. It was assumed that at a low F_n, a lubricating layer of a solvent as a fluid was formed. This can be rationalized by the fact the μ value at a lower F_n (= 2 nN) is dependent on v (as shown by the square symbol in Figure 3-4a). Unfortunately, this

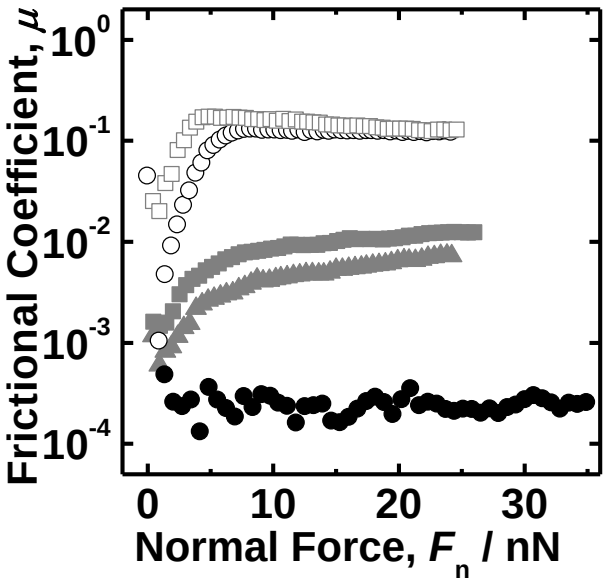

Figure 3-3. Plot of frictional coefficient μ vs normal force F_n measured at a shear velocity v of 6 μm/s between hydrophobized silica (without brush) surfaces in DEME-TFSI (□) and toluene (○) and between PMMA-brush surfaces in DEME-TFSI (■), EMI-TFSI (▲) and toluene (●).

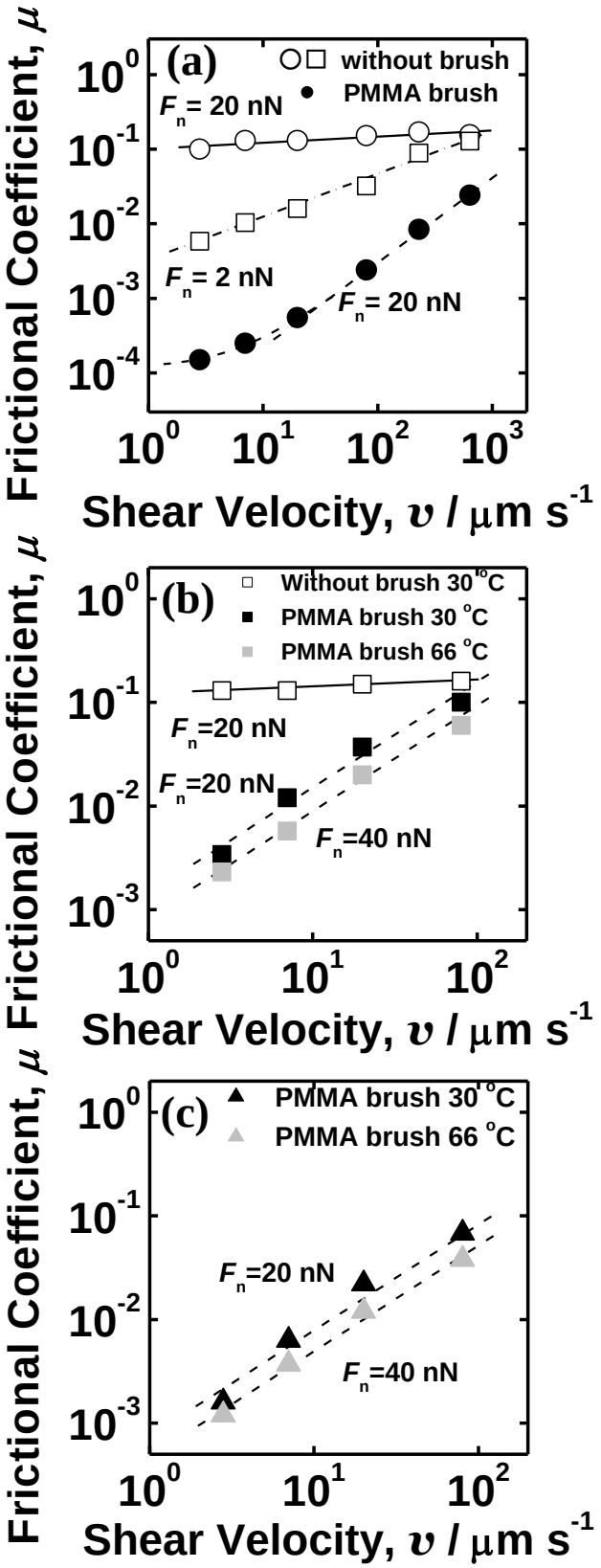

Figure 3-4. Plots of frictional coefficient μ vs shear velocity v in (a) toluene, (b) DEME-TFSI, and (c) EMI-TFSI.

lubricating layer was not maintained up to high F_n values because of high adhesive interactions. This breakdown caused the system shift to boundary lubrication. This regime of lubrication was characterized by F_s being approximately proportional to F_n and thus an almost constant value of μ (Amonton-Coulmb's law[9]) independent of v. Interestingly, an approximately same μ value was obtained both in toluene and DEME-TFSI, regardless of the differences in viscosity. This is due to the fact that the system is in the regime of boundary lubrication.

The addition of the CPB greatly improved the lubrication. As discussed in Chapter 2, the CPB of PMMA showed a compression-independent super lubrication, which was described by two lubrication mechanisms: boundary lubrication giving μ values on the order of 10^{-4} (observed in a lower-v region) and hydrodynamic lubrication having v-dependent μ values.

The CPB of PMMA lowered the frictional properties even in ILs. As observed in the system without brushes, the μ value increased with increasing F_n, approaching a constant value. This may imply the formation of a solvent-lubricating layer between the two CPB-modified surfaces at a lower F_n region. However, it is difficult to unequivocally confirm this conclusion with the present data. As an almost-saturated and representative value, the μ data at 20 nN for 30 ºC and 40 nN for 58 ºC (measured at two different temperatures) are plotted in Figure 3-4. The v-dependency of μ indicates the hydrodynamic lubrication regime, while no evidence for the boundary lubrication was obtained. The suppression of attractive interactions effectively lowers the friction in the boundary lubrication, to the same levels of μ as in toluene, and thus allows hydrodynamic lubrication to dominate.

The temperature had a slight impact on the frictional property in the two ILs. It should be noted that approximately the same slope of the line in Figure 3-4 was obtained under all conditions, even though the μ value of the ILs was about 100 times greater than that in toluene. Here, the author discusses the relationship between μ vs v in hydrodynamic lubrication according to Equation (2-5). The slope of the line in Figure 3-4 corresponds to $\alpha \sim 1$ for all the systems, suggesting that the

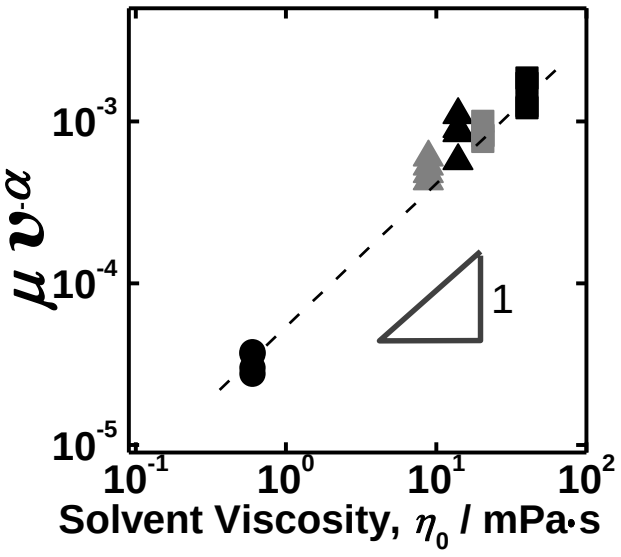

Figure 3-5. Plot of frictional coefficient normalized with shear velocity, $\beta = \mu\upsilon^{-\alpha}$, vs bulk solvent viscosity, η_0. in toluene at 30 ºC (●), DEME-TFSI at 30 ºC (■) and 58 ºC (▲), and EMI-TFSI at 30 ºC (■) and 58 ºC (▲).

solvent-swollen CPB behaves like a Newtonian fluid, by contrast the concentrated polymer solution exhibits non-Newtonian behavior due to the entanglement of polymer chains. This can be possibly attributed to the fact that in the CPB layer, the graft-polymer chains are highly stretched and hence reduce in chain entanglement. The parameter of β in Equation (2-5) can be defined as follows.[10]

$$\beta = \eta/h \tag{3-1}$$

where η and h are the viscosity and the effective thickness, respectively, of a lubricating layer. Figure 3-5 plots $\beta = \mu \cdot \upsilon^{-\alpha}$ (with $\alpha = 1$ as discussed above) as a function of viscosity of solvent in bulk η_0. The parameter β can be interpreted as the local viscosity in a solvent-swollen brush layer because of the similar degree of swelling at each solvent condition. Good correlation was obtained between β and η_0; the slope of the line in Figure 3-5 was almost unity. This implies that the local viscosity of the brush layer is linearly related to the solvent viscosity. The viscosity of a liquid can be determined by the size of the molecules and the intermolecular interactions (leading to clustering of molecules in some cases). In a polymer solution especially of a dilute concentration, the viscosity is proportional to the solvent viscosity,[11] unless a polymer segment affects the intermolecular interaction. From this

point of view, the observed proportionality is a special case, presumably due to the solvent-swollen CPB possessing a highly stretched-chain conformation. The above-mentioned data do not show clustering to have a significant effect. The formation of a lubricating layer in concert with the solvent-swollen CPB layer in the IL system can be readily explained in terms of the hydrodynamic lubrication mechanism.

3-4. Conclusions

The AFM-microtribologic technique was used to investigate the frictional properties of PMMA CPBs in highly viscous ILs (DEME-TFSI and EMI-TFST) and toluene, which are all good solvents for PMMA. In the ILs, little adhesive interaction between the brush surfaces was observed, which caused a dramatic decrease in the frictional coefficient μ in the boundary lubrication regime to values on the order of 10^{-4} , as was the case in toluene. This decrease allowed the hydrodynamic lubrication mechanism to dominate. In this regime, the v-dependence of μ followed power-law scaling with an α value close to unity. It was suggested that the thus produced lubricating layers should have similar thicknesses in toluene as well as ILs and that the frictional property could be simply related to the solvent viscosity. These friction/lubrication properties can be attributed to the unique features of the CPBs in a good solvent: the polymer chains are highly stretched due to high osmotic pressure. The author has suggested that the local viscosity of the lubricating layer on or in the brushes is proportional to that of the solvent in bulk. Finally, the author concludes that the addition of the CPB layer improved the friction even in ILs, where the hydrodynamically lubricating layer was successfully produced and maintained under all the conditions studied. The combination of ILs and CPB may lead to the development of a novel route toward the control of lubrication in practical applications.

References

(1) (a) Dupont, J. ; de Souza, R. F. ; Suarez P. A. Z. *Chem. Rev.* 2002, **102**, 3667-3691. (b) Kirchner, B., Eds.; *Ionic Liquids*; Springer: Heidelberg, 2007. (c) Freemantle, M. *An Introduction to Ionic Liquids*; Royal Society of Chemistry: London, 2010.

(2) (a) Carmichael, A. J.; Haddleton, D. M.; Bon, S. F. A.; Seddon, K. R. *Chem. Commun*. **2000**, *14*, 1237-1238. (b) Biedron, T.; Kubisa, P. *Macromol. Rap. Comm*. **2001**, *22*, 1237-1242. (c) Kubisa, P. *Prog. Polym. Sci*. **2004**, *29*. 3-12. (d) Susan, M. A.; Kaneko, T.; Noda, A.; Watanabe, M. *J. Am. Chem. Soc*. **2005**, *127*, 4976-4983.

(3) (a) Carper, W. R.; Pflug, J. L.; Elias, A. M.; Wilkes, J. S. *J. Phys. Chem*. **1992**, *96*, 3828-3833. (b) Fuller, J.; Carlin, R. T.; Delong, H. C.; Haworth, D. *Chem. Commun*. **1994**, *3*, 299-300. (c) Elaiwi, A.; Hitchcock, P. B.; Seddon, K. R.; Srinivasan, N.; Tan, Y. M.; Welton, T.; Zora, J. A. *Dalton Trans*. **1995**, *21*, 3467-3472. (d) Suarez, P. A. Z.; Einloft, S.; Dullius, J. E. L.; de Souza, R. F.; Dupont, J. *J. Chim. Phys*. **1998**, *95*, 1626-1639.

(4) (a) Seddon, K. R.; Stark, A.; Torres, M. J. *Pure Appl. Chem*. **2000**, *72*, 2275-2287. (b) Huddleston, J. G.; Visser, A. E.; Reichert, W. M.; Willauer, H. D.; Broker, G. A.; Rogers, R. D. *Green Chem*. **2001**, *3*, 156-164.

(5) (a) Wang, H. Z.; Lu, Q. M.; Ye, W. M.; Cui, Z. J. *Wear* **2004**, *256*, 44-48. (b) Kamimura, H.; Kubo, T.; Minami, I.; Mori, S. *Tribol. Int*. **2007**, *40*, 620-625. (c) Sanes, J.; Carrion, F. J.; Bermudez, M. D.; Martinez-Nicolas, G. *Tribol. Lett*. **2006**, *21*, 121-123. (d) Bhushan, B.; Palacio, M.; Kinzig, B. *J. Coll. Int. Sci*. **2008**, *317*, 275-287.

(6) Ohno, K.; Morinaga, T.; Koh, K.; Tsujii, Y.; Fukuda, T. *Macromolecules* **2005**, *38*, 2137-2142.

(7) Brandrup, J.; Immergut, E. H.; Grulke, E. A., Eds.; *Polymer Handbook*; John Wiley & Sons Inc: New York, 1999.

(8) Chen, Y. K.; Chang, K. C.; Wu, K. Y.; Tsai, Y. L.; Lu, J. S.; Chen, H. *Appl. Surf. Sci.* **2009**, *255*,

8634-8642.

(9) Amonton, G. *Mem. del'Academie Royale A* **1699**, 275-282

(10) Barnes, H. A.; Hutton, J. F.; Walters, K. *An Introduction to Rheology*; Elsevier: Amsterdam, 1989.

(11) Atkins, P. W. *Physical Chemistry Sixth Edition*; Oxford University Press: Oxford, 1978.

(12) Santos, F.; de Castro, C.; Dymond, J.; Dalaouti, N., Assael, M., Nagashima, A. *J. Phys. Chem. Ref. Data* **2006**, *35*, 1-8.

Chapter4

Super Lubrication and its Mechanism between Immiscible Concentrated Polymer Brushes in Good Solvent

4-1. Introduction

In Chapter 2, the author found out the boundary and hydrodynamic lubrication features in the friction of CPBs. The friction force in hydrodynamic lubrication is determined by the effective viscosity and thickness of lubricating layer. The author revealed that the friction force of CPBs in hydrodynamic lubrication state was scaled with the degree of swelling (Chapter 2) and viscosity of swelling solvents of brush layer (Chapter 3). Meanwhile, the boundary lubrication is the lubrication state in which the interaction between confronted friction surfaces determines the friction force. The strong resistance of brush layer against mixing drastically reduces the friction force in boundary lubrication. The boundary and hydrodynamic lubrication features can be distinguished from the v-dependence on friction force; the friction force in hydrodynamic lubrication depends logarithmically on the shear velocity obeying the definition of viscosity, while the shear velocity has a less significant effect on the friction force in boundary lubrication.

As mentioned above, CPBs successfully achieved super lubrication by restriction of interpenetration of graft polymer chains. The friction mechanism of super lubrication of CPB would be classified into boundary lubrication in the view point of graft chains related surface interaction. However, the polymer brush surface interaction is still not clearly evaluated and the relevance with frictional property of polymer brushes remains undetermined. Actually, the graft polymer chains of CPBs have certain chain length distributions that would allow a little interpenetration of polymer chains at free ends. This small interpenetration would be inevitable even if the CPBs are fabricated through ideal LRP process.[1] It can be considered that small quantity of contamination at free ends of graft chain determines the value of μ of 10^{-4} order of super lubrication of CPB. Further reduction of

frictional coefficient, especially in boundary lubrication state, is expected by restricting the contamination more efficiently.

Introduction of repulsive interaction on graft polymer chains is an approach to suppress the contamination. Using CPBs of dissimilar polymers would be one way to enhance the repulsive effect. As it is known well, dissimilar polymers are often immiscible because the mixing entropy of dissimilar polymer is quite lower than low molecular weight solvent.[2] Such an immiscible character would inhibit undesired interpenetration for lubricating polymeric materials to improve their frictional property, but that have not previously investigated so far. In this study, the frictional property between CPBs of dissimilar polymers (PMMA and PS) was studied and compared to that of similar CPBs and SDPBs. The interaction between approached brush layers was also simulated with self-consistent field (SCF) calculation based on dynamic mean-field approximation to reveal the appearance of polymer chains interpenetration. The author will discuss the boundary lubrication feature of the friction of CPBs in the relevance of graft chains interpenetration.

4-2. Experimental Section

4-2-1. Materials

Silicon wafer (Ferrotec Corp., Japan, thickness 0.5 mm) was used as substrates for polymer brush surfaces. Silica particle (SiP, HIPRESICA SP, diameter 10 μm) obtained from Ube Nitto Kasei Co., Ltd., was used as prove of AFM for friction measurement. CPBs of PMMA and PS were fabricated on the surfaces of silicon wafer and SiP by surface-initiated ATRP, as described in Chapter 2 and Chapter 3. The characteristics of polymer brushes used in this study were summarized in Table 4-1. Toluene (Wako Pure Chemicals., 99%, spectroscopic grade) was used as solvent for friction measurement.

4-2-2. AFM Measurements

Normal and friction forces were measured by an atomic force microscope (AFM) (JPK Instruments Inc., Germany, NanoWizard) equipped with a rectangular-shaped cantilever (Olympus

Table. 4-1 Molecular Characteristics PMMA and PS Brush Samples

Brush Samples		M_n	M_w/M_n	L_d / nm	σ / chains nm^{-2}	σ*
CPB of PMMA	Wafer 1	57,000	1.24	39	0.49	0.27
	Wafer 2[(a)]	60,000	1.18	44	0.53	0.29
	Probe 1	49,000	1.21	-	-	-
CPB of PS	Wafer 1	38,000	1.19	32	0.53	0.35
	Wafer 2[(b)]	38,000	1.19	26	0.44	0.29
	Probe 1	33,000	1.17	-	-	-
SDPB of PMMA	Wafer[(c)]	50,000	1.13	2	0.03	0.02
	Probe 1[(c)]	50,000	1.13	-	-	-

(a) The data were reprocessed from Chapter 3. (b) The data were reprocessed from Chapter 2. (c) The data were reprocessed from reference 5.

Optical Co., Ltd., Japan, OMCL-RC800, vertical spring constant, k_n = 0.1 N/m). A brush-modified or hydrophobized SiP was attached on the cantilever with two-component epoxy resin adhesive. The detailed procedures are given in section 2-2-3.

4-2-3. SCF Calculation.

The "Simulation Utilities for Soft and Hard Interfaces (SUSHI)" in the OCTA system was used for the prediction of compositions of graft chains on confronted surfaces.[3] SUSHI is a simulator for polymeric materials on mesoscopic scale with SCF calculation based on dynamic mean-field approximation. The calculations were performed on three models ((i) similar SDPBs, (ii) similar CPBs, and (iii) dissimilar CPBs) in one dimensional simulation box with the length of *L*. Polymer A and polymer B were grafted at one chain ends on opposing two ends of the simulation box. The segment number *N* of each polymers was 100 ($N_A = N_B = 100$). The polymer grafted surfaces were soaked in solvent C with polymer volume fractions of φ_A and φ_B. The volume fractions were fixed as $\varphi_A = \varphi_B = 0.006$ for SDPBs ((i)) and $\varphi_A = \varphi_B = 0.4$ for CPBs ((ii) and (iii)). The thermodynamic interaction parameter χ between the segments of polymers and solvent were zero ($\chi_{AC} = \chi_{BC} = 0$). The similarity of polymers was introduced in the thermodynamic parameter χ between the polymers ($\chi_{AB} = 0$ for the calculation models of (i) and (ii), $\chi_{AB} = 0.4$ for (iii)).

4-3. Results and Discussion

The normal load dependence on frictional μ of confronted CPBs of PMMA-PMMA, PS-PS, and PMMA-PS were plotted in Figure 4-1. Toluene was used as solvent for swelling the brush layers, as it was adequately good solvent for both polymer brushes. The μ of SDPBs of PMMA plotted also in Figure 4-1 (open triangle) shows clear frictional transition around F_n = 5 nN and reached almost constant value of μ on the order of 10^{-1}. SDPB having lower graft density (typically less than 0.1 chains/nm^2) shows so small osmotic pressure that the brush layer is easy to be compressed against normal load.[4] The frictional transition of SDPBs was previously ascribed to the interpenetration of the brushes beyond a critical normal load.[5] On the contrary, the μ of CPBs never transferred to high friction state and kept quite low μ. This shows the development of ultra-low frictional property of CPBs by restricting the interpenetration of the brushes. In the case of the friction of the CPBs of PMMA-PS (closed gray circle), the μ value was half value of the PMMA-PMMA (closed black circle) and PS-PS (open circle) ones. This would insist that the friction of dissimilar CPBs also

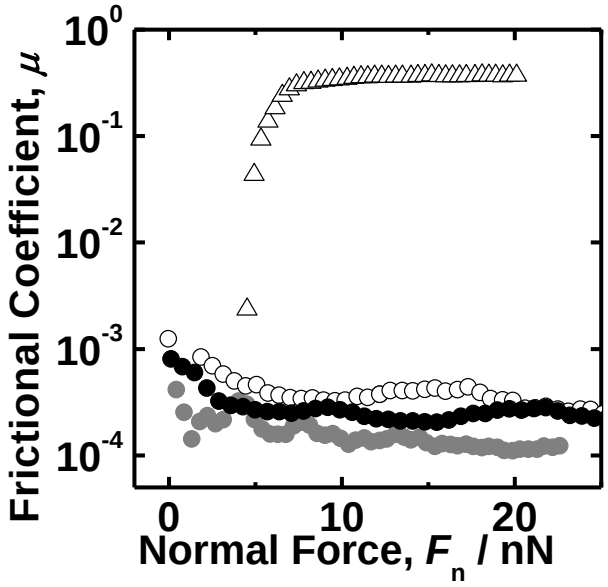

Figure 4-1. Plot of frictional coefficient μ vs normal load F_n at shear velocity υ of 6 μm/s for the SDPBs of PMMA (△,Wafer 1/Probe 1, the data was reprocessed from the reference 5), CPBs of PMMA (●,Wafer 1/Probe 1) and PS (○,Wafer 1/Probe 1), and dissimilar CPBs of PMMA-PS (●,CPB of PS Wafer 1/CPB of PMMA Probe 1).

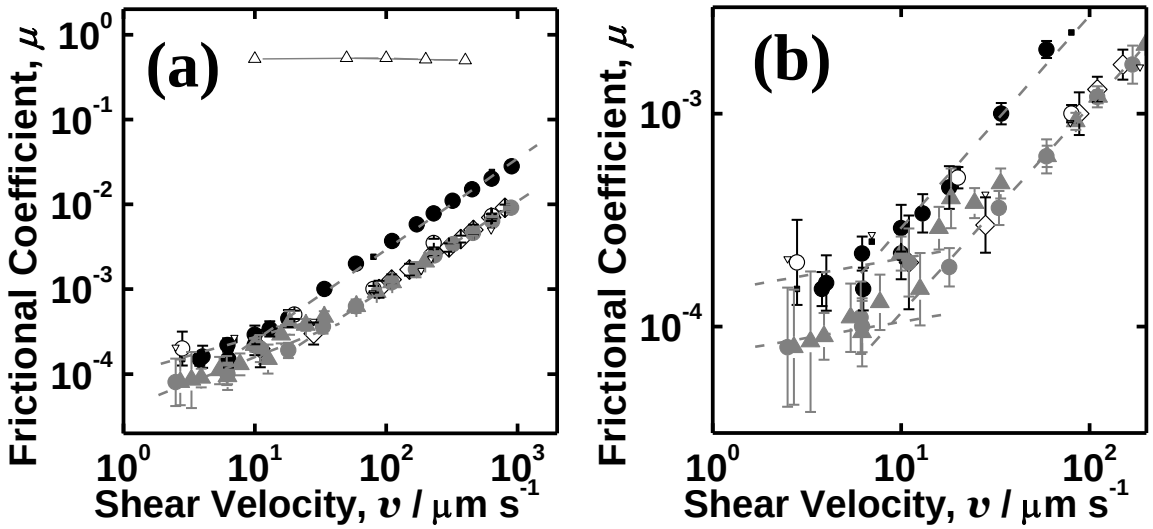

Figure 4-2. Plots of frictional coefficient μ vs shear velocity υ measured at a normal force of F_n 20 nN. Between CPBs of PMMA; Wafer 1/Probe 1 (●) and Wafer 2/Probe 1 (■, the data were reprocessed from Chapter 3). Between CPBs of PS; Wafer 1/Probe 1 (○) and Wafer 2/Probe 1 (▽, the data were reprocessed from Chapter 2). Between CPBs of PMMA and PS; CPB of PS Wafer 1/CPB of PMMA Probe 1 (● and ▲, different sets of data are presented). Between SDPBs of PMMA; Wafer 1/Probe 1 (△, the data were reprocessed from reference 5). The Figure (b) shows magnified drawing of the Figure (a).

develops ultra-low frictional property but the μ is more efficiently reduced by inhibiting the graft chain interpenetration in a more restrict way.

Figure 4-2 shows υ-dependency on μ at F_n = 20 nN. The μ values of SDPBs of PMMA showed little υ-dependency. This implies the friction of SDPBs is in boundary lubrication and suggests that the interaction between the confronted brushes is too strong to achieve the hydrodynamic lubrication. Meanwhile, the three friction surfaces of CPBs showed similar υ dependence; the μ value increased along with υ, but the υ-dependence became smaller below around 30 μm/s of υ. This shows the shift of lubrication mechanisms of CPBs; their friction states in hydrodynamic lubrication at high υ region turn into boundary lubrication state when the υ decreases, as previously noted in Chapter 2. The μ of CPBs and SDPBs shown in Figure 4-1 is in boundary lubrication state.

The friction shift of CPBs from hydrodynamic to boundary lubrication state can be recognizable as graft chains interaction between confronted brush layers. The graft chains of lubricating two brush layers in hydrodynamic lubrication state are difficult to interpenetrate each

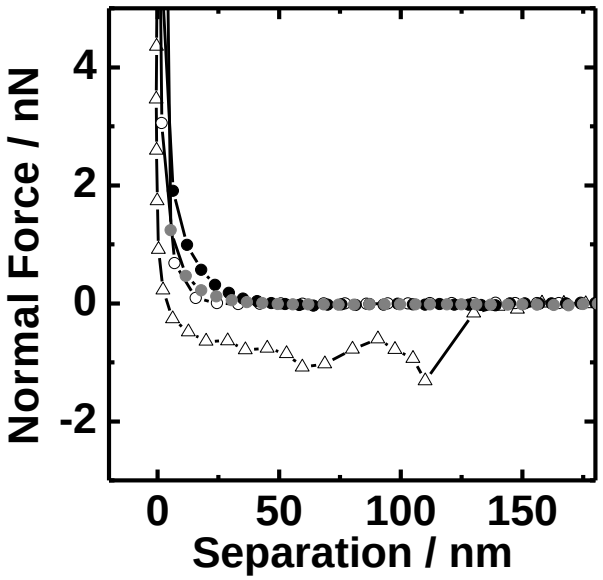

Figure 4-3. Typical retractive force curve profiles of SDPBs of PMMA (△, Wafer 1/Probe 1), CPBs of PMMA (●, Wafer 1/Probe 1) and PS (○, Wafer 1/Probe 1), and dissimilar CPBs of PMMA-PS (●, CPB of PS Wafer 1/CPB of PMMA Probe 1).

other when the v is high. The friction force is mainly produced from viscosity resistance of lubricating brush layer at this friction state. Along with decreasing v, however, the graft chains become easier to interpenetrate, producing resistance force to untangle the interpenetration of chains. This makes the friction state at lower v region is in boundary lubrication state. Typical force curve profiles in retractive mode of brushes were shown in Figure 4-3. While the SDPBs clearly showed adhesion force around 1 nN during repelling the surfaces, the CPBs did not show any detectable adhesion forces. The little adhesive interaction force should decrease the μ determined by boundary lubrication mechanism to develop ultra-low frictional property of CPBs. Of course, there would be no direct correlation between adhesion force (vertical force) and friction force (lateral force). Although, adhesion would be a good indicator of the friction force in boundary lubrication state, as the both forces are related to confronted surface interaction.

It was hitherto explained that the confronted CPBs never interpenetrated each other at any normal load. However, actual CPB samples have some concentration distributions depending on graft density or chain length. It can be expected that this structural unevenness of brush layer of CPB

allows a small portion of interpenetration at free ends of graft chains, which would determine the μ in boundary lubrication state. The author simulated the graft chains composition distribution of confronted two brush surfaces with SUSHI, simulation utilities of SCF calculation based on dynamic mean-field approximation.[3] In Figure 4-4, the volume fraction of graft polymers on two grafted surfaces much close to each other were plotted against the separations. The schematic illustrations of their graft chains on each surface were also depicted in Figure 4-4. The calculation model for SDPBs (i) easily interpenetrated each other along with approaching the surfaces. It can be considered that the interpenetration of SDPBs produced adhesive interaction force against repelling the surfaces (as shown in Figure 4-3) and hence higher μ value on the order of 10^{-1} in boundary lubrication. On the contrary, the interpenetration was gratefully suppressed in the case of CPBs model (ii), however, suggesting that the graft chains of CPBs are somewhat contaminating at free ends surfaces. This results from non-uniform concentration distribution of graft chains. The highly extended polymer structures of CPB are somewhat disrupted to allow the small interpenetration. The actual samples of CPBs have some certain distribution of graft chain length, which would certainly spread the interpenetrate region of graft chains, though not to extent to the SDPBs case. Either way, it can be considered that the small portion of interpenetration determines the μ of 10^{-4} order in boundary lubrication state.

Introduction of thermodynamic interaction parameter (χ) between confronted polymer segments is a way to reduce the small interpenetration of CPBs. When the parameter $\chi_{AB} = 0.4$ was introduced between segments of two graft polymer chains of CPBs, the interpenetration at free ends was suppressed as shown in Figure 4-4 (iii). As it is known that phase separation of A-B block polymer is occurred when the parameter of $\chi_{AB}N$ is over 10.5,[6] the parameter of χ_{AB} ($N_A + N_B$) = 80 of (iii) would be enough to segregate the graft polymers of A and B. As PMMA and PS are immiscible polymers each other, the calculation model of (iii) is attributed to the confronted CPBs of PMMA-PS case. The CPBs of PMMA-PS showed lower μ value as half as that of the PS-PS and PMMA-PMMA cases. Although these simulations do not give us quantitative evaluation of the

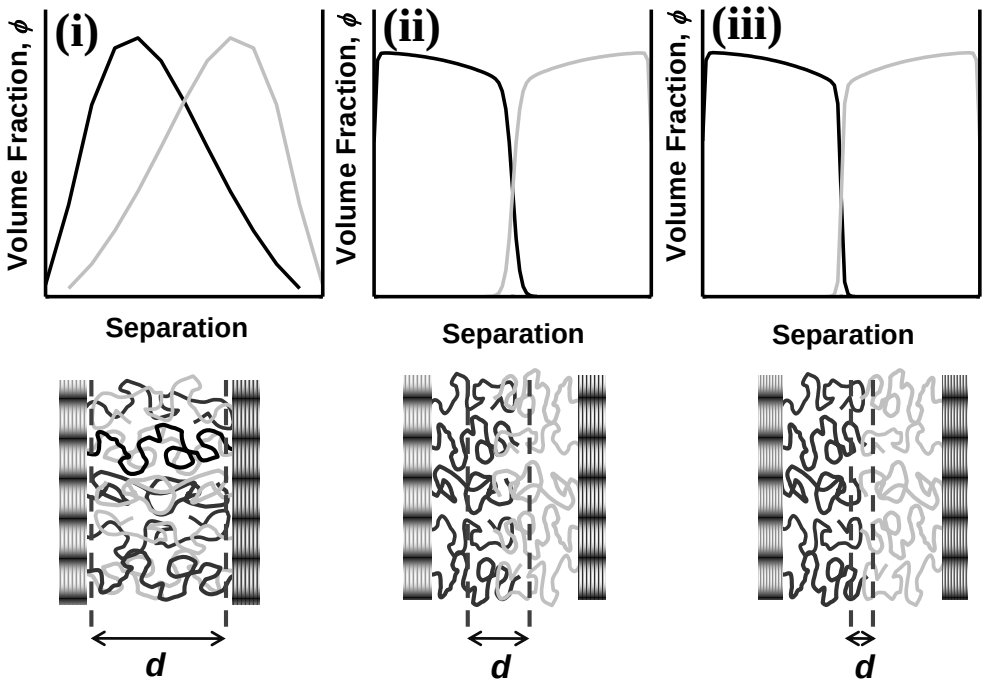

Figure 4-4. Volume fraction profiles of graft polymers represented against separations of the grafted surfaces. The results for adequately approached surfaces of the simulated models for (i) SDPBs (L = 12), (ii) similar CPBs (L = 80), and (iii) dissimilar CPBs (L = 80) were displayed in upper stand. The schematic illustrations of graft polymer distributions were also depicted in lower stand. The d in the illustrations denotes the region of interpenetrated graft chains within the brush layers.

interpenetrations and hence the frictional force, the depicted illustrations from the calculation results qualitatively explain well the friction behaviors of SDPBs and CPBs in boundary lubrication state.

Turning now to hydrodynamic lubrication at high shear rate region. As shown in Figure 4-2b, the μ of CPBs of PMMA-PS and PS-PS in hydrodynamic lubrication state (v > 50 μm/s) were reduced to one-third of that of the CPBs of PMMA-PMMA. The lower μ value of CPBs of PMMA-PS than that of PMMA-PMMA indicates that interaction between graft chains actually have certain effect on hydrodynamic lubrication of CPBs, as the reduced interpenetration of graft chains decreased the μ in boundary lubrication state. The difference of CPBs of PS-PS and PMMA-PMMA suggests that PMMA and PS brush chains differently affect their hydrodynamic lubrication layers, if the thicknesses or graft chain lengths do not affect the interaction in measured range of this study. Either way, they do not certainly tell us how the interaction affects the hydrodynamic lubrication

layer. Further experiment is necessary to clarify the mechanism of hydrodynamic lubrication of CPBs.

4-4. Conclusions

The frictional property and graft chains interactions of confronted CPBs were investigated. Previous friction study of CPBs insisted that CPBs developed ultra-low μ value on the order of 10^{-4} order by inhibiting the graft chains interpenetration. In this study, however, it was revealed that suppressed but small interpenetration of graft chains actually occurred to determine the low μ value of CPBs in boundary lubrication state. The introduction of thermodynamic interaction parameter was a way to suppress the small interpenetration to decrease the μ, and it was confirmed in the friction of CPBs of dissimilar polymers system (PMMA-PS) which lowered the μ as half as the value of their similar-polymer systems. It was also confirmed that dissimilar CPBs also reduced the μ in hydrodynamic lubrication, confirming that some interaction between graft polymer chains was occuring to affect the hydrodynamic lubrication layer.

References

(1) When polymers are obtained through ideal living polymerization process, the chain lengths of each polymer chain obey poisson distribution. In that sense we can never obtain uniform polymer through living polymerization process, although we can produce nearly monodisperse polymer ($M_w/M_n \sim 1$). In addition, some termination reaction between two propagation radicals is inevitable in living radical polymerization process, which somehow increases the breadth of the distribution. The detailed mechanism of living radical polymerization can be referred to, Matyjaszewski, K., Eds.; *Controlled / Living Radical Polymerization: Progress in ATRP, NMP, and RAFT (ACS Symposium Series)*; American Chemical Society: Washington, DC, 2000.

(2) Flory, P. J. *Statistical Mechanics of Chain Molecules*; John Wiley & Sons: New York, 1969.

(3) Honda, T.; Kodama, H.; Roan, J. R.; Morita, H.; Urashita, S.; Hasegawa, R.; Yokomizo, K.; Kawakatsu, T.; Doi, M. *SUSHI Users Manual*; OCTA: Nagoya, 2004 (http://octa.jp).

(4) Tsujii, Y.; Ohno, K.; Yamamoto, S.; Goto, A.; Fukuda, T. *Adv. Polym. Sci.* **2006**, *197*, 1-45.

(5) Tsujii, Y.; Okayasu, K.; Nomura, A.; Ohno, K. Fukuda, T. *Submitted to Macromolecules.*

(6) (a) Leibler, L. *Macromolecules* **1980**, *13*, 1602-1617. (b) Matsen, M. W.; Bates, F. S. *Macromolecules* **1996**, *29*, 1091-1098.

Chapter 5

Controlled Synthesis of Hydrophilic Concentrated Polymer Brushes and Their Friction/Lubrication Properties in Aqueous Solutions

5-1. Introduction

In Chapter 2 ~ 4, the lubrication mechanism of the CPBs was discussed. These mechanistic studies will allow for the design of friction/lubrication-controlled materials, which is one of the most promising applications. Another potential application of polymer brushes has been directed toward bio-interfaces with the intent of tuning the interactions between solid surfaces and biological materials.[1] Recently, the hydrophilic CPBs of poly (2-hydroxyethyl methacrylate) (PHEMA), poly (2-hydroxyethyl acrylate) (PHEA) and poly (poly(ethylene glycol)methylether methacrylate) (PPEGMA) were prepared via surface-initiated ATRP and revealed to extremely suppress non-specific adsorption of proteins (for the PHEMA brush) and thereby cell adhesion[2]. Such bio-inertness was ascribed to the entropically driven size-exclusion effect specific to the structure of the CPB, providing a new potential for biomaterials. In addition to bio-inertness, good lubricity is also required for some biomaterial applications. The PHEMA brush was, therefore, investigated on its friction property, unfortunately giving less improvement than expected as mentioned above. This may be due to insufficient hydrophilicity of PHEMA.[3]

The surface modification by polyelectrolytes is known to be effective in improving the mater lubrication thanks to charged groups. Raviv et al. obtained a μ value on the order of 10^{-4} in water between anionic-polyelectrolyte brushes prepared by the grafting-to method;[4] electrostatic interaction is responsible to such super lubrication, even though this brush can be regarded as a SDPB from a relatively low graft density. Zwitterionic polymers including poly (2-methacryloyloxyethyl phosphorylcholine) (PMPC) with good bio-compatibility[5] were also end-grafted to tune the surface properties. Kobayashi et al. succeeded in densely grafting such

polymers via surface-initiated ATRP[6] and reported frictional property ($\mu \sim 10^{-1}$) and wear resistance better than the corresponding spin-coated film by a so-called tribometer with a stainless steel or glass probe.[7] More recently, Chen et al. reported super lubrication in water between the brushes of zwitterionic polymers (whose graft density was not reported) and ascribed it to the effective formation of hydration sheet.[8]

To the best of our knowledge, it was still challenge to demonstrate super lubrication in water by the concentrated-brush effects and clarify the mechanism of such water lubrication between the CPBs of hydrophilic polymers. Among them, hydrophilic and neutral polymers with PEG side chains exhibit hydration force and bio-compatibility depending on the number or the terminal structure of PEG units,[9] which may also influence the frictional property. Thus, the CPBs of such PEG-containing polymers would enable the author to make a systematic study on the friction and biocompatibility in aqueous systems. An electrically neutral chain would be preferred in this study because electrostatic interaction should be less important, manifesting the potential concentrated-brush effects in an aqueous system. Additionally, their properties are expected to serve even under a high salt-concentration condition, e.g., our body fluid containing about 1 wt% salt electrolytes.

In this study, the author newly synthesized the CPBs of water-soluble polymers, poly (2-hydroxyethyl acrylate) (PHEA) (PEG-unit number, n = 1) and poly (poly(oxyethyleneglycol)methylether acrylate) (PPEGA) (n = 8.5) via photo-induced organotellurium-mediated radical polymerization (TERP). TERP is known to have high tolerance to functional groups, better controllability and applicability for acrylates.[10] For such brush samples, the author studied the frictional property in water media using an colloidal-probe technique on an AFM. The lubrication mechanism of these brushes is discussed in the view point of boundary and hydrodynamic lubrication described in Chapter 2 ~ 4.

5-2. Experiment

5-2-1. Materials

2-Hydroxyethyl acrylate (HEA) (99%, Wako) was purified according to the literature.[11] Poly (ethyleneglycol)methylether acrylate (PEGA) (Aldrich, M_n ~ 454) was passed through a column of basic alumina to remove inhibitors before use. Tellurium compounds, ethyl 2-methyl-2-(methyltellanyl)propanoate (EMA-TeMe) and dimethylditelluride ($(TeMe)_2$), were prepared according to the method previously reported by Yamago et al.[10(b)] All other reagents including 2-iodo-2-methylpropanenitrile (CP-I, 99 %, Tokyo Chemical Industry Co., Ltd., Japan) were used as received.

A silicon wafer (Ferrotec Corp., Japan, one side chemical/mechanical polished, 525 μm thickness) was cleaned by ultrasonication in $CHCl_3$ for 15min and ultraviolet (UV) / ozone treatment for 10min just before fixation of an initiator. A silica particle (SiP, HIPRECICA SP, radius *R* of 5 μm) was received from Ube Nitto Kasei Co., Ltd., and was used as a probe of AFM.

5-2-2. Synthesis of IHE

As a fixable initiator for photo-induced TERP, an iodine-type surface initiator, (2-iodo-2-methyl)propionyloxyhexyl triethoxysilane (IHE), was newly synthesized by the halogen-exchange reaction from (2-bromo-2-methyl)propionyloxyhexyl triethoxysilane (BHE, synthesized according to the literature[12]). BHE (4 g, 9.7 mmol) was added dropwise to a solution of sodium iodine (7.3 g, 48 mmol) in dry acetone (70 ml) and magnetically stirred for 5 days at 50 ºC. The reactant was evaporated to dryness under reduced pressure. The residue was diluted with dry $CHCl_3$ (300 ml) and passed through a filter paper. The evaporation of $CHCl_3$ from the filtrate gave IHE as a brown oil (2.5 g, 56 % yield); ^{1}H NMR ($CDCl_3$): δ 0.64 (t, 2H, SiCH_2), 1.23 (t, 9H, CH_3CH$_2$OSi), 1.32-1.54 and 1.60-1.75 (br, 8H, CH_2), 2.08 (s, 6H, CCH_3), 3.81 (q, 6H, CH$_3$CH_2OSi), 4.15 (t, 2H, CH_2O). Anal. Calcd for $C_{16}H_{33}IO_5Si$: C, 41.74; H, 7.22; I, 27.56. Found: C, 41.05; H, 7.01; I, 27.62.

5-2-3. Synthesis of Concentrated PHEA and PPEGA Brushes via Photo-induced TERP

A silicon wafer was immersed in an ethanol solution of IHE (1 wt%) and 28%-aqueous NH_3 (5 wt%) for 12 h at room temperature in dark condition to immobilize the initiating groups and then washed with ethanol. For the synthesis of PHEA brushes, the IHE-immobilized wafer was immersed in a degassed HEA (in bulk) containing $(TeMe)_2$ (0.3 mM) and a free initiator (0.1 mM), CP-I or EMA-TeMe, sealed under argon atmosphere in a flat grass cell (3 mm thick) and irradiated with visible light (450~530 nm) at 80 ºC for a prescribed time. Irradiation was made with a 300 W xenon-light source (MAX-302, Asahi Spectra Co., Ltd.) through a bandpass filter of the desired wavelength. After polymerization, the solution was diluted with *N*,*N*-dimethylformamide (DMF) to a known concentration and analyzed by gel permeation chromatography (GPC) to determine the molecular weights and conversion. The substrate was copiously rinsed with methanol to remove physisorbed free polymers and impurities. For the synthesis of PPEGA brushes, the IHE-immobilized substrate was immersed in a degassed DMF solution of PEGA (1 M), $(TeMe)_2$ (0.1 mM) and EMA-TeMe (0.2 mM) and treated in the same way as above described. SiPs were also modified with PHEA and PPEGA brushes by the same procedure, in which the concentration of SiPs was kept 0.5 wt% for all steps.

5-2-4. AFM Measurement for Swelling and Frictional Property of PHEA and PPEGA Brushes

An atomic force microscope (Seiko Instruments Inc., Japan, SPI400) was used to evaluate the microscopic surface character of the PHEA and PPEGA brush surfaces. For the measurement of equilibrium swollen thickness, a bare (unmodified) SiP was attached on a V-shaped cantilever (Olympus Optical Co., Ltd., Japan, vertical spring constant k_n = 0.15 N/m) with two-component epoxy resin adhesive and used as a probe. For the measurement of friction force and adhesive force between the brush surfaces, the above-mentioned brush-modified SiP was attached on a rectangular-shaped cantilever (Olympus Optical Co., Ltd, k_n = 0.1 N/m, lateral spring constant k_s = 23 N/m). The detailed procedures were described in section 2-2-3.

5-2-5. Other Measurements

The GPC analysis was made on a Shodex GPC 101-series high-speed liquid chromatograph

(Tokyo) equipped with a differential refractometer (Shodex RI-101). DMF solution of 10 mM LiBr was used as eluent with a flow rate of 0.8 mL/min at 40 ºC. Two Shodex gel columns LF804 (300mm length × 8.0 mm inner diameter; bead size = 6 μm) were used and calibrated with standard poly (methyl methacrylate)s (PMMAs). Sample detection was also made with a multiangle laser light-scattering (MALLS) detector, a Wyatt Technology DAWN HELEOS (Santa Barbara, CA), equipped with a Ga-As laser (λ = 658 nm) The refractive-index increments d*n*/d*c* were determined to be 0.061 and 0.045 mL·g^{-1} for PHEA and PPEGA, respectively, by a Wyatt Technology Optilab rEX differential refractometer (λ = 658 nm).

The thickness of the brush layer in a dry state was determined by a compensator-rotating, spectroscopic ellipsometer (M-2000U^{TM}, J. A. Woolam, NE, USA) equipped with a D2 and QTH lamps. The polarizer angle was 45º, and the incident angle was 70º. For analyzing thus obtained ellipsometric data, the optical constants were determined for the spincast film with a thickness of ca. 200 nm for each polymer.

5-3. Result and discussion

5-3-1. Graft Polymerization of HEA and PEGA by Photo-induced TERP Technique

The LRP of HEA was firstly reported via ATRP.[13] Recently, better control of molecular weight and molecular weight distribution of PHEMA was achieved by photo-induced TERP.[15] The TERP technique developed by Yamago et al. is one of novel LPRs equipped with good tolerance to functional groups and easy transformation of end groups. The key process, i.e., the reversible activation of dormant species to propagating radical, of TERP includes the degenerative (exchange) chain transfer (Scheme 5-1b) as well as the homolytic dissociation of a C-Te bound (Scheme 5-1a). Under usual conditions, the thermal dissociation insufficient occurs so that a conversional radical initiator is needed for control of polymerization. Yamago et al. succeeded in photochemically enhancing such homolytic dissociation and hence in better controlling the polymerization without radical initiator.[13] However, it still remained a challenge to synthesize low-polydispersity PHEA of

higher M_n, e.g., on the order of 10^5. With decreasing concentration of dormant initiator and then increasing target molecular weight, the polydispersity (M_w/M_n) index increased especially in the above-mentioned molecular-weight region. The author anticipated too slow deactivation of propagating radical in this case and hence added $(MeTe)_2$, which had already been demonstrated to be an efficient deactivator in TERP (Scheme 5-1d).[14] In addition, $(MeTe)_2$ can be photochemically dissociated to a tellanyl radical $MeTe^{\bullet}$ (Scheme 5-1c)[15], which will serve as an activator of the dormant P-X (Scheme 5-1d, e) but not as an initiator for monomers.

In this study, the author achieved well controlled polymerization of HEA (in bulk) by adding a small amount of EMA-TeMe (0.1 mM) and $(MeTe)_2$ (0.3 mM); under this condition, $(MeTe)_2$ was mainly photoexcited (see the reference 16 for the absorption spectra of relevant compounds). Figure 5-1 shows the M_n and M_w/M_n values of produced polymers in this case as a function of monomer conversion, suggesting relatively low polydispersities ($M_w/M_n < 1.3$) even in a high M_n range (below 2×10^5 in M_n and 2% in conversion). Here, the M_n and M_w/M_n are the values reduced with standard PMMAs in GPC. The absolute values of M_n (open circle symbols) obtained by GPC-MALLS for selected samples were also plotted in Figure 5-1, indicating good agreement between these two values and also with the theoretical value (depicted by the solid line) calculated from the

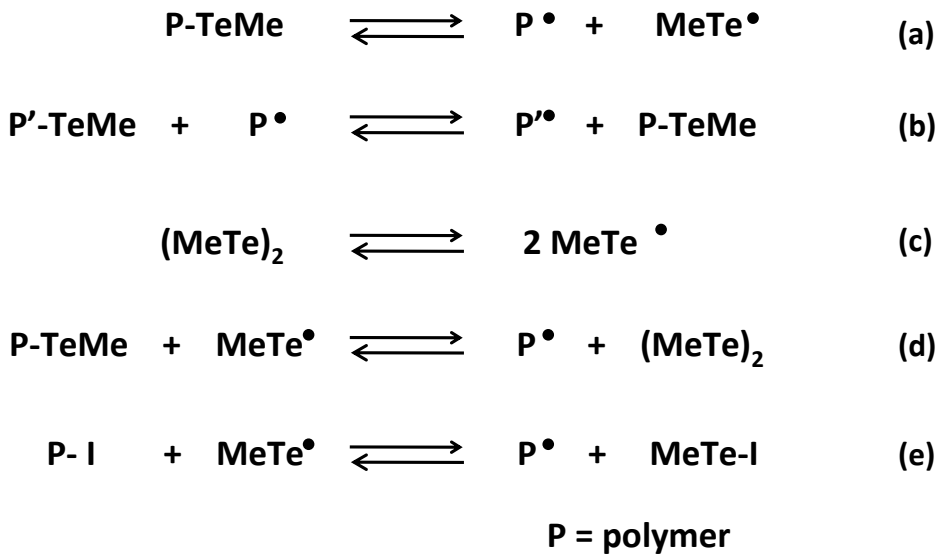

Scheme 5-1. Plausible mechanism of reversible activation in photo-induced TERP with EMA-TeMe or CP-I initiator.

feed-monomer/initiator molar ratio and conversion. Thus, it was concluded that the PMMA-reduced M_n well approximated the absolute value. It should be noted that thanks to exceptionally low concentrations of EMA-TeMe and $(MeTe)_2$, more homogeneous irradiation of polymerization solution was attained and high molecular weight polymers were obtained at low conversions; the latter is especially an advantage for graft polymerization. Another strategy in this study was to use IHE with a C-I group as an ease-to-use fixable initiator for surface-initiated graft polymerization, since the C-TeMe group is sensitive to air. Using an iodine-type (free) initiator, CP-I, the polymerization hardly proceeded without $(TeMe)_2$ but was well controlled in the presence of it similarly to the case of EMA-TeMe as shown in Figure 5-1. This means that the C-I bound was effectively activated by $TeMe^{\bullet}$. As the dormant end-group, the C-I bond would be readily replaced

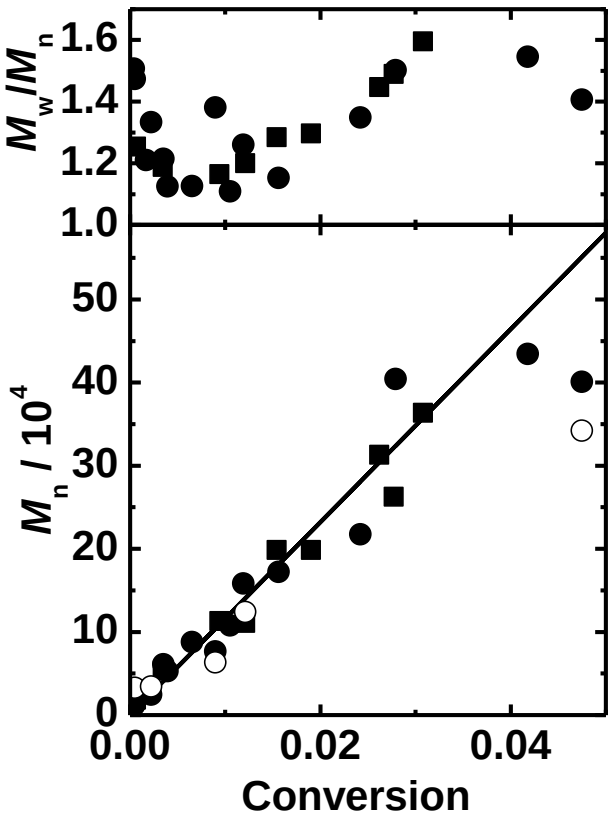

Figure 5-1. Plots of M_n and M_w/M_n vs conversion for photo-induced TERP of HEA with EMA-TeMe (■) and CP-I (●) as free initiators. Absolute M_n values determined by MALLS-GPC for selected samples were also plotted (○).

with the C-TeMe under the studied condition that the concentration of $(TeMe)_2$ was sufficiently higher than that of CP-I.

Finally, this polymerization condition was applied to surface-initiated graft polymerization on the IHE-immobilized substrate. Here, the polymerization was carried out under the condition that the number of initiating groups immobilized on the substrate was negligibly small (less than 1%) as compared with that of the free initiator CP-I. As a good measure in M_n and M_w/M_n for graft polymers,[17] the free polymers simultaneously produced from the free initiators had relatively narrow distribution in molecular weight similarly as mentioned above. In addition, a linear increase of the graft layer thickness with increasing M_n was observed as shown in Figure 5-3a. These results suggest well-controlled graft polymerization.

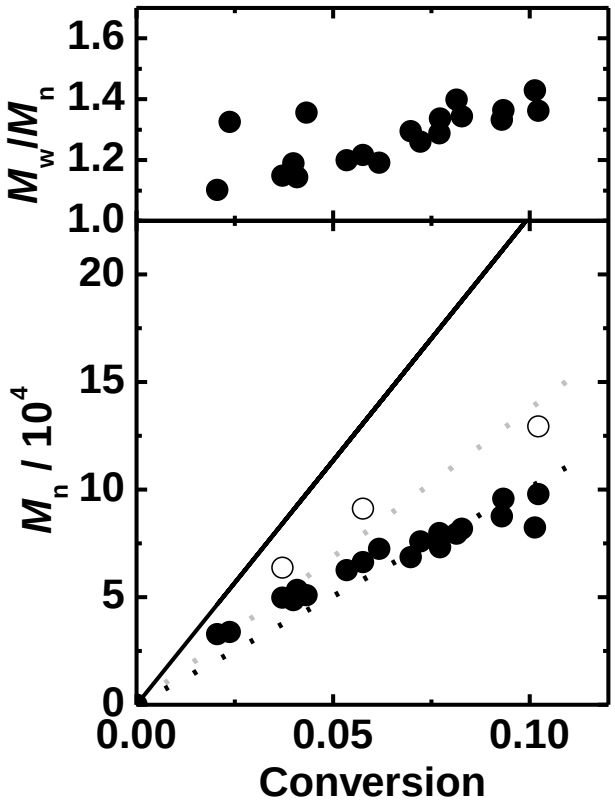

Figure 5-2. Plots of M_n and M_w/M_n vs conversion for photo-induced TERP of PEGA with EMA-TeMe (●) as a free initiator. Absolute M_n values determined by MALLS-GPC for selected samples were also plotted (○).

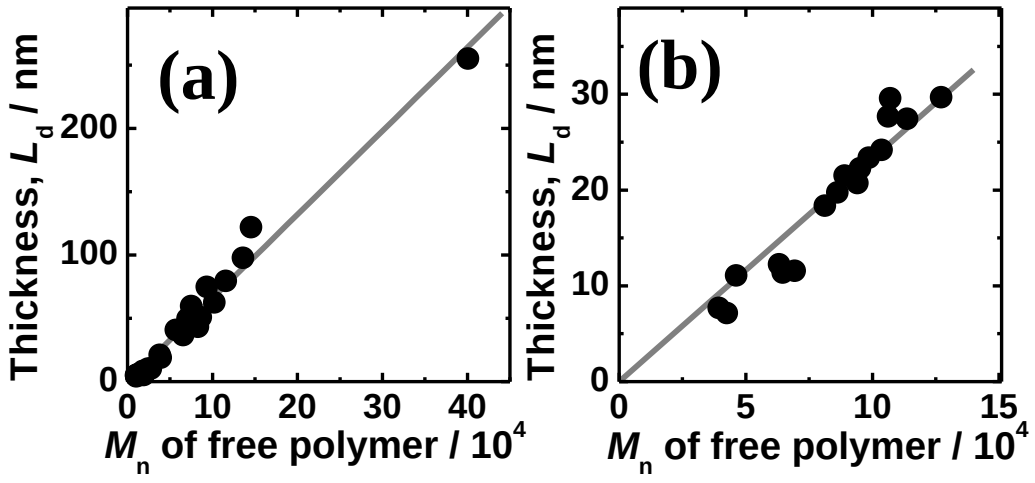

Figure 5-3. Relationship between the brush thickness L_d and M_n of corresponding free polymer for (a) PHEA and (b) PPEGA brushes.

According to the same strategies, the author carried out the surface-initiated graft polymerization of PEGA and succeeded in well controlling it as was the case with HEA (see Figures 5-2 and 5-3b); the M_n value of free polymers of relatively low M_w/M_n (< 1.4) and the L_d value of graft layers are proportional to conversion, giving a good correlation between them (as shown in Figure 5-3b). Here, the estimated M_n values are also the PMMA-reduce ones, being lower than the theoretical value. This was reasonably understood by the fact that the (hydrodynamic) size of PEGA monomer is much larger than those of HEA or MMA monomers. The absolute values of M_n (open circles) was determined for some samples by GPC-MALLS and plotted by open symbols. The determined values were smaller than the theoretical line. The reason for this is unclear at this moment. As follows, however, the PMMA-reduced M_n value was corrected to the absolute value using the ratio in slopes of the lines in the figure (multiplied by a factor of 1.3).

The proportionality between M_n and L_d in Figure 5-3 suggests uniform growth of graft polymers with constant surface densities for the polymerization of HEA and PEGA. From the slope of the lines, the graft densities σ_{PHEA} and σ_{PPEGA} were calculated to be 0.42 and 0.14 chains/nm^2, respectively, using the equation of $\sigma = \rho L_d N_A / M_n$, where ρ is the polymer density in bulk (ρ = 1.0 g/cm^3 was adopted here for both PHEA and PPEGA) and N_A is the Avogadro constant. To discuss

Table 5-1. Characteristics of PHEA- and PPEGA-Brush Samples.

PHEA Brush	M_n /g mol^{-1}	M_w/M_n	L_d / nm	σ / chains nm^{-2}	σ*
Wafer 1	24,000	1.33	10	0.25	0.19
Wafer 2	75,000	1.25	54	0.43	0.33
Wafer 3	86,000	1.16	51	0.36	0.27
Wafer 4	135,000	1.30	98	0.44	0.34
Probe 1	13,000	1.29	-	-	-
Probe 2	67,000	1.20	-	-	-
Probe 3	148,000	1.43	-	-	-

PPEGA brush	M_n /g mol^{-1}	M_w/M_n	L_d / nm	σ / chains nm^{-2}	σ*
Wafer 1	47,000	1.35	11	0.14	0.42
Wafer 2	64,000	1.19	12	0.11	0.34
Wafer 3	99,000	1.26	23	0.14	0.42
Probe 1	8,000	1.06	-	-	-

the conformation of graft chains on a surface and to categorize their constructing polymer brushes, the dimensionless graft density or surface occupancy σ* is a useful measure, defined as $\sigma^* = s_c\sigma$, where s_c is the cross-sectional area per monomer unit (see section 2-3-1). The σ* for the PHEA and PPEGA brushes was estimated to be $\sigma^*_{PHEA} = 0.32$ and $\sigma^*_{PPEGA} = 0.42$, respectively. These values are higher than the critical value ($\sigma^* \sim 0.1$) at crossover between the SDPB and CPB regimes. Thus, it was concluded that the surface-initiated, photo-induced TERP under the optimized condition successfully provided the CPBs of PHEA and PPEGA with the thicknesses reaching 100 nm and 30 nm, respectively. Table 5-1 lists the characteristics of the CPB samples used for the following studies on their structure and frictional properties in aqueous solutions.

5-3-2. Swelling property of PHEA and PPEGA brushes

Figure 5-4 shows typical force curves (force vs separation profile) of the CPBs of PHEA and PPEGA observed in the approaching mode against the bare (brush-unmodified) silica probe in water with and without NaCl. Here, the separation is the distance between the surfaces of substrate and probe by correcting the "offset" distance. The upper abscissa gives the value normalized by the

weight-average contour length of graft chain, $L_{c,w}$. The force curves of both CPBs in pure water clearly suggest the contribution of two components of repulsion forces with different compressibilities, i.e., different slopes in the curve. The component observed in a longer range of separation was characterized as a long tail beyond the fully-stretched chain length (especially much larger than the $L_{c,w}$ for the PPEGA brush) and nearly the same compressibility for both. Thus, it was reasonably ascribed to an electrostatic repulsion due to the surface charges of substrate and silica probe. Form the slope of the line, the so-called Debye length was estimated to be ca. 100 nm, corresponding to the case of 10^{-5} M NaCl aqueous solution, for both brushes; such a low level of salt concentration is understood as possible contamination even for Milli-Q water. When the probe further approached, much steeper increase in repulsion force was observed, being ascribed to steric repulsion by the swollen brushes. These two repulsion forces are originated from the osmotic pressures mainly caused by counter ions and polymer segments. Such assignments were also confirmed by the force profiles in 0.1 M NaCl-aqueous solution, in which the Debye length is about 1 nm; the longer-range interaction disappeared, and then the shorter-range one remained almost

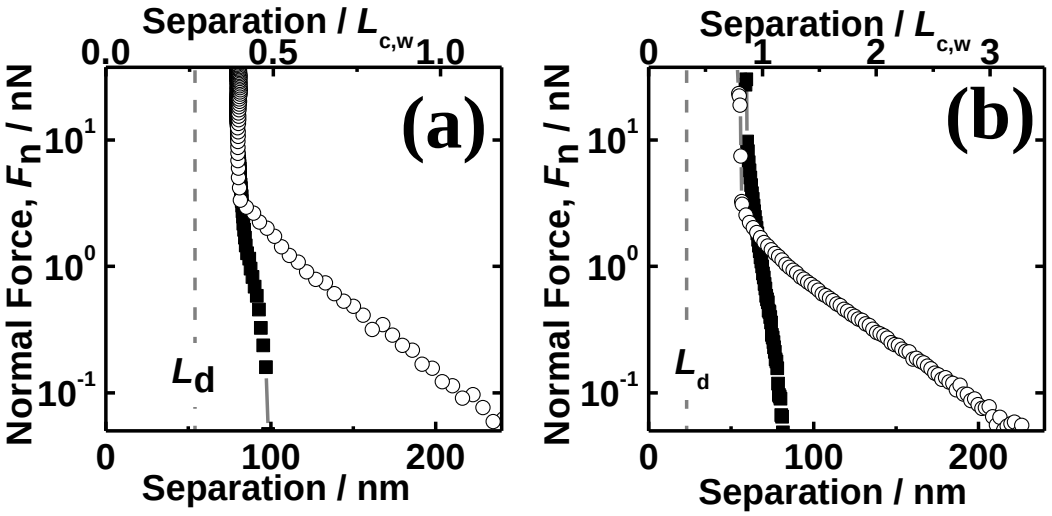

Figure 5-4. Approaching-mode force profiles of (a) PHEA brush (Wafer 2, $L_{c,w}$ = 203 nm) and (b) PPEGA brush (Wafer 3, $L_{c,w}$ = 69 nm) measured in water (○) and 10^{-1} M NaCl aqueous solution (■) using a bare silica probe.

unchanged. Good coincidence in the force profile at high compression (F_n > 5 nN) also suggests that the CPBs were similarly swollen in water with and without NaCl. This enabled us to precisely determine the equilibrium thickness L_e of the brushes in aqueous solutions, where L_e is the critical distance at which a repulsive force is detectable. In this study, it was taken as the distance at F_n = 0.05 nN and compared with the $L_{c,w}$ value (see the upper abscissa in Figure 5-4). The $L_e/L_{c,w}$ value was about 0.5 and 1.2, respectively, for the CPBs of PHEA and PPEGA. The estimation error of these values is possibly 20 - 30% mainly owing to that of the absolute molecular weight. Nevertheless, the CPB of PPEGA was concluded to be highly swollen, as had been previously observed for the CPBs of PS and PMMA in toluene ($L_e/L_{c,w}$ = 0.6 - 0.8). By contrast, the CPB of PHEA was less swollen in aqueous solution. This means that the solvent quality of water is insufficient for the CPB of PHEA in spite of the fact that water can dissolve PHEA.[3] The CPB is expected to be more difficult to be swollen in a solvent because of larger elastic stress caused by its highly stretched chain conformation, as compared with an equivalent free chain. For PPEGA more hydorophilic than PHEA, water was good enough to highly stretch away the chains in its Such difference in solvent quality was confirmed as the difference in interaction between the CPBs in

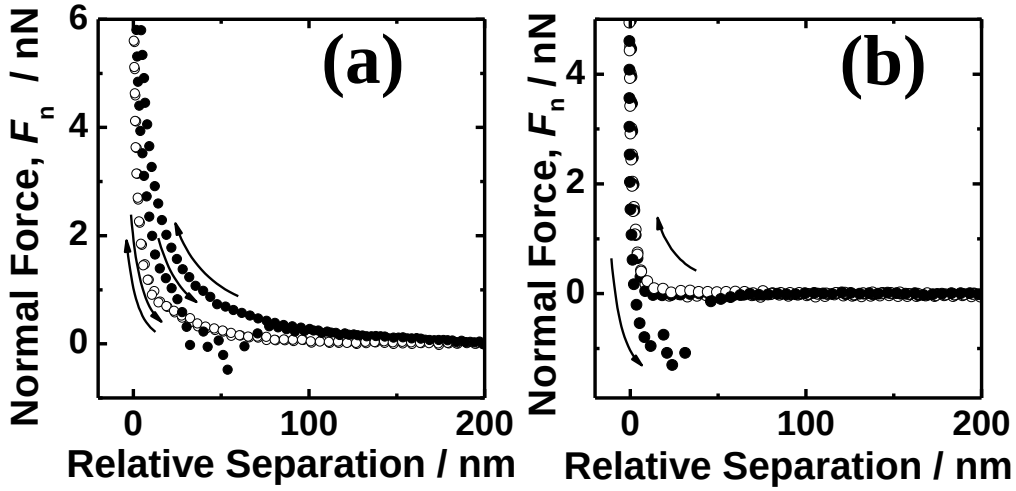

Figure 5-5. Approaching and retracting-mode force curve profiles measured between PHEA brushes and PPEGA brushes in (a) water ((●) PHEA Wafer 1/Probe 1 and (○) PPEGA Wafer 1/Probe 1) and in (b) 10^{-1} M NaCl aqueous solution ((●) PHEA Wafer 1/Probe 1 and (○) PPEGA Wafer 2/Probe 1).

aqueous solutions. Figure 5-5 shows typical force profiles measured in the approaching and retracting modes between the confronted CPBs (using the brush-modified probe) in (a) pure water and (b) 0.1 M NaCl aqueous solution; the abscissa in this figure is relative separation, since the "off-set" distance was not determined using the brush-modified probe. The above-mentioned, long-ranged repulsion force owing to the electrostatic interaction was also seen between the CPBs only in pure water. More importantly, an adhesive interaction was clearly observed in each aqueous solution between the CPBs of PHEA but not between the CPBs of PPEGA. This indicates the attractive interaction between the PHEA segments in water and hence insufficient solvent quality of water for PHEA. The observed adhesion force was estimated to be about 1.5 nN in average both in pure water and in salt-aqueous solution. This strongly affected the frictional property between the CPBs, as will be discussed.

5-3-3. Frictional property of PHEA and PPEGAA brush

Figure 5-6 shows the F_n-dependence of μ for the concentrated brushes of PHEA and PPEGA measured at v = 7 μm/s in pure water and 0.1 M NaCl aqueous solution. Since an adhesion force acts as an additional normal load as previously indicated (section 2-2-2), the μ value was corrected by adhesion force F_a as $\mu = F_s / (F_n + F_a)$ and plotted in the figure, suggesting that such correction had little effect on the following discussion. At low loads, the μ increased with F_n in any case, and for each brush system, the value in water was significantly smaller than that in the presence of 0.1 M NaCl. These presumably suggest that the lubricating layer of solvent was constructed between the confronted CPBs and that the electrostatically repulsive interaction was contributed to stabilize it, but that such layer was easily destroyed by applying normal force even in water. The contribution of electrostatic interaction was limited only at low loads, since it was not originated from the brush component but possibly from a small amount of charges remaining on the silica-substrate surfaces.

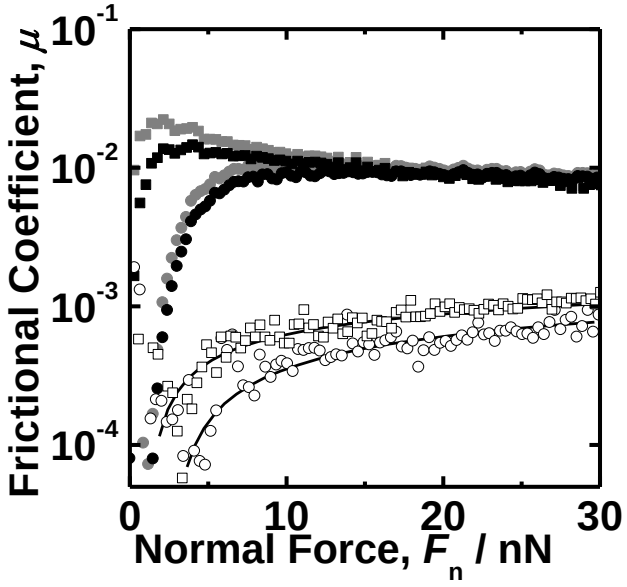

Figure 5-6. Plot of frictional coefficient μ vs normal force F_n measured at a shear velocity v of 7 μm/s between PHEA brushes (closed symblos) and PPEGA brushes (open symbols). PHEA; (●) Wafer 1/Probe 1 in water and (■) Wafer 1/ Probe 1 in 10^{-1}M NaCl aqueous solution, PPEGA; (○) Wafer 1/Probe 1 in water and (□) Wafer 2/Probe 1 in 10^{-1}M NaCl aqueous solution. For PHEA brushes, the data corrected by adhesion force (see text) were also plotted by black symbols.

As a more important issue, the author discusses the friction/lubrication at sufficiently high loads. Each brush system gave nearly the same μ value in spite of the addition of salt. This is consistent to the fact that the electrostatic interaction was not so large in these systems as mentioned above. In contrast, a quite large difference in μ (by an order of magnitude) was observed for the two brush systems, which will be discussed below. The μ value at F_n = 20 nN (as the saturated value in Figure 5-6) was plotted against v on the double-logarithmic scale in Figure 5-7. The author detected little differences in μ with and without NaCl (i.e., little contribution of electrostatic interaction) as well as the brush thickness in the examined ranges. The detailed studies on these factors are underway in our laboratory. Here, the author focuses on the difference between the two brush systems. The data of v-dependence of μ enabled us to discuss the lubrication mechanism in detail. For the CPBs of PMMA and PS in non-aqueous solvents, the author previously proposed two mechanisms; i.e., the hydrodynamic and boundary lubrications. These two mechanisms were observed as v-dependent and less dependent μ values at higher and lower v regions, respectively. Figure 5-7 clearly suggests these two regions for each brush system. It was rather difficult to precisely determine the slope in the

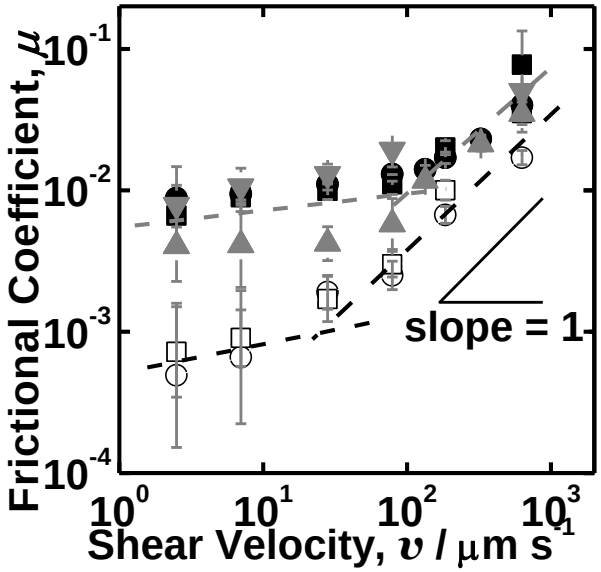

Figure 5-7. Plot of frictional μ vs shear velocisy υ measured at a normal force of 20 nN between PHEA brushes and between PPEGA brushes in water (circles and triangles) and 10^{-1} M NaCl aqueous solution (squares). PHEA; (●) Wafer 1/Probe 1, (▲) Wafer 3/Probe 2 and (▼) Wafer 4/Probe 3 in water, (■) Wafer 1/Probe 1 in 10^{-1} M NaCl aqueous solution, PPEGA; (○) Wafer 1/Probe 1 in water and (□) Wafer 2/Probe 1 in 10^{-1} M NaCl aqueous solution.

hydrodynamic lubrication regime (υ > 200 μm/s), but it seemed to follow the dependency with a slope of unity (i.e., Equation (2-5) with α = 1), as expected for the Newtonian fluid. This was the case with our previously studied CPBs in solvents (α = 0.7 - 1). In this case, the slight difference in μ and hence β between the two brush systems was presumably ascribed to the difference in solvent quality and hence the degree of swelling.

Then, the author discusses the boundary lubrication, where the interaction between the confronted brushes dominates the friction. Especially, the solvent-swollen CPB was characterized by much improvement of lubrication in this regime, reaching the order of 10^{-4} in μ under good-solvent condition. Figure 5-7 clearly show the boundary lubrication with the order of 10^{-4} in μ for the CPB of PPEGA but with higher μ for the CPB of PHEA. The difference between the two brush systems was also understood by the difference in solvent quality and hence the degree of swelling; the author already demonstrated that the adhesive interaction in e.g., insufficiently good solvents increased the friction.

5-4. Conclusion

By optimizing the polymerization condition of photo-induced TERP, the author succeeded in synthesizing CPBs of hydrophilic and electrically neutral polymers, PHEA and PPEGA, with molecular weights up to $M_n = 2 \times 10^5$ for PHEA and 1×10^5 for PPEGA as well as relatively narrow polydispersities of $M_w/M_n < 1.3$. The L_d of the produced graft layers increased up to ca. 100 nm for PHEA and 30 nm for PPEGA proportionally with M_n, suggesting constant σ. The σ values corresponded to σ* = 0.31 for PHEA and 0.42 for PPEGA, being high enough to be categorized into the regime of concentrated brush. The degree of swelling and frictional property of these CPBs in water media were measured using a colloidal-probe AFM technique. The PPEGA brush gave a L_e value comparable to the fully-stretched length of graft chain, while the PHEA brush did not as well. This was ascribed to the difference in hydrophilicity of these two polymers or in solvent quality of water for them. The v-dependencies of μ were well understood on the basis of the lubrication mechanism, boundary and hydrodynamic lubrications, previously proposed for non-aqueous CPBs. The poorer hydrophilicity of PHEA induced some adhesion force between the brush surfaces and hence increased the μ to the order of 10^{-2} in boundary lubrication. In contrast, the concentrated PPEGA brush achieved a μ value on the order of 10^{-4} similarly to the previously reported non-aqueous CPBs. Because the graft polymers have no charged groups, the addition of salt little affected the above-mentioned swollen structure and frictional properties. This means that such super lubrication was achieved without help of electrostatic interaction, being common to the CPB under good-solvent condition. This study would offer a promising route for designing novel bio-medical materials demanding not only bio-compatibility but also good lubrication.

References

(1) (a) Majewski, J.; Kuhi, T. L.; Gerstenberg, M. C.; Israelachvili, J. N.; Smith, G. S. *J. Phys. Chem. B* **1997**, *101*, 3122-3129. (b) Wagner, M. L.; Tamm, L. K. *Biophys. J.* **2000**, *79*, 1400-1414. (c) Currie, E. P. K.; Norde, W.; Stuart, M. A. C. *Adv. Coll. Interf. Sci.* **2003**, *100*, 205-265. (d)Nagase, K.; Kobayashi, J.; Kikuchi, A.; Akiyama, Y.; Kanazawa, H.; Okano, T. *Langmuir* **2008**, *24*, 511-517. (e) Tam, T. K.; Ornatska, M.; Pita, M.; Minko, S.; Katz, E. *J. Phys. Chem. C* **2008**, *112*, 8438-8445.

(2) (a) Yoshikawa, C.; Goto, A.; Tsujii, Y.; Fukuda, T.; Yamamoto, K.; Kishida, A. *Macromolecules* **2005**, *38*, 4604-4610. (b) Yoshikawa, C.; Goto, A.; Tsujii, Y.; Fukuda, T.; Kimura, T.; Yamamoto, K.; Kishida, A. *Macromolecules* **2006**, *39*, 2284-2290. (c) Yoshikawa, C.; Goto, A.; Tsujii, Y.; Ishizuka, N.; Nakanishi, K.; Fukuda, T. *J. Polym Sci. Part A: Polym. Chem.* **2007**, *45*, 4795-4803. (d) Yoshikawa, C.; Hashimoto Y, Hattori, S.; Honda, T.; Zhang, K.; Terada D.; Kishida, A.; Tsujii, Y.; Kobayashi, K. *Chem. Lett.* **2010**, *39*, 142-143.

(3) Brandrup, J.; Immergut, E. H.; Grulke, E. A., Eds.; *Polymer Handbook*; John Wiley & Sons Inc: New York, 1999.

(4) Raviv, U.; Giasson, S.; Kampf, N.; Gohy, J. F.; Jerome, R.; Klein, J. *Nature* **2003**, *425*, 163-165.

(5) (a) Ishihara, K.; Nomura, H.; Mihara, T.; Kurita, K.; Iwasaki, Y.; Nakabayashi, N. *J. Biomed. Mater. Res.* **1998**, *39*, 323-330. (b) Feng, W.; Zhu, S. P.; Ishihara, K.; Brash, J. L. *Langmuir* **2005**, *21*, 5980-5987. (c) Zhang, Z.; Chao, T.; Chen, S. F.; Jiang, S. Y. *Langmuir* **2006**, *22*, 10072-10077.

(6) (a) Matsuda, Y.; Kobayashi, M.; Annaka, M.; Ishihara, K.; Takahara, A. *Langmuir* **2008**, *24*, 8772-8778. (b) Kobayashi, M.; Terada, M.; Terayama, Y.; Kikuchi, M.; Takahara, A. *Macromolecules* **2010**, *43*, 8409-8415.

(7) (a) Sakata, H.; Kobayashi, M.; Otsuka, H.; Takahara, A. *Poly. J.* **2005**. *37*, 767-775. (b) Kobayashi, M.; Terayama, Y.; Hosaka, N.; Kaido, M.; Suzuki, A.; Yamada, N.; Torikai, N.; Ishihara, K.; Takahara, A. *Soft Matter* **2007**, *3*, 740-746. (c) Kobayashi, M.; Takahara, A. *Chem.*

Rec. **2010**, *10*, 208-216. (d) Ishikawa, T.; Kobayashi, M.; Takahara, A. *ACS Appl. Mater. Interf.* **2010**, *2*, 1120-1128.

(8) Chen, M.; Briscoe, W. H.; Armes, S, P.; Klein, J. *Science* **2009**, *323*, 1698-1701.

(9) (a) Han, S.; Hagiwara, M.; Ishizone, T. *Macromolecules* **2003**, *36*, 8312-8319. (b) Tanaka, M.; Mochizuki, A. *J. Biomed. Mater. Res. Part A* **2004**, *68A*, 684-695. (c) Hua, F. J.; Jiang, X. G.; Li, D. J.; Zhao, B. *J. Polym. Chem. Part A: Polym. Chem.* **2006**, *44*, 2454-2467.

(10) (a) Yamago, S.; Iida, K.; Yoshida, J. *J. Am. Chem. Soc.* **2002**, *124*, 2874-2875. (b) Yamago, S.; Lida, K.; Yoshida, J. *J. Am. Chem. Soc.* **2002**, *124*, 13666-13667. (c) Yamago, S.; Iida, K.; Nakajima, M.; Yoshida, J. *Macromolecules* **2003**, *36*, 3793-3796. (d) Yamago, S. *Chem. Rev.* **2009**, *109*, 5051-5068.

(11) Coca, S.; Jasieczek, C. B.; Beers, K. L.; Matyjaszewski, K. *J. Polym. Sci. Part A: Polym. Chem.* **1998**, *36*, 1417-1424.

(12) Ohno, K.; Morinaga, T.; Koh, K.; Tsujii, Y.; Fukuda, T. *Macromolecules* **2005**, *38*, 2137-2142.

(13) Yamago, S.; Ukai, Y.; Matsumoto, A.; Nakamura, Y. *J. Am. Chem. Soc.* **2009**, *131*, 2100-2101.

(14) Kwak, Y.; Goto, A.; Fukuda, T.; Kobayashi, Y.; Yamago, S. *Macromolecules* **2006**, *39*, 4671-4679.

(15) Bell, W.; Colehamil, D. J.; Culshaw, P. N.; Mcqueen, A. E. D., Shenaikhatkhate, D. V.; Walton, J. C.; Hails, J. E. *J. Organomet. Chem.* **1992**, *430*, 43-52.

(16) Kwak, Y.; Tezuka, M.; Goto, A.; Fukuda, T.; Yamago, S. *Macromolecules* **2007**, *40*, 1881-1885.

(17) (a) Tsujii, Y.; Ejaz, M.; Sato, K.; Goto, A.; Fukuda, T. *Macromolecules* **2001**, *34*, 8872-8878. (b) Morinaga, T.; Ohkura, M.; Ohno, K.; Tsjii, Y.; Fukuda, T. *Macromolecules* **2007**, *40*, 1159-1164.

Chapter 6

Synthesis and Frictional Property of Thermo-Responsible Concentrated Polymer Brushes

6-1. Introduction

In Chapter 5, the CPBs of hydrophilic polymers were newly synthesized and super lubrication was achieved for one of them in water media, which would offer a new surface modification technique for bio-medical devices. Meanwhile, the ability to control and manipulate friction is extraordinarily important in many applications ranging from bio-lubricating systems[1] to micromechanical devices.[2] However, the understanding of friction especially in bio-systems,[3] achieving intelligent friction[4] still remains great challenges for advanced applications.

Poly (*N*-isopropyl acrylamide) (PNIPAM) is one of the well known polymers with thermo-responsibility in water media sharply changing its conformation and solubility, according to a LCST-type phase separation around 32 ºC.[5] Due to its transition temperature at around ambient and body temperature of our living sphere, PNIPAM has been widely used ranging from the fundamental studies on polymer-solution properties to application researches for bio-medical materials. As one of the most intensively studied applications, PNIPAM was grafted on membrane surfaces to control cell adhesion by changing the wettability of the outermost surfaces.[6] However, those PNIPAM-grafted membranes had insufficiently well organized, discouraging the closer fundamental study on transitions in solubility, hydrophilicity, and lubricity.

In order to control the structural parameters, the surface-initiated LRP would be one of the most useful approaches, as the author achieved in the former Chapters. The fabrication of CPB of PNIPAM would offer us novel model surfaces not only to investigate the swelling and friction properties of polymer brush as a function of temperature but also for the evolution of bio-lubricating materials. In this study, CPB and SDPB of PNIPAM are fabricated through surface-initiated ATRP and studied on their swelling and friction properties as a function of temperature to discuss the

detailed mechanism of friction/lubrication and its temperature-induced transition.

6-2. Experiment

6-2-1. Materials

N-Isopropyl acrylamide (NIPAM, Wako Pure Chemicals, Japan, 98%) was recrystallized three times from a toluene/hexane mixture prior to use. Copper(I) chloride (Cu(I)Cl, 99.9%), copper(II) chloride (Cu(II)Cl_2, 99.9%), dimethyl sulfoxide (DMSO) (dehydrated, 99%), allylamine (98%), propylamine (98%), 2-chloropropionyl chloride (95%), and 3-chloropropyltriethoxysilane (CPT) (97%) were purchased from Wako Pure Chemicals and used as received. Tris[2-(dimethylamino)ethyl]amine (Me_6TREN) was prepared as described in the literature.[7] Triethoxysilane (99%) was obtained from Chisso Corp., Tokyo, Japan, and distilled before use. A solution of platinum catalyst (Karstedt's catalyst) (Pt-114, platinum content: 3 wt%) was received from Johnson Matthey Catalysts, Royston, UK. All other reagents were used as received from commercial sources.

6-2-2. Synthesis of *N*-propyl-2-chloropropanamide (PCP)

A free initiator, *N*-propyl-2-chloropropanamide (PCP), was synthesized by the amidation of allylamine with 2-chloropropionyl chloride. 2-Chloropropionyl chloride (25 g, 197 mmol) was added dropwise to a solution of propylamine (12 g, 204 mmol) and triethylamine (20 mL, 198 mmol) in dry THF (200 mL) at 0 °C. The mixture was magnetically stirred for 3 h at 0 °C and then for another 10 h at room temperature. After the reaction, the solution was passed through a filter paper, and the filtrate was evaporated to dryness under reduced pressure. The residue was diluted with chloroform (200 mL) and washed twice with 1 N HCl aqueous solution (2 × 200 mL), twice with $NaHCO_3$-saturated aqueous solution (2 × 200 mL), and with water (500 mL). After the solution was dried over Na_2SO_4 and filtered off, the solvent was evaporated, giving a brown oil. This crude product was subsequently purified by flash chromatography on a column of silica gel with a mixture of hexane and ethyl acetate (5/1, v/v) as an eluent to yield PCP as a transparent liquid (32 g, 86%).

^{1}H NMR ($CDCl_3$): δ 0.95 (t, 3H, CH_2CH_3), 1.60 (m, 2H, $CH_3CH_2CH_2$), 1.73 (d, 3H, $CHCH_3$), 3.2 (q, 2H, CH_2CH_2NH), 4.40 (q, 1H, $COCHClCH_3$), 6.8 (br, s, 1H, NH). ^{13}C NMR ($CDCl_3$): δ 11.1 (CH_3CH_2), 22.4 ($CHCH_3$), 22.5 (CH_3CH_2), 41.4 (CH_2CH_2NH), 55.8 ($COCHClCH_3$), 169.4 (NHCO). Anal. Calcd for $C_6H_{12}NOCl$: C, 46.21; H, 8.40; O, 10.69, N, 9.36, Cl, 23.70. Found: C, 46.37; H, 8.46; O, 10.72, N, 4.38, Cl, 11.53.

6-2-3. Synthesis of 2-chloro-*N*-(3-(triethoxysilyl)propyl)propanamide (CTP)

A surface-immobilizable initiator, 2-chloro-*N*-(3-(triethoxysilyl)propyl)propanamide (CTP), was newly designed and synthesized via the two-step reaction as follows. First, *N*-allyl-2-chloropropanamide was synthesized according to the same procedure as described for PCP. Finally, a colorless oil was obtained with a 90% yield. ^{1}H NMR ($CDCl_3$): δ 1.75 (d, 3H, $CHCH_3$), 3.91 (q, 2H, $CHCH_2NH$), 4.45 (q, 1H, $COCHClCH_3$), 5.15-5.25 (m, 2H, CH_2=CH), 5.80-5.92 (m, 1H, CH_2=CH), 6.82 (s, 1H, NH). ^{13}C NMR ($CDCl_3$): δ 22.6 ($CHCH_3$), 42.0 ($CHCH_2NH$), 55.7 ($COCHClCH_3$), 116.5 (CH_2=CH), 133.3 (CH_2=CH), 169.3 (NHCO). Anal. Calcd for $C_6H_{10}NOCl$: C, 48.82; H, 6.83; O, 10.84, N, 9.49, Cl, 24.02. Found: C, 46.93; H, 6.62; O, 12.00, N, 9.03, Cl, 24.45.

Then, CTP was synthesized via the hydrosilylation reaction between *N*-allyl-2-chloropropanamide and triethoxysilane in the presence of Karstedt's catalyst. The reaction was carried out in a glovebox purged with argon gas. In brief, *N*-allyl-2-chloropropanamide (15 g, 101 mmol) and dry toluene (50 mL) were charged into a two-neck round-bottom flask equipped with a magnetic stir bar and a rubber septum. Freshly distilled triethoxysilane (100 mL, 0.54 mol) and subsequently a solution of Karstedt's catalyst (200 μL) was added dropwise into the flask by a syringe. The reaction mixture was magnetically stirred under an argon atmosphere at room temperature for 48 h. The complete consumption of *N*-allyl-2-chloropropanamide was confirmed by ^{1}H NMR spectroscopy. Excess triethoxysilane and toluene were removed under vacuum at 50 °C to afford CTP as a slightly yellow liquid in a quantitative yield. ^{1}H NMR ($CDCl_3$): δ 0.65 (t, 2H, $SiCH_2$), 1.25 (t, 9H, CH_3CH_2OSi), 1.60 (m, 2H, $CH_2CH_2CH_2$), 1.75 (d, 3H, $CHCH_3$), 3.30 (q, 2H, $CHCH_2NH$), 3.84 (q, 6H, CH_3 2OSi), 4.30 (q, 1H, $COCHClCH_3$), 6.80 (s, 1H, NH). ^{13}C NMR

(CDCl3): δ 7.5 (Si*C*H2), 18.2 ($SiOCH_2CH_3$), 22.7 ($CH_2CH_2CH_2$, $CHCH_3$), 42.0 (CH_2CH_2NH), 56.0 ($COCHClCH_3$), 58.4 ($SiOCH_2CH_3$), 169.3 (NH*C*O). Anal. Calcd for $C_{12}H_{26}NO_4ClSi$: C, 46.21; H, 8.40; N, 4.49, Cl, 11.37. Found: C, 46.37; H, 8.46; N, 4.38, Cl, 11.53.

6-2-4. Synthesis of PNIPAM Brushes via Surface Initiated ATRP

A silicon wafer (Ferrotec Corp., Japan, thickness 0.5 mm) treated with ultraviolet (UV) / ozone for 15 min was immersed for 12 h at room temperature in an ethanol solution containing CTP/CPT mixture (1 wt%) and 28%-aqueous ammonium (5 wt%) and then copiously rinsed with ethanol. Under an argon atmosphere, the CTP-immobilized wafer was immersed in a degassed DMSO solution of NIPAM (3.0 M), Cu(I)Cl (2.9 mM), $Cu(II)Cl_2$ (1.0 mM), Me_6TREN (3.9 mM), and PCP (1.5 mM) at room temperature for a given time. PCP was used as a "sacrificial" free initiator producing a free polymer as a useful reference in molecular weight and molecular weight distribution for the graft polymer.[8] The polymerization solution was directly analyzed by gel permeation chromatography (GPC) and ^{1}H NMR to estimate the molecular weights of free polymers and the monomer conversion, respectively. The as-prepared sample was rinsed in a Soxhlet apparatus with methanol for at least 10 h to remove physisorbed free polymers and impurities. The thicknesses of dried and swollen PNIPAM brushes were measured by ellipsometry and AFM. No characteristic structure was observed by AFM on the surfaces either before or after graft polymerization, suggesting that the initiating groups were immobilized on the surface randomly in a scale smaller than the AFM resolution.

The same protocol was used to prepare PNIPAM brushes on silica spheres (SiP, HIPRESICA SP, diameter 10 μm, obtained from Ube Nitto Kasei Co., Ltd.), which were suspended with help of magnetic stirring in the mixture solution of surface initiator and then the polymerization solution. The brush-modified silica particles thus obtained were rinsed by repeated dispersion/centrifugation cycles in methanol.

6-2-5. Frictional Force Measurement by AFM

An AFM (JPK Instruments Inc., Germany, Nano Wizard) was used to characterize the structure

and properties of PNIPAM brush surfaces. For the measurement of equilibrium swollen thickness, a bare unmodified SiP was attached on a V-shaped cantilever (Olympus Optical Co., Ltd., Japan, k_n = 0.15 N/m) with two-component epoxy resin adhesive and used as a probe. The detailed procedures of the AFM measurements were described in section 2-2-3. For the measurement of friction and adhesive forces between the brush surfaces, a brush-modified SiP prepared above was attached on a rectangular-shaped cantilever (Olympus Optical Co., Ltd, vertical spring constant, k_n = 0.73 N/m, lateral spring constant, k_s = 86 N/m) and used as aprobe.

6-2-6. Other Measurement

The GPC analysis for PNIPAM was made on a Tosoh CCP & 8020 series high-speed liquid chromatograph (Tokyo, Japan) equipped with a Tosoh differential refractometer RI-8020. DMF containing 10 mM LiBr was used as an eluent with a flow rate of 0.8 mL/min (40 °C). Two Shodex gel columns LF804 (300 × 8.0 mm; bead size = 6 μm; pore size = 20 - 3000 Å) (Tokyo) were installed and calibrated with poly (methyl methacrylate) (PMMA) standards. The M_w/M_n value was estimated according to this calibration. To estimate the absolute value of M_n, sample detection was also made with a multiangle laser light scattering (MALLS) detector, a Wyatt Technology DAWN EOS (Santa Barbara, CA), equipped with a Ga-As laser λ = 690 nm. The refractive index increment d*n*/d*c* was determined to be 0.0774 $mL \cdot g^{-1}$ by a Wyatt Technology OPTILAB DSP differential refractometer.

The thicknesses of the PNIPAM-brush layers in dry state (L_d) were determined by a compensator rotating, spectroscopic ellipsometer (M-2000U, J.A. Woolam, Lincoln, NE) equipped with D_2 and QTH lamps. The polarizer angle was 45°, and the incident angles were 60°, 65°, and 70°. The thickness was calculated using the refractive index determined for the spin-cast PNIPAM film with a thickness of ca. 200 nm.

^1H (300 MHz) and ^{13}C NMR (75 MHz) spectra were obtained on a JEOL/AL300 spectrometer.

6-3. Results and discussion

6-3-1. Preparation and Characterization of PNIPAM Brushes

The PNIPAM brushes were prepared by surface-initiated ATRP. Some previous reports dealt with LRP of NIPAM,[9] but sufficiently well control of chain length and its distribution was not achieved for the synthesis of CPB of PNIPAM. The author made an independent effort to optimize polymerization conditions to meet the purpose of this study, referring the report of ATRP of acrylamides using copper / tripodal amine catalytic system.[10] Figure 6-1 shows the polymerization result (the plot of M_n and M_w/M_n vs monomer conversion determined by GPC analysis) of ATRP of NIPAM with Cu(I)Cl / $Cu(II)Cl_2$ / Me_6TREN catalyst system using a chlorine type of free initiator PCP, where PMMA was used for the GPC calibration (filled circle symbols). The absolute values of

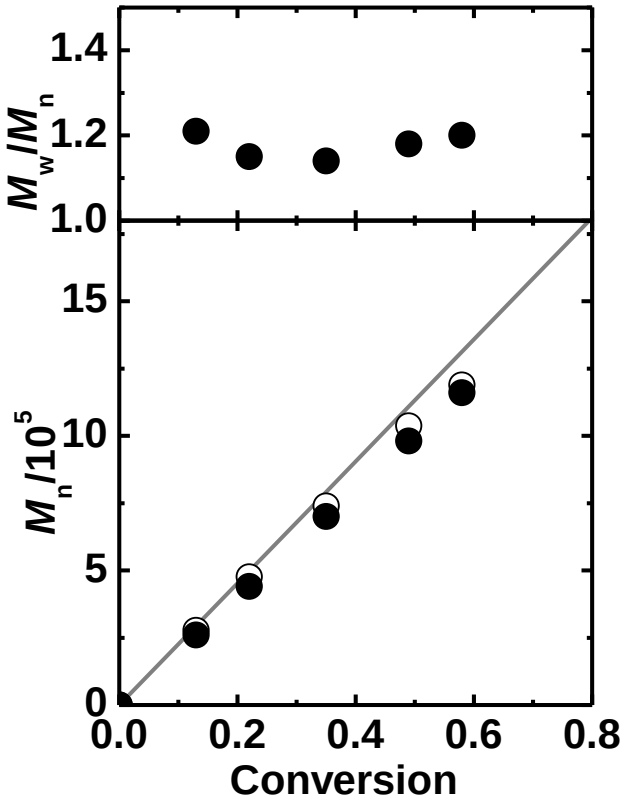

Figure 6-1. Plots of M_n and M_w/M_n vs conversion for the ATRP of NIPAM (●): the closed and open symbols represent the molecular weight data determined by the PMMA calibration and MALLS (as an absolute value), respectively.

M_n (open circle symbols) obtained by GPC-MALLS system were also plotted in Figure 6-1. The M_n proportionally increased with conversion and kept relatively low value of M_w/M_n (M_w/M_n < 1.2) throughout the polymerization. The absolute M_n are very close to the theoretical value (straight line), which is calculated from the monomer/initiator molar ratio and the conversion. These results suggest the controlled polymerization of NIPAM over 100,000 of M_n for the first time.

For applying the ATRP of NIPAM to surface-initiated graft polymerization, a chlorine type of surface initiator CHE corresponding to the free initiator PCP was newly synthesized. Silicon wafers immobilized with CHE on its surface were subjected to the ATRP of NIPAM. Figure 6-2 shows the L_d of resulting PNIPAM brush layers plotted against M_n of PNIPAM simultaneously produced from the free initiator PCP. There is a certain evidence to believe that the molecular weights of graft polymer are approximated to those of free polymer.[8] The thickness of PNIPAM brush layers linearly increased with increasing M_n, suggesting uniform growth of graft polymer with a constant surface density. From the slope of the line in Figure 6-2, the graft density σ of PNIPAM turned out to be ca. 0.7 chains/nm^2, using the equation in section 2-2-2 (bulk density ρ of PNIPAM was assumed to be

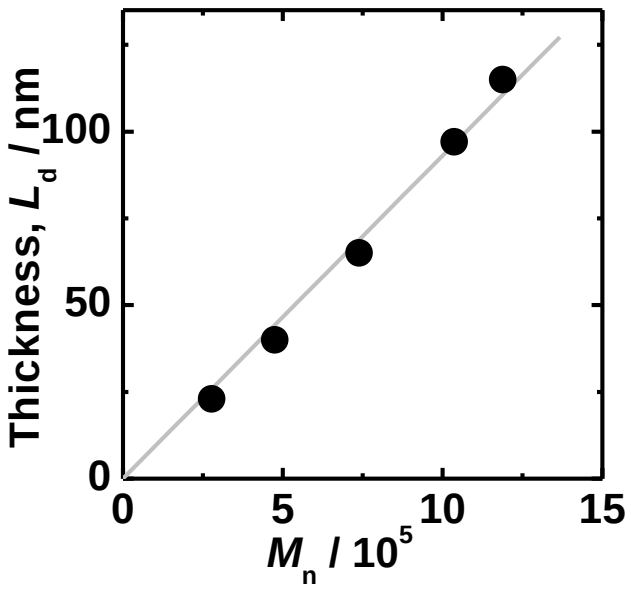

Figure 6-2. Relationship between the brush thicknesses in dry state, L_d, and the M_n of free polymer.

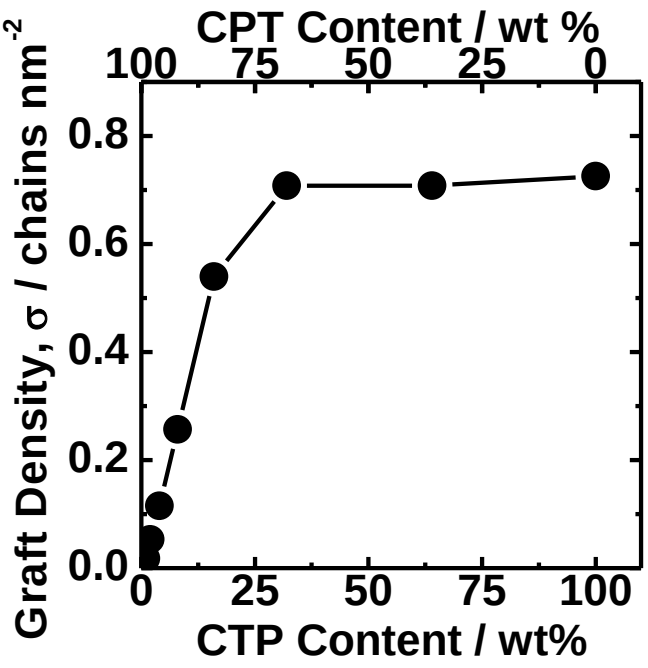

Figure 6-3. Graft density σ of grafted PNIPAM brushes plotted against the composition of surface initiator (CTP) in a solution used during the immobilization process for silicon wafer.

1.0 g/cm^3). This graft density corresponds to a dimensionless graft density σ* of 0.5, higher than the critical value (σ* = 0.1) at the crossover between SDPB and CPB regime. Thus, the prepared PNIPAM brush was concluded to be in the CPB regime.

The graft density of the PNIPAM brush was able to be successfully controlled by mixing an inert silane-coupling agent, CPT, with CTP and immobilizing them on silicon wafers and SiPs. Figure 6-3 shows the graft density of the PNIPAM brushes on thus prepared substrates as a function of CTP content in an immobilization solution. On the silicon wafer with only CPT immobilized, almost no propagation of brush layer was observed after the polymerization, confirming that CPT is

Table 6-1. Characteristics of PNIPAM Brush Samples

PNIPAM Brush Samples	M_n	M_w/M_n	L_d / nm	σ / chains nm^{-2}	σ*
CPB on wafer	51,000	1.15	60	0.7	0.5
CPB on SiP	50,000	1.14	-	-	
SDPB on wafer	52,000	1.17	4	0.05	0.04
SDPB on SiP	53,000	1.15	-	-	

totally inert for the graft polymerization in this study. As Figure 6-3 shows, the graft density increased with increasing CTP content and approached a constant and maximum value over the 30 wt%-CTP content. This means that not all of surface initiators and but 30% of them are effective as surface-initiation points, when the substrate surface was fully covered with CTP. In such cases, the graft density is determined by a steric effect of polymer segment in the surface-initiated polymerization but not by the density of initiator on the surface.[11]

6-3-2. Swelling and Friction Properties of PNIPAM Brushes

Typical PNIPAM brush samples used for the following study were tabulated in Table 6-1, including the brushes of high graft density (σ = 0.7 chains nm^{-2}, corresponding to CPB) and low graft density (σ = 0.05 chains nm^{-2}, corresponding to SDPB) prepared on wafers and SiPs (used as probes for the friction measurement between PNIPAM brush surfaces). Figure 6-4 shows the equilibrium swollen thickness L_e in water plotted against temperature. Here, the L_e value was normalized with the weight-average full length of graft chains in the all-trans conformation $L_{c,w}$. The L_e of CPB of PNIPAM was also measured in ethanol, a good solvent for PNIPAM and plotted as the

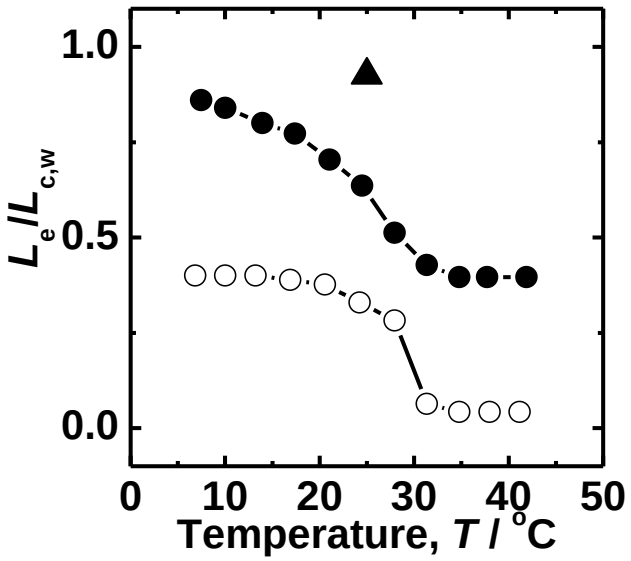

Figure 6-4. Temperature T dependence of degree of swelling $L_e/L_{c,w}$ in water for CPB (●, $L_{c,w}$ = 129 nm) and SDPB of PNIPAM (○, $L_{c,w}$ = 134 nm). The $L_e/L_{c,w}$ of CPB of PNIPAM in ethanol at 25 ºC was also plotted (▲).

triangle symbol. The $L_e/L_{c,w}$ in ethanol reached 0.9, suggesting that this PNIPAM brush extended to nearly full stretched length of the graft chains, as expected for the CPB (see section 1-1-7). This, in addition to the above-mentioned high value of σ*, confirmed that this PNIPAM brush is in the regime of CPB. The $L_e/L_{c,w}$ of the PNIPAM brush in water at 8 ºC also showed a high value (0.8), which indicated that water at 8 ºC is also a good solvent for PNIPAM like ethanol, but gradually decreased with increasing of water temperature and became constant around 0.5 above 30 ºC. This should be attributed to decreasing hydrophilicity and dehydration of PNIPAM with temperature, which is peculiar to PNIPAM having LCST-type phase behavior in water.[5] The $L_e/L_{c,w}$ of the CPB of PNIPAM above 30 ºC suggested almost non-swollen state. Meanwhile, the $L_e/L_{c,w}$ of SDPB sample showed smaller values at low temperature and more sharply changed from a swollen to non-swollen state with increasing temperature at around 30 ºC, than the case of CPB one. The temperature-induced change in degree of swelling observed for the SDPB of PNIPAM was approximated by the coil-to-globule transition for the dilute solution of free PNIPAM[4]. Comparing those two swelling properties of CPB and SDPB of PNIPAM, the gradual shrinkage of the CPB of

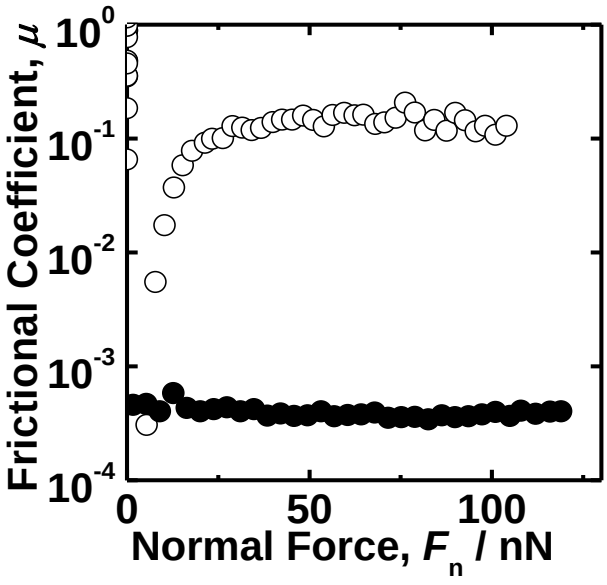

Figure 6-5. Plot of frictional coefficient μ vs normal force F_n measured at a shear velocity v of 6 μm/s for the CPB (●) and SDPB (○) of PNIPAM in water of 8 ºC.

PNIPAM would result from its highly stretched chain conformation even in non-swollen state. A larger cost (better solvent quality) is needed to further extend a more highly stretched chain than the case of non-stretched chain, which would broaden the change in the degree of swelling with temperature. Therefore, the gradual shrinkage of CPB of PNIPAM can be considered as one of the unique characters of CPB.

Water lubrication between the brushes was measured. First, the author discusses the result at a temperature of 8 ºC at which water is good enough as a solvent for PNIPAM as described above. Figure 6-5 shows the μ plotted against normal load F_n for the CPB and SDPB of PNIPAM at a shear velocity of 6 μm/s shear velocity. The SDPB of PNIPAM has two different lubrication regimes; at low applied loads, the μ is very low (< 10^{-3}), and then at an onset of the threshold, it steeply increases with increasing F_n, approaching a constant μ value about 0.1 at higher normal loads. Such a transition from low to high-frictional stages is usually found in SDPBs due to mutual interpenetration of confronted brushes at higher normal forces, as mentioned in Chapter 1. On the

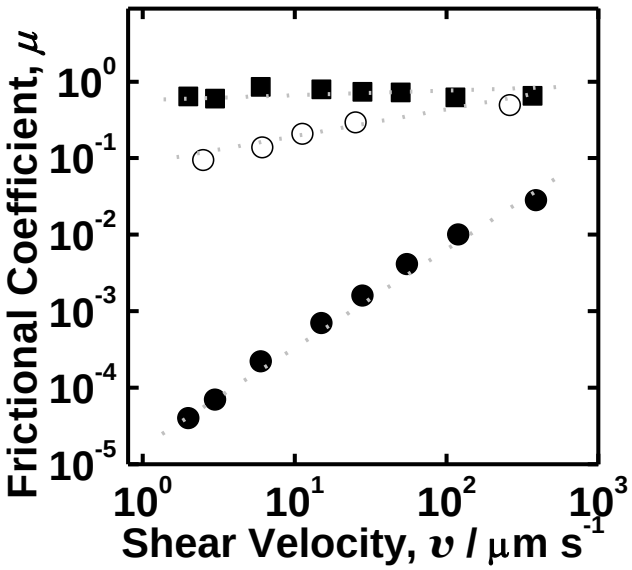

Figure 6-6. Plot of frictional coefficient μ vs shear velocity v measured at a normal force F_n of 100 nN for the CPB (closed symbols) and SDPB (open symbols) of PNIPAM at 8 ºC (circles) and 43 ºC (squares).

other hand, the μ between the CPBs of PNIPAM showed no such transition, staying at exceptionally low values of 4×10^{-4} in the applied normal loads up to 120 nN. Such excellent water lubrication was also observed for the CPB of PPEGA but not for that of PHEA (see Chapter 5). Sufficient hydorphilicity and swollen state of brush layers are requisite for developing ultra-low frictional property in water media.

Figure 6-6 shows the v-dependence on μ for the CPB and SDPB of PNIPAM at F_n = 100 nN. The CPB of PNIPAM at temperature of 8 ºC showed a good power-law relationship between μ and v, suggesting the hydrodynamic lubrication regime as mentioned in Chapter 2. The boundary lubrication regime of μ less dependent on v (expectedly at lower v region) was not seen in the examined range of v. This would imply the μ in boundary lubrication state is lower than the 10^{-4} order in this case. The power-law exponent (the slope in the Figure 6-6) of hydrodynamic lubrication between the CPBs of PNIPAM was close to unity, as like the case of other CPBs. On the other hand, the μ values between the CPBs of PNIPAM at 43 ºC and the SDPBs of PNIPAM at 8 ºC were less

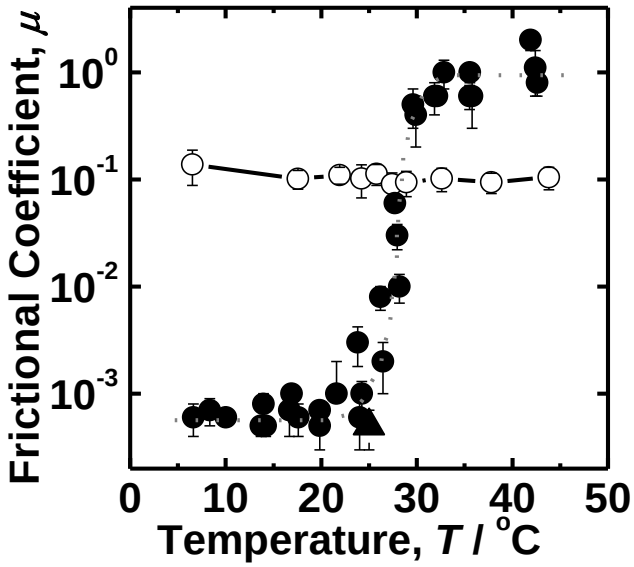

Figure 6-7. Temperature T dependence of frictional coefficient μ for the CPB (●) and SDPB (○) of PNIPAM in water. The measurement condition is normal force F_n of 100 nN and shear velocity v of 6 μm/s. The frictional coefficient of the CPB of PNIPAM measured in ethanol was also plotted at 25 ºC (▲).

dependent on v, indicating the boundary lubrication state. Interestingly, the CPB of PNIPAM at 43 ºC showed a higher μ than the SDPB of PNIPAM, which is presumably related to the fact that the former is totally in non-swollen state.

Figure 6-7 shows the temperature dependence of between the CPBs and between the SDPBs. The SDPB of PNIPAM gave an almost constant μ ca. 0.1 in the temperature range of 8 ºC < T < 44 ºC. The exact reason for little change in μ above and below the transition temperature is not clear at present, but it may be ascribed to the complementary interaction by interpenetration and adhesion (will be discussed in following section) at low and high temperatures. In contrast, the CPB of PNIPAM showed a sharp frictional transition triggered by increasing temperature; the μ was on the order of 10^{-4} at low temperatures (T < 20 ºC) and rapidly increased in a temperature range of 20 ºC < T < 30 ºC, reaching an almost constant μ of ca. 1 above 30 ºC. This means that the μ changed by more than three orders of magnitude within a small span of temperature. Even in a non-swollen state, the CPB layers hardly interpenetrate each other. Therefore, the rapid increase in μ would be caused by change in the degree of swelling or interaction between the chain segments near the brush surfaces. It should be noted that the μ of CPB of PNIPAM in a good solvent ethanol was also in the

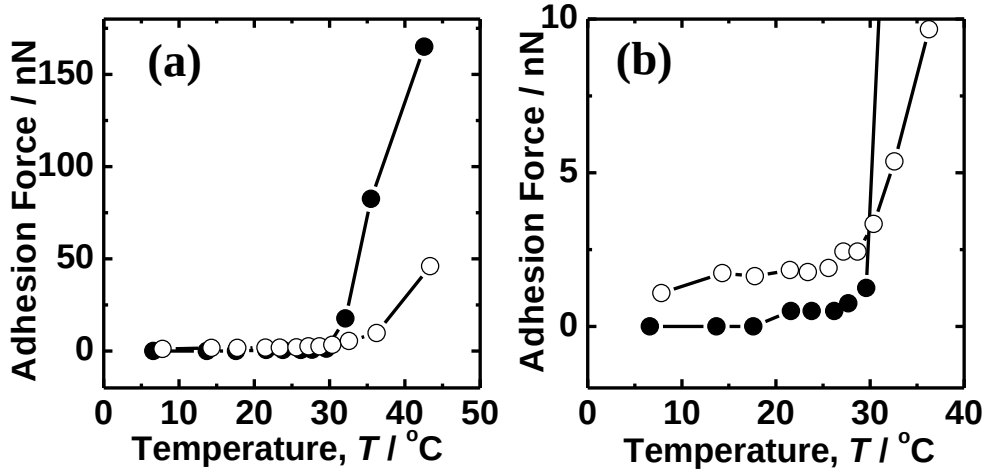

Figure 6-8. Temperature T dependence of adhesion force for the CPB (●) and SDPB (○) of PNIPAM in water. The Figure (b) shows magnified drawing of the Figure (a).

order of 10^{-4}.

Figure 6-8 shows the adhesion force between the confronted brushes measured without modulation, clearly suggesting that both SDPB and CPB of PNIPAM gave a rapid increase in adhesion forces at around 30 ºC due to their dehydration. The adhesion force between the CPBs of PNIPAM was larger than that between the SDPBs of PNIPAM above 30 ºC, which is consistent with the fact that the former had higher μ values than the latter in this temperature range. This would imply the stronger segment-segment interaction between the CPBs of PNIPAM, presumably owing to lower surface roughness and hence larger contact area in a shrunken state. As shown in Figure 6-8 (b), the adhesion force between SDPBs of PNIPAM at low temperatures (T < 20 ºC) showed a small but detectable value (~ 2 nN), which is ascribed to the interpenetrating interaction between them. By contrast, the adhesion force between the CPBs of PNIPAM did not show any detectable value, which should be responsible for super lubrication in boundary lubrication state.

In order to discuss the relationship between the frictional property and swollen structure of the

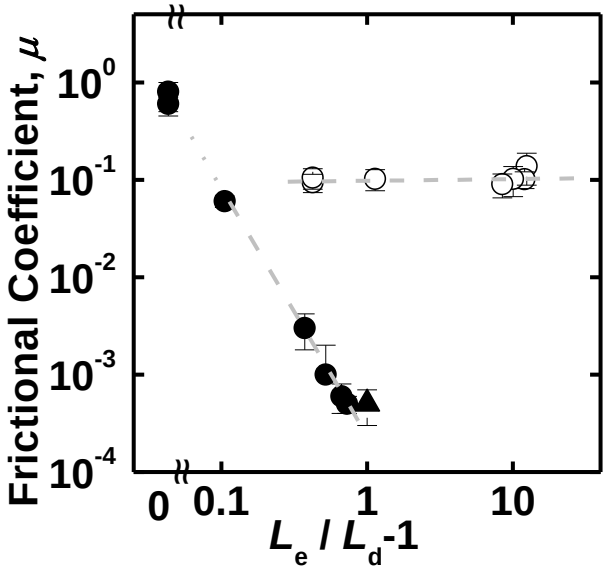

Figure 6-9. Plots of frictional coefficient μ of PNIPAM brushes vs their degree of swelling L_e/L_d-1. Each symbol denotes the results of the CPB of PNIPAM in water (●) and ethanol (▲) and the SDPB of PNIPAM in water (○). The applied normal force is 100 nN.

PNIPAM brushes, the μ of SDPBs and CPBs of PNIPAM were plotted against the degree of swelling, L_e/L_d-1, in Figure 6-9 in double logarithmic scale. As mentioned in Chapter 2, the degree of swelling plays crucial role in determining friction in the hydrodynamic lubrication but little affect the boundary lubrication state. In fact, the SDPB of PNIPAM gave little dependency in the studied condition, in which it was in boundary lubrication state as already discussed in Figure 6-6. In contrast, the CPBs of PNIPAM showed good scaling below 30 ºC. This indicates the hydrodynamic lubrication state in this temperature range. The increase of frictional coefficient in the temperature range of 20 ºC < T < 30 ºC in Figure 6-7 is attributed to gradual shrinking of the brush layer. The exponent in this scaling was about -2.5, which is presumably understood by the change in the degree of swelling simultaneously affecting the viscosity and thickness of effective hydrodynamic lubrication layer as shown by Equation (2-5).

6-4. Conclusion

The PNIPAM brushes were synthesized via surface-initiated ATRP, and their graft densities were widely controlled by changing the density of initiator on the surface from the SDPB to CPB regimes. The CPB of PNIPAM in water of 8 ºC had nearly fully stretched chain conformation and F_n-independent μ on the order of 10^{-4}, achieving excellent water lubrication, similarly to the CPBs of PPEGA in Chapter 5. The v-dependence of μ revealed that under the studied condition, the CPB of PNIPAM was in the hydrodynamic lubrication state, while the SDPB of PNIPAM was in the boundary lubrication one. Both brushes showed swelling/shrinking behaviors with temperature owing to the LCST-type hydration/dehydration. However, the swelling/shrinking curve of the CPB of PNIPAM was broader than that of the SDPB of PNIPAM, reflecting their highly stretched chain conformation. The CPB of PNIPAM showed a rapid increase in μ in a small range of 20 ºC < T < 30 ºC. This sharp change like a transition was brought about by shrinkage of brush layer simultaneously affecting the effective thickness and viscosity of lubricating brush layer. These results revealed that the CPB of PNIPAM could control the lubrication by temperature, which would offer new insight

into tribology of polymer-brush-modified surfaces.

References

(1) (a) Urbakh, H.; Klafter, J.; Gourdon, D.; Israelachvili, J. *Nature* **2004**, *430*, 525-528. (b) Moro, T.; Takatori, Y.; Ishihara, K.; Konno, T.; Takigawa, Y.; Matsushita, T.; Chung, U. IL.; Nakamura, K.; Kawaguchi, H. *Nat. Mater.* **2004**, *3*, 829-836.

(2) (a) Durr, M.; Kentsch, J.; Muller, T.; Schnelle, T.; Stelzle, M. *Electroporesis* **2003**, *24*, 722-731. (b) Wang, T.; Kelly, K. W. *J. Micromech. Microeng.* **2005**, *15*, 81-90.

(3) (a) Lee, S.; Spencer, N. D. *Science* **2008**, *319*, 575-576. (b) Klein, J. *Science* **2009**, *323*, 47-48.

(4) (a) Forster, A. M.; Mays, J. W.; Kilbey, S. M. *J. Polym. Sci. Part B: Polym. Phys.* **2006**, *44*, 649-655. (b) Chang, D. P.; Dolbow, J. E.; Zauscher, S. *Langmuir* **2007**, *23*, 250-257. (c) Nordgren, N.; Rutland, M. W. *Nano Lett.* **2009**, *9*, 2984-2990.

(5) Schild, H. G. *Prog. Polym. Sci.* **1992**, *17*, 163-249.

(6) (a) Mizutani, A.; Kikuchi, A.; Yamato, M.; Kanazawa, H.; Okano, T. *Biomaterials* **2008**, *29*, 2073-2081. (b) Nagase, K.; Kobayashi, J.; Okano, T. *J. Royal Society Interface* **2009**, *6*, S293-S309.

(7) Ciampolini, M.; Nardi, N. *Inorg. Chem.* **1966**, *5*, 41-44.

(8) (a) Tsujii, Y.; Ejaz, M.; Sato, K.; Goto, A.; Fukuda, T. *Macromolecules* **2001**, *34*, 8872-8878. (b) Morinaga, T.; Ohkura, M.; Ohno, K.; Tsjii, Y.; Fukuda, T. *Macromolecules* **2007**, *40*, 1159-1164.

(9) (a) Yusa, S.; Shimada, Y.; Mitsukami, Y.; Yamamoto, T.; Morishima, Y. *Macromolecules* **2004**, *37*, 7507-7513. (b) Convertine, A. J.; Ayres, N.; Scales, C. W.; Lowe, A. B.; McCormick, C. L. *Biomacromolecules* **2004**, *5*, 1177-1180. (c) Bontempo, D.; Li, L. C.; Ly, T.; Brubaker, C. E.; Maynard, H. D. *Chem. Comm.* **2005**, *37*, 4702-4704. (d) Gibbons, O.; Carrol, W. M.; Aldabbagh, F.; Yamada, B. *J. Polym. Sci. Part A: Polym. Chem.* **2006**, *44*, 6410-6418.

(10) Teodorescu, M.; Matyjaszewski, K. *Macromol. Rap. Comm.* **2000**, *21*, 190-194.

(11) Yamamoto, S.; Ejaz, M.; Tsujii, Y.; Fukuda, T. *Macromolecules* **2000**, *33*, 5608-5612.

Chapter 7

Synthesis of Well-defined Bottle Brushes with Concentrated-Brush Effect and Frictional Property of Their Gel

7-1. Introduction

Concerning the lubrication mechanism of CPBs, it can be expected that the super lubrication of CPBs is not developed with grafted polymer on flat wafer but also on porous surface, sphere particle, clay, fiber, polymer, etc. Among them, grafted polymer (bottle brush polymer) can form gel material (graft-type of gel) by cross-linking. Gel is one of the attracted polymeric materials for lubrication, since it represents excellent lubrication system of body tissue (bio-tribology), such as joints, eyes, vessels, etc, which are generating much interest of the research of biomedical materials.[1] Osada et al. found super lubrication in charged hydro-gel attaining the μ of 10^{-4} order in water media.[2] They insist that electrostatic repulsion force derived from charged polymer network prevent the polymer to attach to the friction surface to produce pure solvent layer which actually acts as effective lubricant. Aside from their system, the lubrication mechanism of CPBs would provide further lubricating gel materials without the help of electrostatic repulsion effect, as the CPB lubrication depends on the conformation of brush structure rather than chemical structure.

Whether the super lubrication of CPB can be introduced to graft type of gel or not is totally depends on the conformational structure of bottle brush polymer of gel network; the precise control of graft chain and cross-linking. The structure of bottle brush polymer can be considered with columnar model (Figure 7-1). The effective graft density, the number of graft chains per columnar surfaces, decays along with the chain length. The shorter graft chains rather maintain the stretched structure determined by the initial graft density on the stem polymer. As the required effective graft density for CPB is over 0.1 (see section 2-3), the columnar model suggests us that the bottle brush polymer exhibit CPB structure when consisted of grafted chains on each monomer segment of stem

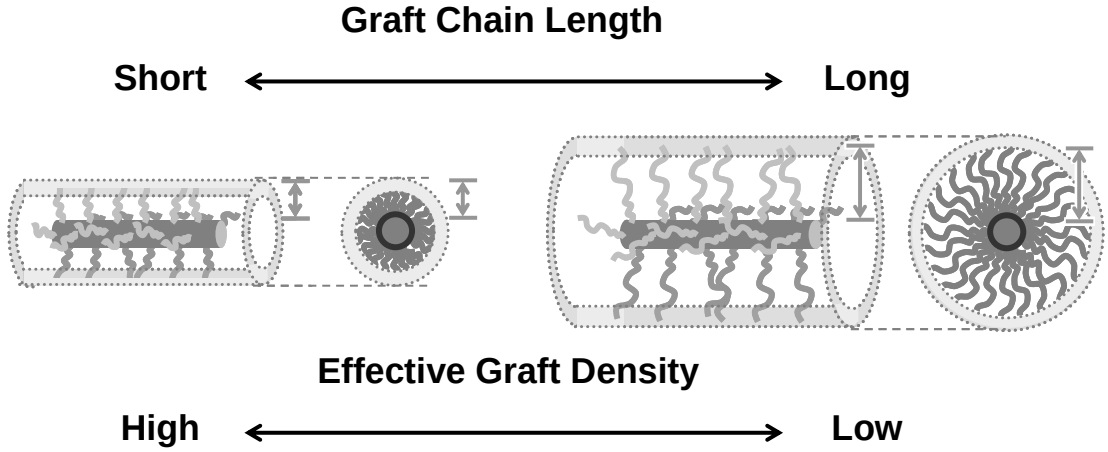

Figure 7-1. Schematic illustration of tubular model for bottle brush polymers. When the following assumptions are taken into account, graft density σ on peripheral of bottle brush polymer with *x*-mer graft polymer chain can be calculated as $1/(2\pi x \times 0.25 \times 0.25)$ chains/nm^2. The effective graft density σ*, a good measure of σ for various kinds of polymer brushes, is defined as $a^2\sigma$, where a^2 is the cross-sectional area per monomer unit given by $a^2 = v_0/l_0$ with v_0 being he molecular volume per monomer unit and l_0 being the chain length per monomer unit. Assumptions: (i) the graft chains are grafted on each monomer segment of stem polymer. (ii) the grafted chains take fully-stretched structure. (iii) chain lengths per monomer unit of stem and graft polymers are 0.25 nm (vinyl polymer).

polymer and shorter than pentadecamer graft chains. This fascinate us to design graft-type of gel with precisely controlled graft chains for lubricating gel material developing super lubrication effect of CPB. Although some research groups previously fabricated bottle brush polymer with controlled graft chains by grafting-to or grafting-from method using LRP technique,[3] the bottle brush polymer design aiming at developing CPB effect and material design with the polymer have not been reported yet.

Herein, the author newly synthesize a precisely and densely grafted bottle brush polymer, and study the frictional property of the graft-type of gel in a view point of developing super lubrication of CPB. ATRP was exploited to directly graft the brush chain on stem polymer in controlled manner (Scheme. 7-1). First, 2-(2-bromo-2-methylpropanoyloxy)ethyl methacrylate (BIEM, methacrylate type monomer having ATRP initiation sites in side chain) was polymerized via conventional radical polymerization to obtain linear macro-initiator (PBIEM) for the stem chain of bottle bush polymer. Subsequently, St was polymerized from PBIEM macro-initiator with almost full initiation efficiency via ATRP to obtain the bottle brush polymer with precisely controlled graft chain length. The bottle

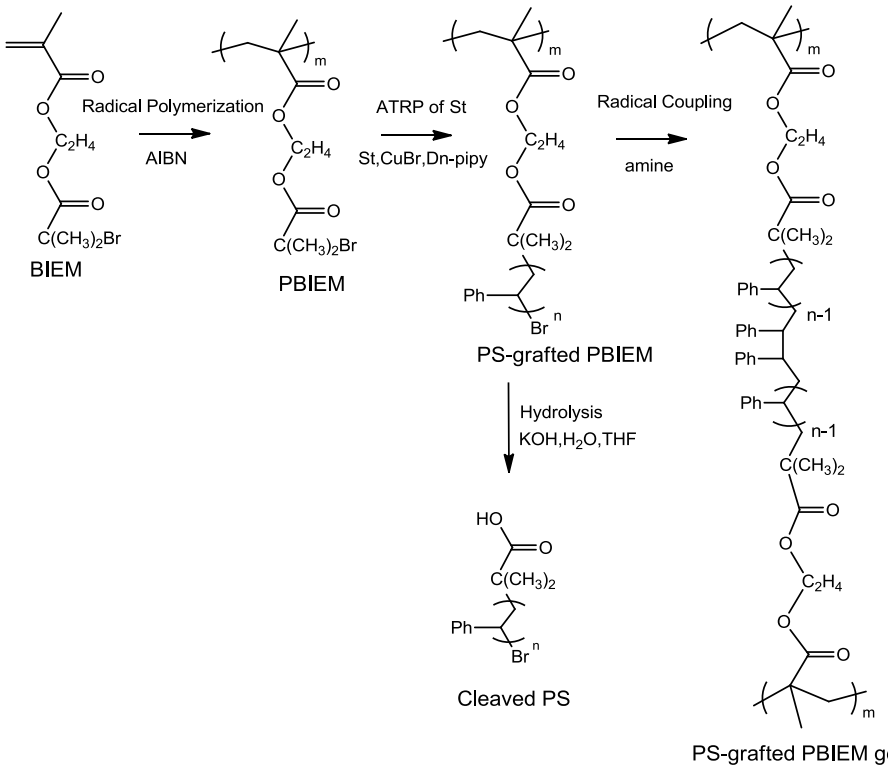

Scheme 7-1. Synthesis of bottle brush polymer (PS-grafted PBIEM) and of its gel (PS-grafted PBIEM gel) with controlled PS graft chain and graft density.

brush polymer was turned into graft-type of gel in thin film by spincoating the bottle brush poymer solution on silicon wafer and cross-linking of the free ends of grafted PS side chains with radical coupling reaction. The frictional property of the graft-type of gel was evaluated by AFM.

7-2. Experimental methods

7-2-1. Materials

2-(2-bromo-2-methylpropanoyloxy)ethyl methacrylate (BIEM) was synthesized according to the literature.[4] Azobisizobutyronitrile (AIBN, 99%, Wako Pure Chemical Ind., Ltd., Japan) was recrystallised from methanol. Ethyl 2-bromoisobutyrate (EBIB, 98%, Tokyo Chemical Industry Co., Ltd., Japan), copper(I) bromide (Cu(I)Br, 99.9%, Wako), copper(II) bromide (Cu(II)Br, 99.9%, Wako) and 4,4’-dinonyl-2,2’-bipyridine (dNbipy, 97%, Aldrich) were used as received. Styrene (St, 99 %, Nacalai Tesque Inc., Japan) was passed through a column of basic alumina to remove inhibitor. All other reagents were used as received from commercial source.

7-2-2. Polymerization of BIEM

An anisole solution of BIEM (2.4 M) and AIBN (1.2 mM) was subjected to Schlenk flask and then heated at 50 °C for 40 h under argon atmosphere to obtain polyBIEM (PBIEM) solution with 77% conversion determined from the gel permeation chromatography (GPC) peak area. The PBIEM, after having purified by reprecipitation from an anisole solution into methanol, had a M_n of 467,000 and a M_w/M_n of 3.35 by PMMA-calibrated GPC.

7-2-3. ATRP of St from PBIEM

An anisole solution of St (4.6 M), PBIEM (21 mM), EBIB (free initiator, 2.3 mM), Cu(I)Br (46 mM), Cu(II)Br (2.3 mM) and dNbipy (92 mM) was subjected to Schlenk flask and then heated at 110 °C under argon atmosphere. After a prescribed time *t*, an aliquot of the solution was taken out with a syringe and quenched to air. The reaction mixture was then diluted with tetrahydrofuran (THF) and analyzed by GPC. The GPC curve showed two clearly divided peaks attributed to PS grafted on PBIEM and free PS chain grown from EBIB respectively. The reaction mixture turned into flabby soft gel when the conversion exceeded about 30%, due to a small proportion of cross-linking by bimolecular termination reaction of growing PS chain from PBIEM. After the gelation, the free PS chain was extracted by washing the gel with THF and analyzed by GPC. The residual gel composed of PS grafted PBIEM was dried under vacuum and hydrolyzed as below. The conversion of St was determined by ^{1}H NMR analysis of the reaction mixture.

For preparation of PS grafted PBIEM for thin gel samples, the ATRP solution of St should be stopped at relatively lower conversion before undesirable gelation. Free initiator EBIB also should not be added to the solution due to the difficulty in separating the PS grafted PBIEM from free PS.

The PS grafted PBIEM for each gel sample was prepared as below.

PS grafted PBIEM for Gel 1 (M_p ~ 1,000)

An 8.0 g anisole solution of St (4.6 M), PBIEM (46 mM), Cu(I)Br (11 mM), Cu(II)Br (1.4 mM) and dNbipy (23 mM) was subjected to Schlenk flask and then heated at 110 °C under argon atmosphere for 5.0 h.

PS grafted PBIEM for Gel 2 (M_p ~ 1,300)

An 8.0 g anisole solution of St (4.6 M), PBIEM (46 mM), Cu(I)Br (11 mM), Cu(II)Br (1.4 mM) and dNbipy (23 mM) was subjected to Schlenk flask and then heated at 110 °C under argon atmosphere for 15.0 h.

PS grafted PBIEM for Gel 3 (M_p ~ 5,600)

An 8.0 g anisole solution of St (4.6 M), PBIEM (4.6 mM), Cu(I)Br (23 mM), Cu(II)Br (2.3 mM) and dNbipy (46 mM) was subjected to Schlenk flask and then heated at 110 °C under argon atmosphere for 7.0 h.

The purified PS grafted PBIEM for each gel sample was obtained by reprecipitation from an anisole solution into methanol. The small portion of the PS grafted PBIEM was hydrolyzed as below to measure the M_n and M_w/M_n of PS chain by GPC or matrix assisted laser desorption ionization time of flight and mass spectrometry (MALDI-TOF MS, microflex & microflex LT, Bruker Daltonics Inc., USA) equipped with a nitrogen laser. The matrix used for the MALDI-TOF MS analysis was dithranol.

7-2-4. Hydrolysis of PS chain from PS grafted PBIEM

The PS grafted PBIEM was dispersed (0.1 wt%) in 5 M KOH aqueous solution/THF/ethanol (6/53/41 wt%) mixture. The system was sealed in glass tube and then heated at 100 °C for 12 h. The residual solution was subjected to GPC analysis to examine the M_n and M_w/M_n of the cleaved PS and hydrolysis efficiency of 90%. For MALDI-TOF MS analysis, the residue was diluted with 10 parts chloroform and washed thrice with water, and then evaporation of solvent gave a polymer film of cleaved PS.

7-2-5. Preparation of Thin Gel Film of PS Grafted PBIEM

PS grafted PBIEM was dissolved (5 wt%) in ethylbenzene containing 73 mM tetrakis(dimethyl)ethylene. The thin gel film of PS grafted PBIEM was obtained by spincasting the PS grafted PBIEM solution onto a silicon wafer (Ferrotec Corp., Japan, thickness 0.5 mm) using a spin coater at spinning speeds of 500 rpm for 5 s and subsequently 3000 rpm for 30 s, followed by

evaporation in vacuum for 10 min and annealing at 120 °C for 1 h in argon atmosphere to obtain water insoluble PS grafted PBIEM gel film. The film was immersed in THF for 60 min and toluene for 24 h to remove residue. The film thickness was measured with AFM (Nano Wizard, JPK Instruments AG, Germany) by scanning the surface image across the boundary between the scratched and unscratched regions on the sample. The equilibrium swollen thickness of the film was also measured with AFM by the combination of force measurement and topographic imaging across the boundary.

7-2-6. Friction Measurement

Frictional force measurement was performed by AFM with a rectangular-shaped cantilever OMCL-RC800 probe (Olympus Optical Co., Ltd., vertical spring constant, k_n = 0.1 N/m, lateral spring constant, k_s = 23 N/m, respectively). A silica particle (SiP) modified with concentrated PS brush (the M_n and M_w/M_n values of the grafted PS chain were 47,000 and 1.26 respectively, prepared according to Chapter 2) on its surface was attached at the tip of cantilever with two-component epoxy resin adhesive. Friction force F_s and normal force F_n between PS grafted PBIEM gel and SiP surfaces were simultaneously measured in toluene as a function of separation using a modified AFM system, as described in section 2-2-3.

7-3. Results and discussion

PBIEM (M_n ~ 467,000 and M_w/M_n ~ 3.35) was obtained through conventional radical polymerization of BIEM using AIBN as radical initiator. The ATRP of St was carried out with PBIEM as macro-initiator. Figure 7-2 shows the plots of M_n and M_w/M_n of free PS chain against conversion. The free PS chain, which would be the indicator of molecular weight of grafted PS chain on PBIEM,[5] was produced from compensating free initiator EBIB added beforehand to the polymerization solution in place of 10% molecular amount of bromoisobutyrate group (ATRP initiation group) of PBIEM macro-initiator. The M_n and M_w/M_n of the free PS chain was able to be determined with direct GPC analysis of polymerization solution distinctively from PS grafted

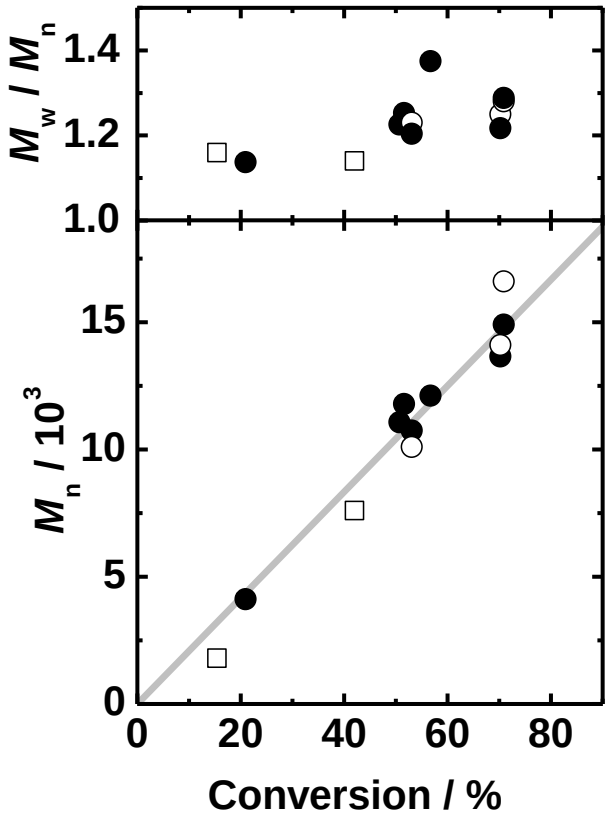

Figure 7-2. Plot of M_n and M_w/M_n vs conversion of the free (●) and cleaved (○) polymers for the polymerization of St. The M_n and M_w/M_n of cleaved polymers polymerized without EBIB free initiator are also plotted (□).

PBIEM. The polymerization proceeded in controlled manner, keeping relatively low polydispersity and good proportionality of M_n with conversion following theoretical molecular weight. It was possible to measure the grafted PS chains cleaved from PBIEM after the polymerization by hydrolysis, following almost same M_n and M_w/M_n values with the free PS chains. Those polymerization results show that the PS chain is grafted on PBIEM consuming almost all of ATRP initiation group with controlling chain length, prerequisite for controlled bottle brush polymer with high graft density.

The purified PS grafted PBIEM was then gelated into thin film to measure the frictional property. Radical coupling reaction between the grafted PS chain ends was used for gelation process. The ethylbenzene solution of the PS grafted PBIEM and tetrakis(dimethylamino)ethylene, the amine which can withdraw bromine end of the grafted PS to generate St radical for coupling,[6] was

Table 7-1. Characteristics of Studied PS Grafted PBIEM Gels for Frictional Property.

Sample	$M_{p,GPC}$[(a)]	$M_w/M_{n,GPC}$[(a)]	$M_{n,MS}$[(b)]	$M_w/M_{n,MS}$[(b)]	Swelling Degree[(c)]	L_d /nm[(d)]
Gel 1	1,000	-	1,070	1.07	12.5	234
Gel 2	1,300	-	1,100	1.14	13.5	245
Gel 3	5,600	1.07	4,970	1.01	13.8	44

(a) Determined by peak top value of GPC curve. (b) Determined by MALDI-TOF MS. (c) Swelling degree was defined as a ratio of equilibrium swollen thickness L_{swell} and dry thickness L_d (L_{swell}/L_d). (d) L_d was determined with AFM image across scratched boundary of gel film.

spincoated on silicon wafer and then annealed under reduced pressure to successfully obtain insoluble gel film about 100 nm thickness. The grafted PS chain was also able to be cleaved from PBIEM main chain after gelation. The GPC curve of the grafted PS chain cleaved after gelation showed another peak at twice molecular weight of the original grafted PS chain but the area is only a few percent of the original one, indicating that only small portion of the grafted PS chain is involving in the radical coupling reaction to turn into thin gel film. It is favorable to fabricate gel for maintaining densely grafted brush structure, avoiding the large part of the brush structure being fractured by forming bridge or loop structure between adjacent PS chain ends. The combination of AFM force measurement and topographic imaging across the boundary revealed that the thin gel films immersed in toluene swell as 10 times thicker as their dry thicknesses. The characteristics of the PS grafted PBIEM thin gels are listed in Table 7-1.

Figure 7-3 shows the v-dependence on μ at F_n of 20 nN. Gel 3 showed relatively high μ value of 0.3 and smaller v-dependency. On the contrary, the μ of Gel 1 and Gel 2 showed lower value and proportionally increased logarithmically with v. In particular, Gel 1, the gel with the shortest graft chain length, exhibited quite small μ value as low as 10^{-4} order at low v region, which is comparable friction behavior to the ultra-low frictional property of CPBs.

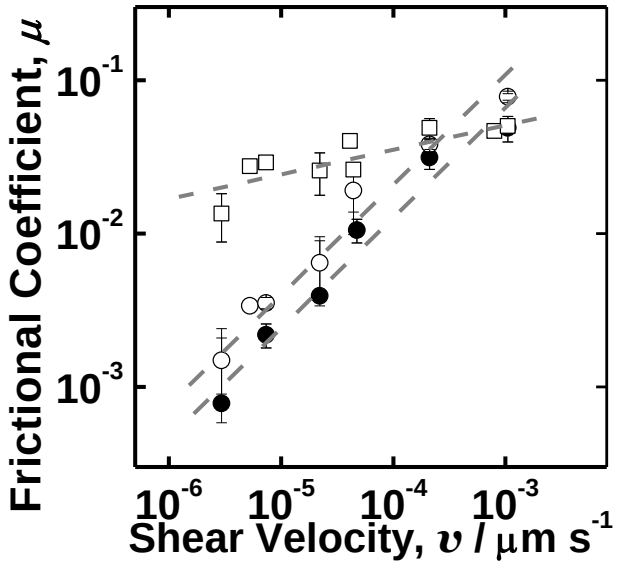

Figure. 7-3. Plot of frictional coefficient μ vs shear velocity v measured at a normal force F_n of 20 nN between the PS-grafted PBIEM gel and CPB of PS on probe silica particle in toluene. Each symbol denotes the result of Gel 1 (●) and Gel 2 (○) and Gel 3 (□), respectively.

Concerning the friction mechanism of CPBs as discussed in Chapter 2, the friction behavior of Gel 1 and Gel 2 is attributed to the development of CPB effect on their bottle brush structures. The friction of each gel sample can be understood by considering effective graft density. Here, the author defines the effective graft density of bottle brush polymer of cylindrical surface of tubular bottle brush polymer. The effective graft density is decreased in inverse proportion to the graft chain length. Gel 3, having the longest grafted PS chain among gel sample, has lower effective graft density of 0.03 which is indeed inadequate for consisting concentrated polymer brush with the grafted PS chain. The low effective graft density allows partial contamination of graft chain segments between the graft chain and confronted CPBs on probe particle, resulting in relatively higher μ value determined with the boundary lubrication nature of Gel 3. In comparison, the effective graft densities of Gel 1 and Gel2, which have shorter grafted PS chain lengths, can be calculated as 0.13 and 0.17. Their effective graft densities are enough to develop CPB effect for bottle brush polymer, as they exceed the crossover effective graft density of 0.1 dividing polymer brush to SDPB or CPB regimes. The CPBs structure developed in PS grafted PBIEM of Gel 1 and Gel 2 dramatically decreased their μ

value in boundary lubrication by preventing the contamination of graft chain segments, which came to exhibit friction manner in hydrodynamic lubrication state. The crossover effective graft density could not be directly applied for tubular bottle brush polymer. However, the friction behaviors of Gel 1 and Gel 2 insist that the effective graft density would be a parameter for the formation of CPB structure with bottle brush polymer, concerning that other parameter for friction such as the gel thickness and degree of swelling is almost same in this friction measurement. Either way, it can be emphasized that the reduction of μ of Gel 1 and Gel 2 is the first successful result of confirmation of CPB effect with bottle brush polymer.

7-4. Conclusion

The author has newly proposed a synthesis of bottle brush polymer precisely designed of its graft chain length and graft density, and studied the frictional property of the thin gel film constituted with the bottle brush polymer. The graft chain length and graft density of bottle brush polymer was accurately controlled by exploiting ATRP initiated from macro-initiator polymer which contains initiation sites in its each monomer segment. The bottle brush polymer was able to be turned into thin gel film with radical coupling reaction between the free living ends of grafted polymer chain. The friction study of the prepared then gel films showed a distinctive lubricating property depending on the grafted polymer chain lengths, which was understood by their effective graft density of each bottle brush polymer. Namely, the bottle brush polymer with shorter graft chain length has higher effective graft density, even if the brushes have a same graft density at the roots of their graft chains. The gel films constructed by the bottle brush polymer with shorter graft chain, the effective graft density of which were particularly more than 0.1, exhibited ultra-low frictional property that resulted from CPB structure on the bottle brush polymer. This work demonstrates the synthesis of well-defined bottle brush polymer, and holds promise for a novel functional polymer material developing CPB effect with single polymer chain.

References

(1) (a) Freeman, M.E.; Furey, M.J.; Love, B.J; Hampton, J.M. *Wear* **2000**, *241*, 129-135. (b) Wang, H.Q.; Ateshian, G.A. *J. Biomech.* **1997**, *30*, 771-776.

(2) (a) Gong, J.; Higa, M.; Iwasaki, Y.; Katsuyama, Y.; Osada, Y. *J. Phys. Chem. B* **1997**, *28*, 5487-5489. (b) Gong, J.; Osada, Y. *J. Chem. Phys.* **1998**, *109*, 8062-8068. (c) Gong, J.; Kagata, G.; Osada, Y. *J. Phys. Chem. B* **1999**, *103*, 6007-6014. (d) Gong, J.; Kurokawa, T.; Narita, T.; Kagata, G.; Osada, Y.; Nishimura, G.; Kinjo, M. *J. Am. Chem. Soc.* **2001**, *123*, 5582-5583.

(3) (a) Subbotin, A.; Saariaho, M.; Ikkala, O.; Ten Brinke, G. *Macromolecules* **2000**, *33*, 3447-3452. (b) Zhang, M.; Müller, A.H.E. *J. Polym. Sci. Part A: Polym. Chem*. **2005**, *43*, 3461-3481. (c) Sheiko, S.S.; Sumerlin, B.S.; Matyjaszewski, K. *Prog. Polym. Sci*. **2008**, *33*, 759-785.

(4) Von Werne, T.A.; Germack, D.S.; Hagberg, E.C.; Sheares, W.; Hawker, C.J.; Carter, K.R. *J. Am. Chem. Soc*. **2003**, *125*, 3831-3838.

(5) (a) Tsujii, Y.; Ejaz, M.; Sato, K.; Goto, A.; Fukuda, T. *Macromolecules* **2001**, *34*, 8872-8878. (b) Morinaga, T.; Ohkura, M.; Ohno, K.; Tsujii, Y.; Fukuda, T. *Macromolecules* **2007**, *40*, 1159-1164.

(6) Nishiyama, Y.; Kobayashi, A. *Tetrahedron Letters* **2006**, *47*, 5565-5567.

Summary

In **Chapter 1**, the background, purpose, and outline of this thesis were described.

In **Chapter 2**, the effect of solvent quality and hence degree of swelling on the frictional property of CPBs was investigated using the polystyrene (PS) brush samples. The degree of swelling of the brush was successfully controlled by varying the solvent composition of toluene/2-propanol mixture. The data of frictional coefficient μ as a function of shear velocity v and solvent composition (and hence degree of swelling) were well understood by two mechanisms of lubrication, boundary and hydrodynamic lubrications. At low v in toluene-rich solvents, the boundary lubrication mechanism afforded μ values less dependent on v and exceptionally small on the order of 10^{-4}, as had previously been observed for the CPB of poly (methyl methacrylate) (PMMA) in toluene and ascribed to effective suppression of interpenetration between polymer brushes. This study more focused on the hydrodynamic lubrication regime observed in a wide range of solvent compositions. The μ data in this regime were well described by the relationship $\mu = \beta \cdot v^{\alpha}$, where the parameter α was almost constant and close to unity and the parameter β was scaled by the degree of swelling, suggesting that the viscosity resistance on and in the solvent-swollen polymer brush dominated the friction.

In **Chapter 3**, the frictional property of the CPB of PMMA was investigated in highly viscous ionic liquids (ILs) (DEME-TFSI and EMI-TFSI) and toluene. These ILs could swell the CPB of PMMA to the same degree as toluene, a more commonly used good solvent of much lower viscosity. As expected between the concentrated polymer brushes in good solvents, little adhesive interaction in the ILs was observed, decreasing the μ in the boundary lubrication regime to values presumably on the order of 10^{-4}, as was the case in toluene. This allowed the hydrodynamic lubrication mechanism to dominate the friction. In this regime, the v dependence of μ followed the above-mentioned power-law scaling with an α value close to unity. Interestingly, the β parameter was simply scaled by the viscosity of solvent even though the viscosity differed by nearly two orders

of magnitude. The study did not only clarify the nature of hydrodynamic lubrication but also suggested the ability, as an excellent-lubrication system, of the CPB combined with IL.

In **Chapter 4**, the frictional property between the CPBs of immiscible polymers, PS and PMMA, was investigated in toluene, a good solvent for both polymers, to clarify the feature in the boundary lubrication of the CPB system. The immiscibility was demonstrated to effectively lower the frictional coefficient, approximately by half, to a value on the order of 10^{-5}. This means that in a good solvent, the confronted CPBs of the identical polymer partly interpenetrate each other at the outermost surface by compression and that this interaction determines the friction in the boundary lubrication (on the order of 10^{-4} in μ).

In **Chapter 5**, the CPBs of water-soluble polymers, poly (2-hydroxyethyl acrylate) (PHEA) and poly (poly(oxyethyleneglycol)methylether acrylate) (PPEGA), were newly synthesized by applying photo-induced TERP to surface-initiated graft polymerization, where TERP refers to the organotellurium-mediated radical polymerization, and their swelling and frictional properties in water media were investigated. In water, the CPBs of PHEA and PPEGA had equilibrium thicknesses of ca. 50% and 120%, respectively, against the weight-average contour length of graft chains. This indicates that water is a reasonably good solvent for PPEGA but not for PHEA. The frictional property of these brushes was well understood by the above-mentioned boundary and hydrodynamic lubrications. Reflecting less quality as a solvent, the PHEA brush showed a higher value of μ in the boundary lubrication, consistent with the fact that adhesive interaction was observed for this system. More interestingly, the CPB of PPEGA gave a μ value on the order of 10^{-4} in pure water as well as in 0.1 M NaCl aqueous solution. Such super lubrication was concluded to be common to the CPBs, e.g., even in an aqueous system.

In **Chapter 6**, the CPB and semi-dilute polymer brush (SDPB) of poly (*N*-isopropyl acrylamide) (PNIPAM) were synthesized via surface-initiated ATRP, and their swelling and frictional properties in water were investigated as a function of temperature. Temperature-induced swelling/shrinking process was observed for both the CPB and SDPB, the former of which had a

more gradual change owing to its highly stretched chain conformation. At low temperatures, the CPB achieved μ values lower than 4×10^{-4}, nearly three orders of magnitude lower than those of the SDPB. More notably for the CPB, a sharp transition in μ was triggered by temperature at around 30 ^{o}C, namely, the μ value changed by more than three orders of magnitude in a narrow temperature span, unlike the SDPB. Such stimulus-responsive water lubrication is of importance in developing novel and advanced applications in technological and biomedical fields.

In **Chapter 7**, the bottle brushes of PS-side chains were synthesized, and the frictional property of thin gel films of these bottle brushes was investigated. The ATRP from a multi-initiator, poly (2-(2-bromo-2-methylpropanoyloxy)ethyl methacrylate) (PBIEM), proceeded with almost complete initiation, giving the bottle brushes with controlled side-chain lengths. Using an amine catalyst, effective radical coupling between side-chain ends was successfully achieved, processing the bottle brushes into thin gel films. Thus prepared films were swollen in toluene, a good solvent for PS, and the μ value on their surfaces was measured against the CPB of PS. Interestingly, the samples of sufficiently short side-chains were much improved in lubrication; the μ value was dependent of v, going down to the order of 10^{-4} in a low v range (almost comparable to the value between the CPBs of PS in toluene). This result was discussed on the basis of the crossover density between the SDPB and CPB by assuming the swollen bottle brush as a column with a radius equal to the fully stretched side-chain length.

Through the thesis, the author revealed the lubrication mechanism of CPBs in solvents and thereby developed new types of lubricating surfaces. The features of lubrication for the CPB are summarized as follows; (i) the boundary lubrication is much improved on the order of 10^{-4} or sometimes 10^{-5} in μ, allowing the hydrodynamic lubrication, and (ii) the hydrodynamic lubrication is well understood by the local viscosity affected by the degree of swelling of the brush and the viscosity of solvent. The author hopes that these fundamental studies shed new light on the science of tribology, leading to new design for sophisticated and intelligent tribomaterials.

List of Publication

Chapter 2.

(1) Lubrication Mechanism of Concentrated Polymer Brushes in Solvents: Effect of Solvent Quality and Thereby Swelling State

Nomura, A.; Okayasu, K.; Ohno, K.; Fukuda, T.; Tsujii, Y. *Macromolecules* **2011**, *44*, 5013-5019.

Chapter 3.

(2) Lubrication Mechanism of Concentrated Polymer Brushes in Solvents: Effect of Solvent Viscosity

Nomura, A.; Okayasu, K.; Ohno, K.; Fukuda, T.; Sato, T.; Tsujii, Y. *Polym. Chem.* submitted.

Chapter 4.

(3) Super Lubrication and its Mechanism between Immiscible Concentrated Polymer Brushes in Good Solvent

Nomura, A.; Okayasu, K.; Ohno, K.; Fukuda, T.; Tsujii, Y. *Macromolecules* to be submitted.

Chapter 5.

(4) Controlled Synthesis of Hydrophilic Concentrated Polymer Brushes and Their Friction/Lubrication Properties in Aqueous Solutions

Nomura, A.; Goto, A.; Tsujii, Y.; Kayahara, E.; Yamago, S. *J. Polym. Sci., Part A: Polym. Chem.* submitted.

Chapter 6.

(5) Thermoresponsive Water Lubrication by Concentrated Polymer Brushes

Gao, W.; **Nomura, A.**; Ohno, K.; Tsujii, Y.; Fukuda, T. *Macromolecules* submitted.

Chapter 7.

(6) Synthesis and Frictional Property of Graft-Type Gel with Concentrated Polymer Brush Structure

Nomura, A.; Nakahara, R.; Ohno, K.; Tsujii, Y. *Adv. Mat.* to be submitted.

Other Associated Publications.

(7) AFM Studies on Microtribology of Concentrated Polymer Brushes in Solvents

Tsujii, Y.; **Nomura, A.**; Okayasu, K.; Gao, W.; Ohno, K.; Fukuda, T. *J. Phys.: Conference Series* **2009**, *184*, 012031.

(8) Use of Alcohol as Initiator for Reversible Chain Transfer Catalyzed Polymerization

Kim, J.; **Nomura, A.**; Fukuda, T.; Goto, A.; Tsujii, Y. *Macromol. React. Eng.* **2010**, *4*, 272-277.

(9) Super Lubrication of Concentrated Polymer Brushes in Good Solvent

Tsujii, Y.; Okayasu, K.; **Nomura, A.**; Ohno, K.; Fukuda, T. *Polymer* submitted.

(10) Synthesis and Characterization of Polystyrene Brushes Using a Surface-initiated Atom Transfer Radical Polymerization for Organic Thin Film Transistors

Hwang, D. -H.; **Nomura, A.**; Kim, J.; Cho, H.; Lee, C.; Ohno, K.; Tsujii, Y. *J. Nanosci. Nanotech.* **2011**, in Press.

Acknowledgements

The present investigations were carried out at the Institute for Chemical Research, Kyoto University in the period from 2006 to 2011.

The author would like to express his sincere gratitude to Professor Yoshinobu Tsujii for his invaluable guidance, stimulating discussions and encouragement throughout this work.

Grateful acknowledgement is due to Emeritus Professor Takeshi Fukuda, Associate Professor Kohji Ohno and Associate Professor Atushi Goto for his enthusiastic guidance, valuable discussion and encouragement.

The author wishes to express his appreciation to Professor Takaya Sato, Professor Shigeru Yamago and Dr. Eiichi Kayahara for their useful suggestions.

Sincere appreciation is due to all of his colleagues in Professor Tsujii's Labolatory for their kind helps, particulary, to Dr. Weiping Gao, Dr. Jeongsik Kim, Mr. Kenji Okayasu and Mr. Ryo Nakahara for their active collaborations in part of the study.

Finally, the author wishes to express his heartfelt thanks to his parents, Ritsuo Nomura and Hiroko Nomura, and his brother Masahiro Nomura, for their devoted support, and to his wife, Akiko Nomura for her heartfelt encouragement.

May, 2011

Akihiro Nomura